University of Alberta

Biological role of the tumor suppressor protein, RASSF1A in Inflammation and Cancer

by

Mohamed El-Kalla

A thesis submitted to the Faculty of Graduate Studies and Research
in partial fulfillment of the requirements for the degree of

Master of Science

in

Medical Sciences-Pediatrics

Spring 2010
Edmonton, Alberta

Examining Committee members:

Supervisor:	Dr. Shairaz Baksh, Pediatrics
Co-supervisor:	Dr. Jason Dyck, Pediatrics
Committee Member:	Dr. Hien Huynh, Pediatrics
Committee Member:	Dr. Karen Madsen, Medicine

Dedication

To my daughter Farida

Abstract

Inflammatory bowel disease (IBD) such as Crohn's disease (CD) and ulcerative colitis (UC) are chronic intestinal diseases characterized by inflammation of the gastrointestinal area resulting in abdominal pain, chronic diarrhoea, and weight loss. IBD affects 1 in 1000 individuals and between 10% and 15% of CD patients are children (with northern Alberta having one of the highest rates of CD in the world). Molecularly, it is characterized by hyperactivation of the transcription factor, nuclear factor κ B (NFκB), and elevated production of pro-inflammatory cytokines. RASSF1A is a tumor suppressor protein required for death receptor dependent cell death (apoptosis) originating from the tumor necrosis factor alpha (TNFα) receptor (TNF-R1). It is one of the most methylated genes identified in human cancers and one of the earliest detectable loss in cancer. Loss of RASSF1A expression arises by methylation of the promoter for exon 1Aα (encoding the N-terminal 119 amino acids) without epigenetic loss of the other isoforms of RASSF1, suggesting selective pressure to silence isoform RASSF1A. We have defined apoptotic regulation by RASSF1A involving death receptors (such as TNF-R1) and its downstream target modulator of apoptosis, MOAP-1. We now define a novel role for RASSF1A in modulating innate immunity. *Rassf1a*$^{-/-}$ mice rapidly become sick following challenge with LPS or dextran sulphate in comparison to wild type animals and cytokine analysis of the peripheral blood reveal an elevated production of NFκB regulated cytokines (IL-6, IL-12, IL-8 and IL-10) *Rassf1a*$^{-/-}$ mice when compared to wild type animals. We propose that RASSF1A is an emerging novel negative regulator of inflammation and maybe a new susceptibility gene for inflammatory diseases.

Acknowledgments

First and foremost, I would like to thank my wife and soul mate, Amira Elkady for all her support and love. I really don't know what to do without you! Love you a lot!

I would like to thank my parents, Prof. Dr. Samir EL-Kalla and Nahed Seada, for everything they have done for me and raising me to be the person that I am today. Without their support and encouragement, I could not do that. I would like also to thank my sisters, Nermin and Nesreen for all their support during my entire life.

My next appreciation goes to my supervisor Dr. Shairaz Baksh for all his support and his research-expertise. I want to express my gratitude to him for inspiration and patience during the period of my studies. I would like to thank my supervisory committee members, Dr. Jason Dyck, Dr. Karen Madsen, and Dr. Hien Huynh for their kindness, guidance, support, patience and valuable suggestions.

My gratitude also goes to all members in Dr. Baksh's lab for their help during this study. I would like to thank especially Dr. Haya Abu Ghazaleh, Christina Onyskiw and Renfred Chow who offered support and help in a numerous ways.

Finally, I would like to thank all my friends who stand behind me in the time of hardships.

Table of Contents

List of Figures

List of Abbreviations

BMDM	Bone marrow derived macrophages
CD	Crohn's Disease
CpG ODN	Double stranded DNA, TLR9 stimuli
CARD15	the other name for NOD2
DSS	Dextran sodium sulfate
FADD	Fas associated death domain protein
IBD	Inflammatory bowel disease
ICC	Intestinal crypt cells
IE	Intestinal epithelial
IKK	IκBα kinase
IRAK	Interleukin 1 receptor associated kinase
LPL	Lamina propri lymophcytes
LPS	Lipopolysaccharide, TLR4 stimuli
MOAP-1	Modulator of apoptosis 1
MSP	Macrophage-stimulating protein
MST1*	Macrophages stimulating 1 gene
MST1	Mammalian STE20-like kinase 1
MST2	Mammalian STE20-like kinase 2
MyD88	Myleoid differentiation response gene 88
NFκB	Nulcear factor κB
NOD2	Nucleotide-binding oligomerization domain containing 2

PAM_3CSK_4	A bacterial lipoprotein, TL2 stimuli
RAPL	Regulator of cell adhesion and polarization enriched in lymphoid tissues
RASSFIA	Ras association domain family 1 isoform A
RIP	Receptor interacting protein
SDS PAGE	Sodium dodecyl sulfate polyacrylamide gel electrophoresis
TAB	TAK associated binder
TAK	TGFβ activated kinase
TGF β	Transforming growth factor β
TLR	Toll receptor
TNBS	Trinitrobenzene sulfonic acid
TNFα	Tumor necrosis factor α
TRADD	TRAF2 associated death domain protein
TRAF	TNFα receptor associated factor
TRAIL	TNF-related apoptosis induced ligand
TRIF	Toll like receptor interacting factor
UC	Ulcerative colitis

Chapter 1

Introduction

Tumour suppressor proteins and oncogenes are some of the major targets of cancer therapy.[1] The identification of appropriate targets for therapy requires an understanding of the molecular changes underlying cancer (both genetic and epigenetic changes).[2] Tumour or neoplastic cells typically resist apoptosis because many oncogene and/or tumor suppressor gene mutations impair apoptotic signaling pathways.[3, 4] These pathways can originate either from the stimulation of cell surface death receptors (the extrinsic pathway) or involve mechanisms of conveying signals directly to the mitochondria (the intrinsic pathway). Mitochondria play a central role in nearly all apoptotic pathways, serving to integrate upstream apoptosis-inducing (pro-apoptotic) signals and promote the release of small apoptogenic molecules[5] that amplify the signal originating from the mitochondria.

RASSF1A (Ras association domain family 1 isoform A) is a tumor suppressor protein located in the 3p21.3 region of the human genome. RASSF1A was discovered in 2000 when Lerman and Minna et al., 2000 noticed that this area (3p21) frequently contained loss of heterozygosity (LOH) in lung cancer. Following the cloning of RASSF1A,[6] it was shown by Baksh et. al (2005) to be required for death receptor dependent cell death (apoptosis) originating from the tumor necrosis factor α (TNFα) receptor suggesting that its cell death function may modulate tumour surveillance.[7] It was subsequently shown to one of the most methylated genes identified in human cancers and one of the earliest detectable loss in some cancers. Loss of RASSF1A expression arises by methylation of the promoter for exon 1Aα (encoding the N-terminal 119 amino acids) without epigenetic loss of the other isoforms of RASSF1. This suggested that there is selective pressure to silence the function of isoform RASSF1A. Our research group has recently defined some of the molecular mechanisms of apoptotic regulation by RASSF1A involving death receptors (such as TNF-R1), its downstream target (modulator of

apoptosis [MOAP-1]) and Bax (a key activator of cell death). The objectives of this thesis are to investigate other biological functions of RASSF1A. We now define (i) a novel role of RASSF1A in modulating innate immunity through affecting the transcription factor, nuclear factor κ B (NFκB), a key modulator of inflammation and (ii) documented the importance of the microtubule binding and disease-associated polymorphisms of RASSF1A to several aspects of RASSF1A biology.

1.1 Inflammatory Bowel Disease (IBD)

1.1.1 Overview

IBD is chronic relapsing and remitting inflammation of the gastrointestinal tract resulting in abdominal pain, diarrhoea and weight loss. It results from an inappropriate immune response to pathogenic insult. It is classified into Crohn's disease (CD) and ulcerative colitis (UC). Crohn's disease can affect any part of gastrointestinal tract from the mouth to the anus and its inflammation is transmural, while ulcerative colitis affects only the colon and the inflammation is limited to the superficial layer (mucosa). In general, the highest incidence rates and prevalence for both CD and UC have been reported from northern Europe, the United Kingdom, and North America, which are the geographic regions that have been historically associated with IBD. In North America, incidence rates for IBD range from 2.2 to 14.3 cases per 100,000 person/year for UC and from 3.1 to 14.6 cases per 100,000 person/year for CD.[8] In Alberta, the incidence rate for CD and UC is 16.5 and 11 cases per 100.00 person/year respectively.[9]

1.1.2 Pathogenesis of IBD

Inflammatory bowel disease is thought to result from inappropriate activation of the mucosal immune system driven by the normal luminal flora. This aberrant response is most likely facilitated by defects in both the barrier function of the intestinal epithelium and the mucosal immune system. Therefore, there are a multiple factors which play a role in the pathogenesis of IBD.

Environmental Factors: Environmental factors are very important for the risk of IBD. Potentially relevant environmental factors include prenatal events, breastfeeding, childhood infections, microbial agents, smoking, oral contraceptives, diet, hygiene, occupation, education, climate, pollution, stress, and miscellaneous components such as toothpaste, appendectomy, tonsillectomy, blood transfusions, contact with animals, and physical activity.[10] Among these, the most established association is with smoking, but the reproducibility and strength of association with other risk factors needs further investigation. The effect of smoking or, curiously, the opposite effect of smoking on the outcome of each form of IBD represents the most interesting connection between environmental factors and IBD. Smoking is an independent risk factor for clinical, surgical, and endoscopic recurrence in CD and influences disease activity after surgery.

A link between diet and IBD is logical because IBD have defective nutrient absorption. Nutritional deficiencies related to defective absorption in IBD patients are well documented, particularly that of zinc in CD with associated immunologic dysfunction.[11] The effectiveness of elemental (containing basic diet nutrients as amino acids, sugars and minimal fat) or special diets in reducing the symptoms or inducing remission of CD has been proposed but not universally accepted, and some studies have found that enteral nutrition (tube feeding) is less effective than

steroids and aminosalicylates.[12, 13] Moreover, the relapse rate does not appear to differ between nutritional and traditional approaches (steroids and parenteral nutrition),[14] even when exclusion diets are implemented.[15] Some data suggest that elemental diet may improve CD by reducing intestinal permeability,[16] but it is not clear why nutritional therapies improve CD but not UC.

Familial and Genetic Factors: One of the most consistent observations in studies of IBD populations is the high incidence of CD or UC among family members. Both vertical and horizontal associations occur, including father-son, father-daughter, mother-son, mother-daughter, and sibling-sibling. In large studies performed in Scandinavian countries, a 10-fold increase in familial risk was interpreted to be strongly suggestive of a genetic cause.[17] An early investigation in a random European population found a significantly increased frequency of HLA-A11 and HLA-A7 in UC and a decreased frequency of HLA-A9 in CD.[18] A French group reported that CD genetic predisposition resides outside of chromosome 6[19] and subsequently reported a susceptibility locus on chromosome 16.[20] A British group reported evidence for susceptibility for both CD and UC on chromosomes 3, 7, and 12, suggesting that these are distinct disorders sharing some, but not all, susceptibility genes.[21] To date, more than 30 potential novel IBD susceptible loci have been found mapping to chromosome 1q32 (encoding for IL-10), 1p.31 (encoding the IL-23 receptor), 16q12 (encoding for NOD2 [nucleotide-binding oligomerization domain containing 2]/CARD15 [caspase recruitment domain family, member 15] and uncharacterized linkages on 3p21 to mention a few.[22-26] For some of these susceptibility genes polymorphisms have been identify that may correlate with the presence of disease. For example, in case of NOD2, 32.4% of CD patients carried one mutant allele within the NOD2[27] suggesting that other genetic changes are required for the pathogenesis of CD. Furthermore, the majority of NOD2 polymorphisms map to an R702W (an arginine [R] to tryptophan [W] change

at amino acid 702), or G908R change (a glycine [G] to R change at amino acid 908) or a cytosine insertion at nucleotide position 3020 (3020insC) that leads to a truncation of the final 3% of the NOD2 protein. [28] Individuals having these NOD2 polymorphisms have 10 to 14 times higher risk of developing CD. It has been demonstrated that the treatment with either bacterial lipopolysaccharide (LPS) or peptidoglycan (PGN) resulted in increased NFκB activity in cells transfected with wild-type NOD2/CARD15.[28] However, the frameshift variant, 3020insC, resulted in a marked hyporesponsiveness toward NFκB activation with LPS treatment.[28] In contrast, the R702W and G908R variants respond to LPS to a greater extent than the frameshift variant, though overall they show a significantly diminished ability to activate NFκB following LPS treatment.[29] The molecular mechanisms of how these variants specifically interfere with NFκB activity are yet to be determined. These and other observations provide new insights into potential IBD genes which may influence the pathogenesis of that disease.

Immune response and inflammatory pathway: For the pathogenesis of IBD, it remains unclear whether the immune system is activated as a result of an intrinsic defect (either constitutive activation or the improper down-regulatory mechanisms) or because of continued stimulation resulting from a change in the epithelial mucosal barrier.[30, 31] Substantial progress has been made in characterizing immune-cell populations and inflammatory mediators in patients with inflammatory bowel disease and in murine models.[32]

There is reasonable agreement that the mucosa of patients with established CD disease is dominated by CD4+ lymphocytes with a type 1 helper-T-cell (Th1) phenotype, characterized by the production of interferon-γ and interleukin-2. In contrast, the mucosa in patients with UC may be dominated by CD4+ lymphocytes with an atypical type 2 helper-T-cell (Th2) phenotype, characterized by the production of transforming growth factor β (TGF β) and interleukin-5 but

not interleukin-4.[33] In murine models, the effects of the activation of Th1 cells may be enhanced by the concomitant decrease in subgroups of suppressor T cells, variously designated Th3 or Tr1, which produce the down-regulatory cytokines interleukin-10 and TGFβ.[34] In addition to that, activated macrophages produce a potent mix of broadly active inflammatory cytokines, including tumor necrosis factor α (TNFα), interleukin-1, and interleukin-6. The activation of central immune-cell populations is eventually accompanied by the production of a wide variety of nonspecific mediators of inflammation. These include many other cytokines, chemokines, and growth factors as well as metabolites of arachidonic acid (e.g., prostaglandins and leukotrienes) and reactive oxygen metabolites such as nitric oxide.[32]

These mediators enhance the inflammatory process itself and tissue destruction, which eventuate in the clinical manifestations of disease. Recruitment of additional leukocytes from the vascular space to sites of disease activity is especially important in maintaining inflammation and depends on the expression of adhesion molecules in the local microvasculature on the various leukocyte populations.[35, 36]

1.1.3 Clinical Manifestation, Investigations, Treatment of IBD

IBD is a chronic, intermittent disease. Symptoms range from mild to severe during relapses and may disappear or decrease during remissions. In general, symptoms depend on the segment of the intestinal tract involved. General symptoms associated with UC and CD include fever, loss of appetite, weight loss, fatigue, night sweats, growth retardation and primary amenorrhea (absence of menstruation). Symptoms related to inflammatory damage of the digestive tract include diarrhea or constipation, abdominal pain and cramps, rectal bleeding and tenesmus (feeling of incomplete defecation). Sigmoidoscopy, colonoscopy are the investigation

of choice in IBD cases. Barium double contrast enema and plain x-ray can be either done in certain cases. Stool and blood examination are generally done for all cases of IBD to detect and check for the amount of blood loss.

Dietary and lifestyle changes are the first line of therapy that may reduce inflammation in IBD patients. There are a lot of medications which have been used for treatment of IBD. Aminosalicylates have been used for treating colitis flare-ups and maintenance of remission. Aminosalicylate may act by blocking the production of prostaglandins, inhibit bacterial peptide induced neutrophil chemotaxis and perhaps inhibiting the activation of NFκB. Corticosteroids (anti-inflammatory) usually provide significant suppression of inflammation and rapid relief of symptoms. Methotrexate (immune suppressor) is used when aminosalicylates and corticosteroids are either ineffective or only partially effective. Anti-TNFα agent as Infliximab has been approved for treatment of moderate to severe cases of IBD when there is inadequate response to standard medications. Surgical intervention may be needed in certain cases of IBD at some point to relieve symptoms when if drug treatment fails or to correct complications.

1.2 Inflammatory Bowel Disease and NFκB Pathways

Nuclear factor-kappa B (NFκB) is a key transcriptional regulator of innate and adaptive immunity. Inflammatory bowel disease and experimental intestinal inflammation are characterized by NFκB activation and increased expression of NFκB target genes such as IFN-γ, IL-6, IL-10 and IL-12.[37, 38]

TNFα stimulation can result in activation of the cell death or activation of the NFκB pathway.[39-42] Activation of NFκB plays an important role in amplifying and extending the duration of the innate immune response and inflammatory pathways.[43, 44] In order to activate

NFκB, TNF-R1 promotes the recruitment of TRADD (TRAF2 associated death domain protein), RIP (receptor interacting protein) and TNFα receptor associated factor (TRAF) to receptor complexes (Fig. 1.1) in order to activate NFκB.[45-47] If these events do not occur, FADD (Fas associated death domain protein) associates with TRADD to promote the activation of caspases leading to apoptosis. TRAFs play key roles in the assembly of protein complexes recruiting RIP and activating IκB kinase (IKK) (Fig. 1.1).[48, 49] IKK, in turn, phosphorylates IκBα, promoting its release from the NFκB complex, stimulating IκBα degradation and nuclear translocation of NFκB to regulate target genes.[40, 50] Dysregulation of NFκB can thus lead to the overproduction of some cytokines associated with a number of chronic inflammatory disorders, some leading to cancer.[43, 51-53]

In addition to TNFα stimulation, NFκB activity can also be modulated by the Toll family of receptors (TLRs). TLRs are type I membrane proteins characterized by an ectodomain composed of leucine rich repeats that recognize specific components of microbial pathogens (Fig. 1.1 and 1.2).[54, 55] TLRs activate a potent immunostimulatory response and serve as our first line of defense against invading pathogens. The signal transmitted from TLRs must therefore be tightly controlled, and there is clear evidence that if TLRs are overactivated, inflammatory diseases can result.[56-58] Eleven TLR isoforms are present that respond to different microorganisms and microbial components (Fig. 1.2).[59] TLR-2, 4, and 6 recognizes bacterial lipid components (such as LPS); TLR-3 recognizes single stranded RNA; TLR-5 responds to bacterial flagellin; TLR-7, 8, and 9 detect nucleic acids derived from viruses and bacteria (such as CpG oligodinucleotides [ODN] DNA motifs also found in viral and bacterial genomes; ODNs bearing unmethylated CpG motifs can mimic the immunostimulatory effects of bacterial DNA). Most TLRs are localized to the plasma membrane with the exception of TLR-3, 7 and 8, which

are localized intracellularly in endosomes (Fig. 1.2).[54, 60] TLR9 has been characterized to be located in endosomes in the endoplasmic reticulum of the resting macrophages and dendritic cells.[61] Moreover, surface expression of TLR9 has been reported in gastric epithelium[62] and intestinal epithelium.[63]. Viral particles are endocytosed and degraded in late endosomes or lysosomes, and this degradation causes the release of viral DNA and RNA allowing TLRs to contact them.

Central to TLR activation and linked to NFκB-induced gene transcription are the adapter proteins, MyD88 (Myeloid differentiation primary response protein), IRAK (Interleukin-1 receptor-associated kinase), and TRAF6 (TNF receptor-associated factor 6) (Fig. 2.1). MyD88 is a universal adapter that activates NFκB activity and is utilized by all TLRs, except for TLR3. MyD88 associates with TLRs via its Toll/interleukin-1 receptor (TIR) domain (Toll/interleukin-1 receptor domain) and stimulates the phosphorylation of members of the IRAK family, especially IRAK1, 2, and 4. Once phosphorylated, IRAKs dissociate from MyD88 and complex with TRAF6 to activate TAK 1 (TGF-β activated kinase 1) and promote TAK1/TAB associations (TAB, TAK associated binder).[54] These associations are essential for IKK activation, IκBα degradation, and nuclear accumulation of NFκB resulting in transcription of pro-inflammatory genes. As such, *Myd88*$^{-/-}$ mice have a loss in responsiveness to ligands for TLR2, 4, 5, 6, and 9.[64] TLR3 does not utilize MyD88, but relies on the function of TIR domain containing adapter inducing IFN-β (TRIF, also called TICAM1).[58, 65, 66] Similarly, toll receptor adapter molecule 2 (TRAM or TICAM2) maybe involved in TLR4 activation independent of MyD88 (Fig. 1.2). Several reports suggest that MyD88 participates in the immediate early response phase to TLR activation, whereas TRIF contributes to the late phase of NFκB activation.[67] However, it is important to recognize that MyD88 may also play a role in TLR-independent pathways. The

neuronal specific MyD88-5 is important for JNK activation in neurons.[68] For this thesis, I will only focus of MyD88 functions linked to TLR function.

1.3 Animal models of IBD

Several animal models of intestinal inflammation have been developed using chemical induction, immune cell transfer, or genetic manipulations.[69] Each has unique advantages for characterizing specific biological mechanisms of gut inflammation but also several limitations.

Chemically induced models: This group of animal models requires administration of an exogenous chemical agent for the induction of colitis. Examples include the trinitrobenzene sulfonic acid (TNBS) (a chemical which induce formation of colonic ulcers for up to 8 weeks with just one dose),[70] dextran sodium sulfate (DSS) (a chemical inducer of ulcerative colitis that irriates the colonic mucosa)[71] and oxazolone (a chemical which induce ulcerative colitis in the distal half of the colon).[72] Chemically induced models are useful for studying biochemical pathways of inflammation. These models are also useful in providing proof of concept for therapeutic interventions in a simple and relatively inexpensive setting. It is still unknown what the molecular mechanisms of action of these chemicals are.

Immunological models: Immunologically mediated models are models of adoptively transferred T cells or bone marrow precursors, which are introduced into immunodeficient recipient mice. Two classical examples are the $CD45RB^{high}$ [73] and bone marrow chimera transfer models.[74] Studies in these models have elucidated the role of pathogenic and regulatory T cells in controlling mucosal immunity and intestinal inflammation and offer strong evidence that Th1 polarization plays a key role in CD pathogenesis.[75] However, the profound immune

abnormalities in recipient mice probably make these models unsuitable for investigating the innate factors causing human CD.

Genetic models: Transgenic and knockout methodologies have revolutionized the field of animal models of IBD. Examples include, T-cell receptor (TCR)α/β[76], IL-10[77], and Gi2-a [78] knockout models. Genetic models greatly contribute to our understanding of the role of key immune-related molecules in the pathogenesis of chronic intestinal inflammation. Collectively, these models have clearly established the requirement for strict regulation of the mucosal immune response and have allowed identification of key components involved in gut immune regulation. For example, IL-10 knockout mouse is one of the models which help in understanding the pathogenesis of IBD. IL-10 is produced by T cells, B cells, macrophages, thymic cells, and keratinocytes, and it downregulates the function of T helper (h)-1 cells. Mice with targeted deletion of the IL-10 gene spontaneously develop chronic enterocolitis after 12 weeks of age with massive infiltration of lymphocytes, activated macrophages, and neutrophils.[77] Administration of recombinant IL-10 or IL-10 gene therapy proved a therapeutic option for colitis in several animal models.[79, 80] This gives an idea about importance of T cell derived IL-10 in the regulation of mucosal T cell responses.

Another important model for IBD is the IL-23 deficient mice. Importance of the IL-23 pathway in IBD has come from mouse models of IBD, in which the IL-23 deficiency or blockade protects from disease.[81, 82] Therefore, genetic polymorphisms in the IL-23 receptor represent one of the strongest associations in IBD.[83]

NOD2 (nucleotide-binding oligomerization domain containing 2) is one the susceptibility genes located on chromosome 16q12, therefore *Nod2*$^{-/-}$ mice could be one of the useful models of IBD. Mutations within the Nod2 gene on chromosome 16 as being associated to CD, but not

UC.[29, 84] On the other hand, *Nod2*$^{-/-}$ mice have not demonstrated spontaneous intestinal inflammation.[85, 86] Furthermore, colonic inflammation is not worse than that of wild type mice upon challenge with an agent leading to acute colitis.[86] Therefore NOD2 may be dispensible for the pathogenesis of acute colitis.

Recently, it has been established that macrophages stimulating 1 gene (MST1*) is one of the susceptibility genes located on chromosome 3p21.22.[87] Macrophage-stimulating protein (MSP), the protein encoded by MST1*, and its receptor MST1R have been reported to be involved in macrophage chemotaxis and activation as well as regulation of inflammatory responses suggesting the role of this gene in the pathogenesis of IBD.[88, 89] However, the molecular pathways involved have yet to be determined.

1.4 RASSF1A

1.4.1 Introduction & Overview

RASSF1A (Ras association domain family 1 isoform A) is a recently discovered tumor suppressor protein located in the 3p21.3 region of the human genome whose inactivation is implicated in the development of many human cancers.[90] The most common contributor to loss or reduction of RASSF1A function is transcriptional silencing of the gene by inappropriate promoter specific methylation.[6, 91] If the inactivation of RASSF1A contributes to the development of the transformed phenotype, then one might expect that re-introduction of RASSF1A into RASSF1A negative cells would impair tumorigenicity. Indeed, this is the case. Re-expression of the gene in RASSF1A-negative cancer cells results in reduced colony formation in soft agar and reduced tumorigenicity in nude mice.[6, 91-93] Two groups have independently knocked out the RASSF1A gene in mice.[94, 95] These animals do not have an overt

phenotype. They demonstrate no altered cell cycle parameters or increased sensitivity to DNA-damaging agents and show no signs of gross genomic instability.[94, 95] On the other hand, they develop tumours in response to chemical carcinogens and spontaneous tumors by 18 months of age especially in the breast, lungs, gastrointestinal tract and the immune systems (especially B cell related lymphomas).[94, 95] Thus, RASSF1A is a tumor suppressor gene that is frequently inactivated in human cancers.

The RASSF1 locus contains two major splice variants (A and C) that arise by multiple promoter usage and alternative splicing. The longer isoform, RASSF1A, consists of 340 amino acids and a unique 119 amino acid amino (N)-terminal region, encoded by exon 1Aα (Fig. 1.4). RASSF1A gene silencing results from methylation of the promoter for exon 1Aα without epigenetic loss of the other isoforms of RASSF1. For example, RASSF1A methylation was reported to be observed in, 79% in small cell lung carcinoma patients,[96] 69% of cholangocarcinoma,[97] 62% of breast carcinoma patients,[98] and 52% of esophageal carcinoma patients[99] to mention a few. In addition to gene silencing, numerous polymorphisms have been identified within RASSF1A in some cancer patients that map to important functional domains.[100] Some of these polymorphisms have been identified in breast cancer, Wilm's tumour and nasopharngeal cancer patients. Nine other genes have been characterized, related to the RASSF1 locus, but with different chromosomal locations (Fig. 1.5).[101-103] Several have been shown to be downregulated in cancer (such as RASSF2, RASSF4, and RASSF6)[103, 104] and one maybe involved in modulating NFκB (RASSF6).[103] All RASSF proteins contain an RBD, but direct association with K-Ras has been only observed for RASSF2, RASSF4, and RASSF5/Nore1A.[105-107]

1.4.2 RASSF Primary Schematic Structure

The RASSF proteins contain several distinct domains that are depicted for each member in (Figs. 1.3 and 1.4). Some have been investigated and demonstrated to function as described. The Ras-association (RA) domain is a characteristic feature of Ras-effectors and Ras-related-GTPases.[108] All RASSF family members have the RA domain that can possibly associate with the Ras family of GTPases to influence cell homeostasis.[6] RASSF2, RASSF4, and RASSF5/Nore1A are the only RASSF proteins that can be observed to associate with K-Ras.[105-107] The C1 domain was named after its high homology with a cysteine-rich diacylglycerol/phorbol ester (DAG)-binding domain that is also known as protein kinase C conserved region 1 (C1). Its central C1 zinc finger[109] is characteristic for the domain and RASSF1A was shown to associate with the TNF-R1 or TRAIL-R1 (TNF-related apoptosis induced ligand) death receptors via its C1 domain (Fig 1.4).[110] The ATM (ataxia telangiectasia mutated) domain corresponds to a putative ATM-kinase phosphorylation site (Fig. 1.4). It was shown, that this peptide becomes phosphorylated by ATM at least *in vitro*.[111] The ATM kinase is of central importance for the regulation of cell cycle checkpoints that lead to DNA damage repair and apoptosis.[112] However, a functional relevance of this ATM domain has not been confirmed *in vivo* yet. The SARAH domain is a protein interacting domain for the Salvador/RASSF1/Hpo pathway that associates with the pro-apoptotic kinase, MST1 (Mammalian STE20-like kinase 1). This domain is characterized by its length of 50 amino acids and its distal C-terminal position which functions to promote heteromeric as well as homomeric interactions,[113] such as association of RASSF1A/RASSF5.[114-116] Ortiz-Vega et al. reported that recombinant RASSF1C exhibits a much weaker ability to homodimerize or heterodimerize with RASSF5 and RASSF1A[114] and thus may not interfere or compensate for RASSF1A function.

Regarding RASSF2 it was shown to associate with RASSF3 and RASSF5[117] and RASSF5 with RASSF1A through their nonhomologous amino-terminal segments.[114]

1.4.3 Biological functions of RASSF1A

1.4.3.1 Microtubule stability

The microtubule network functions as a cell scaffold spanning the cytoplasm and consisting of rigid but adjustable tubulin polymers. The network determines cell shape, takes part in cell motility, provides "tracks" for transport processes, functions as a scaffold for protein–protein interaction and compartmentalizes the cell. Furthermore, it is indispensable for correct sister chromatid separation during mitosis. During interphase, microtubules exist in the form of a network radiating from the MTOC (microtubule organizing center). During mitosis it reorganizes into two spindle networks radiating from two centrosomes. A correct chromatid separation is directly dependent on a functioning microtubule network.[118-120] It was demonstrated that RASSF1A co-localizes with the microtubule network during interphase and is found at the spindles and centrosomes during mitosis.[121, 122] RASSF1A binds to both α- and γ- tubulin,[123] thereby stabilizing microtubules[121, 123-125] and regulating the mitotic progression. RASSF1A overexpression was shown to lead to an arrest at different stages the cell cycle: at metaphase,[121] G1,[126] G2/M,[127] G1 and G2/M[123] and at prometaphase.[122] In the absence of RASSF1A as found in the mouse embryonic fibroblasts from *Rassf1a*$^{-/-}$ mice, cells are more sensitive to nocodazole-induced depolymerization of microtubule (M-phase arresting agent) resulting in tubulin de-acetylation and destabilization.[121, 123] Destabilized tubulin results in inadequate formation of mitotic spindles, possible chromosome missegregation, inheritable aneuploidy and cancer.

RASSF1A was also reported to interact with MAP1B (microtubule-associated protein 1B) and C19ORF5 (chromosome 19 open reading frames 5), both microtubule-associated

proteins.[125, 128, 129] MAP1B is one of the major growth-associated and cytoskeletal proteins in neuronal and glial cells.[130] C19ORF5 is a hyperstabilized microtubule-specific binding protein of which accumulation causes mitochondrial aggregation and cell death.[131] Regarding C19ORF5, it was demonstrated that its knockdown led to mitotic abnormalities,[132] that it localizes to centrosomes and it was stated that C19ORF5 is required for the recruitment of RASSF1A to the spindle poles.[129, 132] Liu et al. reported that RASSF1A caused hyperstabilization of microtubules and the accumulation of C19ORF5 on them.[131] Therefore, it appears that the RASSF1A-C19ORF5 interaction may be an intriguing link between the microtubules, cell cycle control, and apoptosis. The disruption of this pathway may have a large effect on the process of tumorigenesis.

1.4.3.2 Cell death and apoptosis

Apoptosis or programmed cell death can be initiated by intrinsic as well as extrinsic signals, which ultimately leads to the destruction of the cell following a defined cascade. Two types of signalling pathways promote apoptosis by utilizing the mitochondria, the central organelle involved in cell death. The "intrinsic" pathway is activated by noxious agent such as DNA damage. On the other hand, specific death receptor (TNF-R1, TRAIL-R1) stimulate the "extrinsic" pathway.[45, 133, 134] Surface activation results in the formation of receptor complexes stimulating apoptosis by conveying signals to the mitochondria. Following mitochondrial perturbation the release of small apoptogenic factors (such as cytochrome c) proceeds from the mitochondrial matrix into the cytosol. Released cytochrome c [together with caspase 9 and apoptotic protease activating factor 1 (Apaf-1)] assemble into a multi-protein complex, the apoptosome, that activate downstream effector caspases (such as caspase 3);[135, 136] cleaves

several nuclear proteins (such as poly [ADP-ribose] polymerase or PARP); activates DNA endonucleases; and finally results in nuclear/cytoplasmic breakdown and death.[137] Besides maintenance of tissue homeostasis, apoptosis is also implicated in human diseases such as in cancer development, myocardial infarction, and some neurological diseases.[138-141] A promising strategy in cancer therapy is re-establishing the ability of tumor cells to undergo apoptosis through the function of RASSF tumor suppressors.[142, 143]

It was reported by Baksh et al. (2005) that RASSF1A is required for death receptor-induced BAX conformational change and apoptosis.[7] BAX is a proapoptotic protein involved in the permeabilization of the outer mitochondrial membrane leading to the release of cytochrome c and cell death. After receptor stimulation RASSF1A and the modulator of apoptosis-1 (MOAP-1; a BH3-like protein) are recruited to the membrane and form a complex with death receptors (Fig. 1.5). It has been now demonstrated that MOAP-1 was specifically required for RASSF1A association with TNF-R1 and that MOAP-1 residues important for TNF-R1 and (TRAIL-R1) association were distinct from MOAP-1 residues required for RASSF1A association.[110]

In addition, RASSF1A has been recently demonstrated to modulate the activation of the MST2 (Mammalian STE20-like kinase 2) pathway by controlling p73 transcriptional activity linked to PUMA expression (a key pro-apoptotic effector).[144, 145] It can associate with the pro-apoptotic kinases, MST1 and MST2, and function with K-Ras to promote apoptosis.[146-148] Therefore, RASSF1A is important elements of apoptosis and regulate the outcomes of death receptor stimulation. Failure to regulate this key apoptotic pathway results in an increased incidence of cancer.

1.4.3.3 Cell cycle regulation

A lot of studies examining the role of RASSF1A in the cell cycle established a role for RASSF1A at G1-S checkpoint. Shivakumar et al. suggested that RASSF1A negatively regulates accumulation of endogenous Cyclin D1 through a posttranscriptional mechanism leading to inhibition of the cell cycle progression.[149] It was reported that transfection of RASSF1A into A549 cells induces G1cell cycle arrest and down-regulates Cyclin D1 expression.[126] Deng et al. showed that RASSF1A overexpression in a gastric carcinoma cell line led to inhibition of cell growth with G1 arrest. Furthermore, they found that RASSF1A overexpression inhibited AP-1 activity. The Activator protein-1 (AP-1) is a transcription factor involved in cell proliferation, differentiation and apoptosis.[150] It was also reported that Cyclin D1, a target of AP-1, is down-regulated after ectopic RASSF1A expression. Therefore, it was presumed that RASSF1A induces a G1 cell cycle arrest in a gastric carcinoma cell line by down-regulating Cyclin D1 through inhibition of AP-1 activity.[151] Moreover, It was reported that RASSF1A, through interacting with CDC20 (an essential cell cycle regulator required for completion of mitosis) during early prometaphase, is able to inhibit the formation of the APC/C-CDC20 complex (anaphase-promoting complex/cyclosom-cell division cycle 20 homolog).[122, 152] The APC/C complex is part of the ubiquitin-conjugation-system, which marks proteins for the degradation in the proteasome. Through inhibition of this complex, Cyclin A and B do not become proteasomally degraded followed by mitotic arrest. Therefore, RASSF1A might control the timing of normal mitotic progression by regulating APC/C-CDC20 activity. On the other hand, Liu et al. and our lab have been unable to confirm the interaction of RASSF1A with Cdc20.[153] Therefore the role of Cdc20 and APC in RASSF1A mediated cell cycle control needs further investigation.

1.4.4 Other RASSF Family Members

RASSF2: RASSF2 gene, which is located on chromosome 20 (locus 20p12.1), is being transcribed into two different isoforms (Fig. 4.1). Isoform A and C encode the same protein containing the SARAH domain as well as the RA domain that shows 28% identity to that of RASSF1A and 31% identity to that of RASSF5. RASSF2 however lacks the cysteine-rich domain of RASSF1A and RASSF5.[104] Akino et al. reported that primary colorectal cancers, which showed KRAS or BRAF mutations, also frequently showed RASSF2 methylation, and that inactivation of RASSF2 enhanced KRAS-induced oncogenic transformation. RASSF2A exhibits several tumor suppressor properties, like inhibition of cell growth and induction of apoptosis.[104, 154] In addition, patients with a methylated RASSF2A promoter presented a higher frequency of lymph node metastasis.[154]

RASSF3: The RASSF3 gene, which is located on chromosome 12 (locus 12q14.2), contains a RA domain and a SARAH domain. RASSF3 shares almost 60% homology, at the amino acid level, with RASSF1 (Fig. 4.1).[155] Its transcript is present in all tested normal tissues and tumor cell lines and no inactivating mutations in the coding region of RASSF3 in lung and breast tumors were found.[155] Overall only few data exist on RASSF3 and up to date no promoter methylation was detected in the few tumors studied.[117, 156]

RASSF4: The RASSF4 gene is located on chromosome 10q11.21. RASSF4 harbors both a SARAH and a RA domain (Fig. 4.1) and has 25% homology to RASSF1A and 60% identity with RASSF2.[157] RASSF4 is transcribed from a CpG island region and frequently downregulated by promoter methylation in human tumor cells and in several cancer cell lines, but broadly expressed in normal tissue.[157] RASSF4 shows tumor suppressor properties as indicated by growth inhibition and induction of apoptosis in human cancer cell lines.[157]

RASSF5: RASSF5, often called NORE1 (Novel Ras Effector 1), was the first member of the RASSF family to become characterized [158]. RASSF5 is up to 60% homologous to RASSF1 and the RASSF5 gene is localized at 1q32.1 (Fig. 4.1).[155] In renal collecting duct carcinoma the same region was earlier reported to be affected by Loss of heterozygosity (LOH) [loss of function of one allele of a gene in which the other allele was already inactivated],[159] whereas others rather found an amplification of the locus 1q32.[160-164] RASSF5 exists in at least three isoforms, as a result of alternative splicing and differential promoter usage; termed RASSF5A /NORE1A, RASSF5B/NORE1B/RAPL (regulator of cell adhesion and polarization enriched in lymphoid tissues) and RASSF5C. RASSF5A and RASSF5C are transcribed from separate CpG islands.[155] The domain structure of these two isoforms shows a RA domain as well as a SARAH domain, whereas the B isoform misses the SARAH domain. It has been reported that RASSF5/NORE1A can form heterodimers with RASSF1A. RASSF5A and RASSF5C were shown to be expressed in most normal tissues, but are down-regulated in various tumor cell lines though not in all studied.[107, 155, 165, 166] RASSF5B/RAPL is a smaller splice of RASSF5. RASSF5B/RAPL deficient mice have defect in B ant T cell trafficking to the lymph nodes.[167] Therefore, this protein regulates lymphocyte adhesion and also been implicated as a tumor suppressor.

RASSF6: The RASSF6 gene, which is located on chromosome 4q13.3, is predicted to be transcribed into two transcripts (Fig. 1.4). RASSF6 contains a RA as well as a SARAH domain.[168, 169] The RASSF6 transcript could be detected in several tumor cell lines, but was often reduced in primary tumors.[103, 169] RASSF6 was able to inhibit the growth and promote apoptosis in specific tumor cell lines.[103, 169] Taken together, the existing data suggest that RASSF6 may play a role in tumorigenesis. In addition to that, RASSF6 has been implicated in determining

susceptibility to infection by the respiratory syncytial virus (RSV).[168] RSV infection activates the eukaryotic NFκB pathway and this activation may play a vital role in the inflammatory response to infection. Moreover, RASSF6 expression inhibits the basal levels of NFκB activity in a lung epithelial cell line, suggesting that defects in RASSF6 may facilitate viral NFκB activation.[103]

RASSF7, RASSF8, RASSF9 and RASSF10: Only recently, four new members joined the Ras-Association Domain Family and were termed RASSF7, RASSF8, RASSF9 and RASSF10. Sherwood et al. reported that the RASSF members 7 to 10 represent the evolutionarily conserved so-called N-terminal RASSF group due to the N-terminal localization of their RA domains.[170] However these 4 members lack the SARAH domain otherwise present in RASSFs.[170] RASSF7 is located at locus 11p15.5 and RASSF8 at 12p12.3. RASSF9 is located at 12q21.31 and RASSF10 at 11p15.2. Interestingly only RASSF7, RASSF8 and RASSF10 are transcribed from CpG island regions. The precise roles of RASSF7, RASSF8, RASSF9 and RASSF10 in tumorigenesis remain to be unclear.

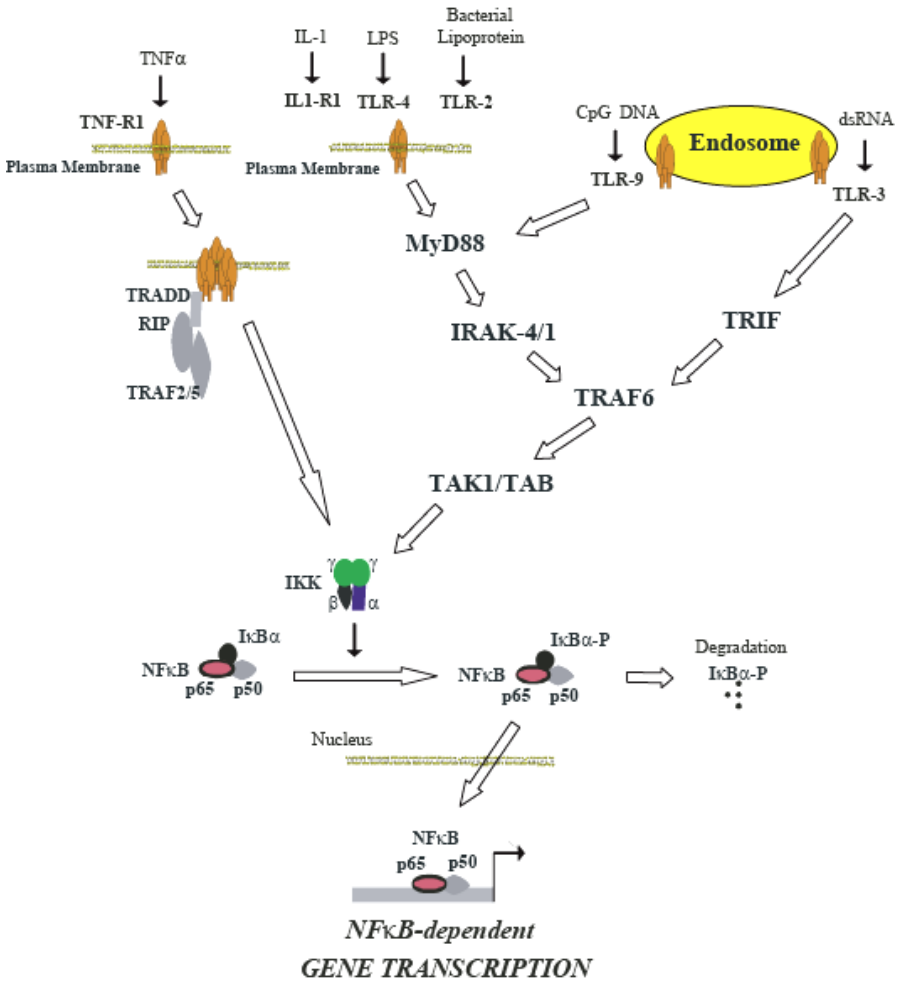

Figure 1.1: Models for NFκB Pathway. TNFα stimulation results in the recruitment of protein complexes to activate IKK (IκBα kinase), IκBα dependent phosphorylation (P) and subsequent degradation as shown. The p65/p50 subunits of NFκB are then free to translocate to the nucleus to turn on gene transcription. Interleukin 1 receptor R1 (IL1-R1) and the family of TOLL receptors (TLRs) can also turn on NFκB dependent gene transcription following stimulation with their respective ligands as indicated. Specific adapters convey these activation signals to IKK. These include MyD88, TAK1/TAB, TRAF6 and TRIF.

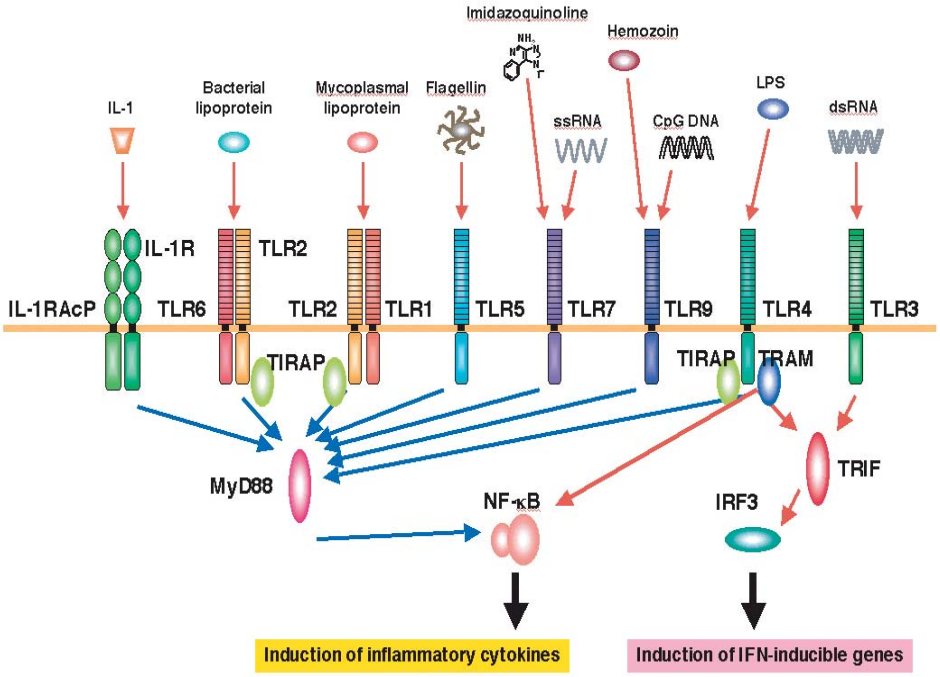

Figure 1.2: The TLR Pathway. Multiple TLRs exist to respond to the invasion of microbial pathogens and components derived from these pathogens. Schematic of TLRs are shown with their respective stimulants. Signaling molecules downstream of TLR activation are indicated that will ultimately lead to the activation of the NFκB transcription factor and induction of pro-inflammatory cytokines. Adapted from Cell Signaling Technology.

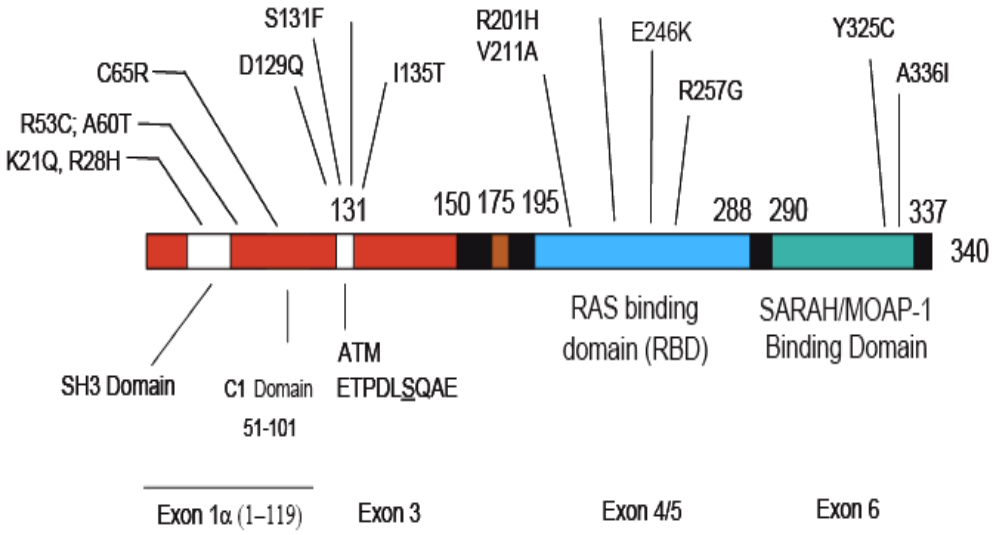

Figure 1.3: RASSF1A schematic and location of polymorphisms identified in some cancer patients. The C1 domain associates with membrane lipids and contains a zinc finger binding motif for protein-protein associations with death receptors. The ATM site is specficially phosphorylated by the DNA damage control kinase, ATM (ataxia telangeictasia mutated). The RAS association/binding domain (RBD) functions to associate with the Ras family of oncogenes (such as K-Ras and H-Ras). Lastly, the SARAH domain is a protein interaction domain for the Salvador/RASSF1/Hpo pathway that associates with the pro-apoptotic kinase, MST1. Several polymorphisms to RASSF1A have been identified as indicated in this figure. Approximate positions of exons are also indicated and a C65R denotes a cysteine to arginine change at position 65 of the amino acid sequence.

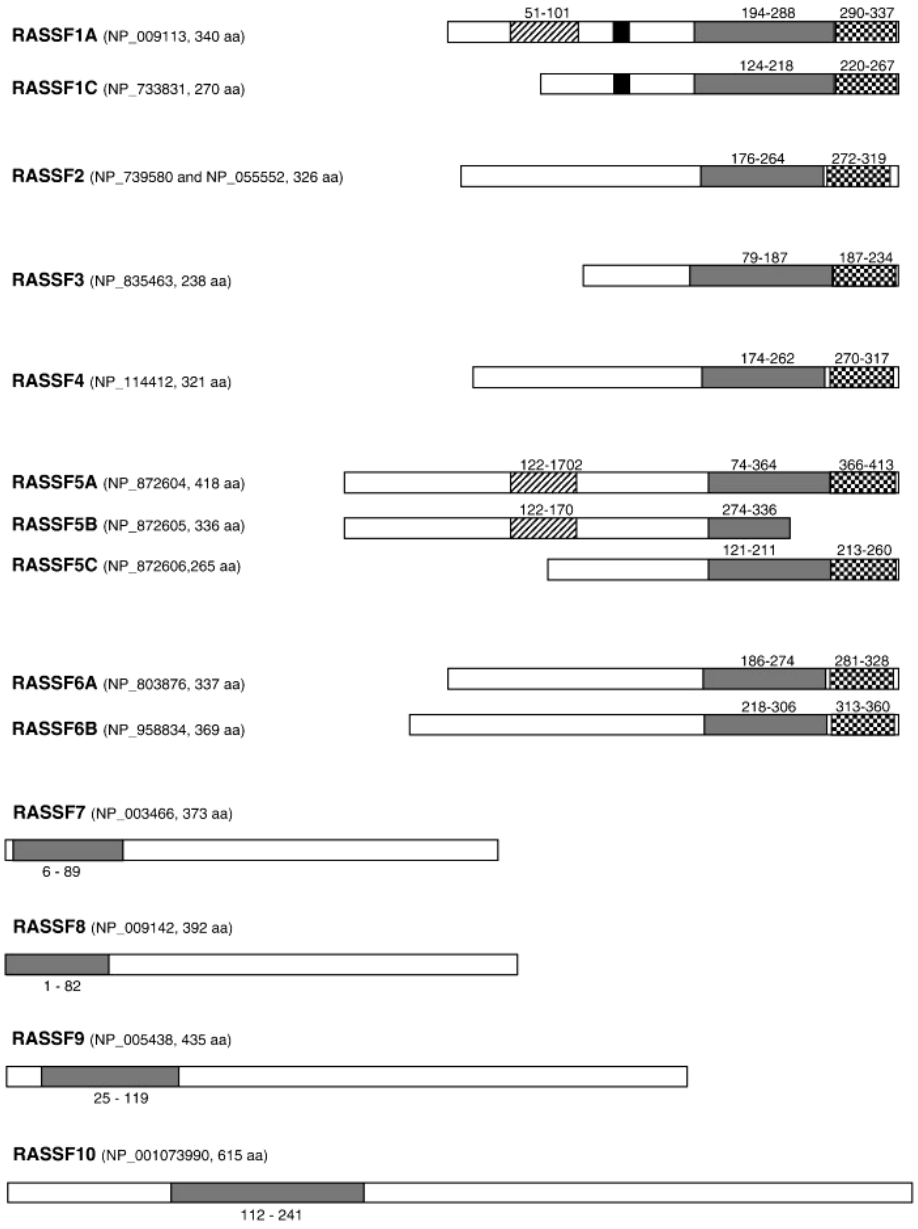

Figure 1.4: Schematic diagram showing RASSF family members. Characteristic domains are the protein kinase C conserved region (C1; striped), the putative ATM-kinase phosphorylation site (black), Ras-association (RalGDS/AF-6) domain (RA; grey) and the Sav–RASSF–Hpo interaction site (SARAH; checkered). Adapted from Richter et al. 2009.

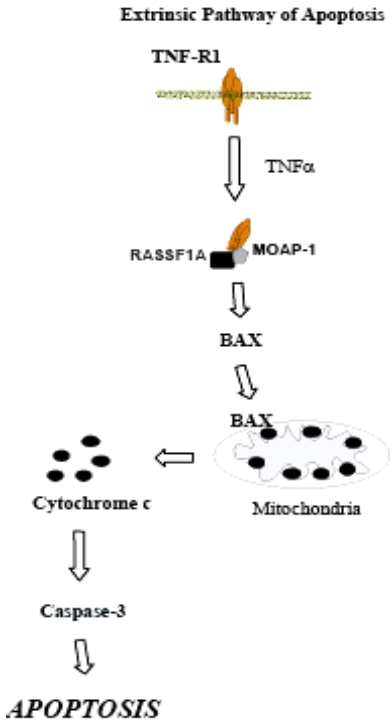

Figure 1.5: RASSF1A-Apoptotic Signaling Pathway. TNFα stimulation results in the formation of RASSF1A/MOAP-1/TNF-R1 complex. This association results in Bax conformational change and insertion into the mitochondrial membrane. The insertion of Bax, together with mitochondrial Bid and Bak, results in mitochondrial membrane perturbation, release of cytochrome c, and activation of the effector caspase, caspase-3. These events lead to the cleavage of key substrates (such as PARP and lamins), followed by DNA and cytoplasmic breakdown and eventual cell death (apoptosis).

Chapter 2

Materials and Methods

2.1 Materials

All chemicals were used according to the manufacturer's specifications as well as in accordance with the protocols set out by the Environmental Health and Safety of the University of Alberta and work Hazardous Materials Information System (WHMIS).

2.1.1 Chemicals, Reagents and other Materials

Acrylamide	Invitrogen
Ammonium persulfate (APS)	BioRad
β-mercaptoethanol	BioShop
Bromophenol blue	Sigma
Cyclohexamide	Calbiochem
DMEM medium	Fisher Scientific
Dextran sulphate (DSS)	MP Biomedical
EDTA	EMD
Ethanol	Commercial Alcohols
Glycine	Fisher Scientific
Hydrochloric acid	Caledon
Igepal	Sigma
Lipopolysaccaride (LPS)	Sigma
MYCOY'S 5A medium	Fisher Scientific
PVDF membrane	Millipore
PEI	Polysciences, USA
RPMI medium	Fisher Scientific

Sodium dodecyle sulphate (SDS)	BioRad
Tris	Fisher Scientific
Trypsin	Fisher Scientific
Whatman Chromatography paper	Fisher Scientific
Nocodazole	Calbiochem
Hydroxyurea	Calbiochem
Taxol	Calbiochem
TNF-α	Peprotech
TRAIL	Peprotech
Anti-Annexin-V Alexa Fluor	Molecular Probes
Protein A Sepharose	GE Healthcare
Protein G Sepharose	GE Healthcare

2.1.2 Antibodies

Primary Antibodies:

Mouse anti-HA	In house produced
Mouse anti-Myc	In house produced
Mouse anti-TNF-R1	Santa Cruz sc-8436
Mouse anti-GFP	Santa Cruz sc-9996
Mouse anti-α-tubulin	Santa Cruz, sc-8035
Mouse anti-α-tubulin	Sigma, T3559
Mouse anti-acetylated α-tubulin	Sigma T7451
Rabbit anti-TLR3	Santa Cruz sc-10740

Rabbit anti-TLR4	Santa Cruz sc- 10741
Rabbit ant-MyD88	Santa Cruz sc-11356
Rabbit anti-TNF-R1	Santa Cruz sc-7895
Rabbit anti-14-3-3	Santa Cruz sc-629
Rabbit anti-PARP	Cell Signaling, #9542
Rabbit anti-γ-tubulin	Santa Cruz sc-10732
Rabbit anti-β-tubulin	Sigma T5201
Goat anti-TRAIL R1	R&D system, AF-347

Secondary Antibodies:

Anti-mouse IgG Horseradish Peroxidase-Linked Whole antibody	GE Heathcare UK
Anti-Rabbit IgG Horseradish Peroxidase-Linked Whole antibody	GE Heathcare UK

2.1.3 Buffers and other solutions

4x Separating Buffer: 1.5M Tris, pH 8.7 and 0.4% SDS

4x Stacking buffer: 0.5M Tris, pH 6.8 and 0.4% SDS

4x SDS-Page loading Buffer: (for 50mL: 13 ml Glycerol, 2.5g SDS, 8.7mL of 1M Tris/HCL pH 6.8 and 10mg Bromophenol blue)

10x SDS Running Buffer: (for 1L: 30.2g Tris, 144g Glycine, 10g SDS)

RIPA Buffer: (for 500mL: 1mL 1M EDTA, 25mL Tris/HCL pH 8, 15mL 5M NaCl, 5mL Igepal, 2.5g Sodium deoxycholate and 2.5 ml 20% SDS)

SB Lysis Buffer: 50 mM HEPES (pH 7.5), 150 mM NaCl, 1 mM $MgCl_2$, 1.5 mM EDTA, 0.5% Triton X-100, 20 mM β-glycerolphosphate, 100 mM NaF, 0.1 mM PMSF.

1x Transfer Buffer: (for 4L: 12g Tris, 57.6g Glycine, 800mL Methanol and then bring to volume with water)

2.2 Methods

2.2.1 Cell culture, Transfection, Lysis and Immunoprecipitation

HCT116 were cultured in DMEM media containing 10% bovine growth serum and kept at 37°C in an incubator containing 95% oxygen and 5% CO_2. Fourty percent confluent cells were used for transfection in a 6 well dish. The cells were transfected using polyethyleneimine (PEI). PEI transfections were carried out by mixing PEI/DNA in a ratio of 4 ul PEI/1 µg DNA in 400 µl of serum. The mixture was allowed to incubate for 15 minutes. While incubating, cells were washed 3 times with serum free media and 2 ml of complete media added after the washes to each well. The PEI/DNA mixture was added to the cells, mixed gently and grown overnight. Media was changed the following day with 1.5 ml of complete media. Different stimulus was added the day after according to the experiment followed by cell lysis for further analysis. Cells were then transferred to 1.5 ml eppendorf tube and washed 2 times with 1X PBS to ensure that no further DMEM media containing bovine growth serum was still present which may interfere with later steps for detection of proteins by western bloat. Following cells washing, 1000 µl of RIPA lysis buffer was added. RIPA buffer containing cells are then vortexed at high speed followed by incubation at 4°C for 15 minutes to ensure complete lysis. Immunoprecipitaion are carried out by adding the of either rabbit antiTLR4 antibody, rabbit anti TLR3 antibody or rabbit anti MyD88 antibody which then incubated overnight. After overnight incubation, samples were added to 50% slurry of either protein A or protein G Sepharose affinity beads for 2 hours

followed by two washes with 1XPBS and bound proteins resolved by SDS-PAGE. For all cell lysate (WCL) immunobloats, ~ 100 µg of protein/lane were used.

2.2.2 Western Blotting

Proteins carried out by SDS-PAGE separation were transferred to PVDF membrane (MilliPore) by 2 hour in a transfer apparatus. Following a successful transfer, the membrane was blocked with 10% skim milk for 30 minutes at room temperature. The membrane was then incubated with the primary antibody (diluted in 2% milk) overnight at 4°C on a shaker. Subsequent washing of the membrane with 3X with 1XTBS-T was needed to get rid from any unbound primary antibody. This wash is followed by the incubation of the membrane with the secondary antibody (diluted in 2% milk) for 2 hours at room temperature on a shaker. Following the incubation, the membrane was washed again 3X using 1XTBS-T for 5 minutes. The membrane is then incubated with the Enhanced chemiluminescence (ECL) detection reagent (GE Heathcare, UK) for 2 minutes followed by developing using X ray films.

2.2.3 Enzyme-linked immunosorbent assay (ELISA)

ELISA Kit was purchased from Fisher Scientific Company. Standards (serial dilution) were made according to the manufacturer's manual. Culture supernatants and serum were diluted using 1:5 or 1:10 dilution using the appropriate diluent. 50 µl of the standards or the samples were added to the each well. The plate is then covered and incubated for 1-2 hours at room temperature. Following incubation, the plate was washed 3 times using 1X washing buffer. 50 µl of biotinylated antibody reagent was added to each well followed by incubation for 1 hour at room temperature. 100 µl of the prepared strepavidin horseradish Peroxidase solution was then

added to each well followed by incubation at room temperature for 30 minutes. The plate was then washed 3 times followed by adding 100µl of the premixed tetramethylbenzidine (TMB) substrate to each well which would yield blue colour when oxidized with hydrogen peroxide (catalyzed by HRP). Finally, the plate was developed in the dark room at room temperature for 30 minutes followed by adding 100 µl of the stop solution to stop the reaction. The absorbance was then measured on a plate reader at 450 nm.

2.2.4 Cell death assays

Human TNFα or TRAIL were added together with 10 µg/ml cyclohexamide (CHX) for the indicated times and Annexin V staining analysis was carried out as previously described. All apoptosis assays were performed at least six times. Data for all immunofluorescence and apoptosis assays were evaluated by Student's t-test (two-tailed), unless otherwise stated.

2.2.5 Surface staining of TNF-R1

Stable cells containing either HA-RASSF1A WT or δMT mutant were generated and stimulated with TNFα. Surface TNF-R1 expression was assessed using antibodies against its extracellular domain (mouse anti-TNF-R1, sc-8436 [Santa Cruz Biotechnology]). Cells were harvested by scraping into 1 X PBS, washed once with 1 X PBS, followed by the addition of primary antibodies (100 µl solution of 3 µg/ml antibody in 1 X PBS + 3 % FBS) for 30 min on ice. Cells were then washed twice with 1 X PBS, followed by the addition of rabbit anti-mouse Alexa 546 secondary antibody (Molecular Probes, 1:200 in same solution as primary antibody) for 30 min on ice. Staining with secondary antibodies alone was used as a negative control. After secondary antibody staining, cells were washed twice with 1 X PBS and then analyzed by FACS

analysis to determine the amount of TNF-R1 remaining on the surface following TNFα stimulation. All experiments were carried out at least four times using single clones and pools of the stable cell lines with similar results.

2.2.6 Cell cycle arrest and release

Cells were treated with either 2 μM nocodazole (for M-phase arrest) or 750 μM hydroxyurea (for S-phase arrest) overnight followed by a release from arrest by washing out either nocodazole or hydroxyurea by changing to media without these drugs. Cell cycle phases were confirmed by FACS (fluorescence activated cell sorting) analysis using a FASC Caliber (Beckman/Coulter).

2.2.7 Animal experiments

Mice were used in our experiment. All mice were 10-12 weeks old, males with the strain background of C57/BL6. Four different genotypes were used, *Rassf1a*$^{+/+}$, *Rassf1a*$^{-/-}$, *Nod2*$^{-/-}$, *Rassf1a*$^{-/-}$*Nod2*$^{-/-}$. All genotypes were confirmed by PCR using genomic DNA from ear or tail biopsies. Genomic DNA was obtained by adding 300 μl of DirectPCR lysis reagent containing freshly prepared 0.4 mg/ml Proteinase K in eppendorf tube to 0.5 cm of tail or ear of selected mouse. This was followed by incubation at 55°C for 6 hrs to overnight with shaking until no tissue clumps are observed. Incubation for another 45 minutes at 85°C was then done. Following the incubation the eppendorf tube containing the samples was spinned down at maximum speed to precipitate the hairs. Supernatant was then stored at - 20°C for further PCR analysis. For RASSF1A PCR reaction, the following primers were used; UMIOAI Primer: 5'-TTGTGCCGTGCCCCGCCCA, LMIIAA Primer: 5'-TGACCAGCCCTCCACTGCCGC, and Neo48U Primer: 5'GGGCCAGCTCATTC-CTCCCAC. The PCR condition was set as the

following; 95°C for 1 minute, 95°C for 4 minutes, 63°C for 1 minutes, 72°C for 1 minute, (95°C for 4 minutes, 63°C for 1 minutes, 72°C for 1 minute) for 2 cycles, 95°C for 1 minute, 63°C for 1 minute, 72°C for 2 minutes, (95°C for 1 minute, 63°C for 1 minute, 72°C for 2 minutes) for 33 cycles, 72°C for 5 minutes and then finally 4°C forever. The multiplex PCR produces a 520-bp band for the wild-type allele and a 380-bp band for the knockout allele and both for heterozygous mice (Fig. 2.1). For NOD2 PCR reaction, the following primers were used; NOD2, 4112 Primer: 5'- ACA gAg ATg CCg ACA CCA TAC Tg, NOD2, 4113 Primer: 5'- Tgg AgA Agg TTg AAg AgC AgA GTC, NOD2, 4114 Primer: 5'- TgA CTg Tgg CTA ATg TCC TTT gTg, NOD2,4115 Primer: 5'- TTC TAT CgC CTT CTT gAC gAg TTC. The PCR condition was set as the following; 94°C for 3 minutes, 94°C for 30 seconds, 66°C for 1 minutes, 72°C for 1 minute, 72°C for 2 minutes, (94°C for 30 seconds, 66°C for 1 minutes, 72°C for 1 minute, 72°C for 2 minutes) for 35 cycles and then 10°C forever. The multiplex PCR produces a 370-bp band for the wild-type allele and a 1000-bp band for the knockout allele and both for heterozygous mice (fig. 2.1).

2.2.7.1 Acute sustained Dextran sulphate (DSS) treatment

Selected mice were separated in individual cages one day before starting the experiment. The following day, normal water was replaced with 3% DSS solution. The mice were exposed to DSS solution in the drinking water for 12-16 days. For all DSS experiment, mice were monitored carefully for signs of colitis including weight loss, piloerction, bloating, tremors and rectal bleeding.

2.2.7.2 Acute unsustained Dextran Sulphate (DSS) treatment

This experiment was carried out as above but these mice were only exposed to 3% DSS solution for 7 days followed by the addition of regular water for another 8 days. These mice were monitored for 15 days.

2.2.7.3 Chronic Dextran Sulphate (DSS) treatment

Selected mice were separated in individual cages one day before starting the experiment. The following day, normal water was replaced with 3% DSS solution. The mice were exposed to DSS solution in the drinking water for 5 days followed by normal water for 10 days followed by DSS solution for 3 days followed by normal water for 7 days then DSS solution until the end of experiment.

2.2.7.4 Lipopolysaccaride (LPS) injection

Selected mice were injected intraperitoneal (IP) with 15 µg/g body weight of LPS (a stimulus of TLR4 function; reagent obtained from sigma, E. coli strain 0111:B4). Mice were monitored for signs of infection including pussy eyes, piloerection and bloating. Survival was followed over 25 days. Alternatively, another group of mice were injected with10 µg/g body weight of LPS and blood harvested by cardiac puncture after 24 hours for cytokine production.

2.2.7.5 Cardiac puncture

Blood was collected from treated mice by doing cardiac puncture. Mice were anesthetized using ether. Twenty five gauge needles were used for blood drainage from the heart. Mice were then sacrificed by CO_2 asphyxiation. Blood was collected in 1.5 ml eppendorf tubes and left to sit for

2 hour until coagulation. After blood coagulation, blood was spinned down at 10.000 rpm for 10 minutes. Plasma were then collected and stored in -80°C for cytokine analysis.

2.2.7.6 Macrophages Isolation and Culture

Selected mice were sacrificed by CO_2 asphyxiation. Skin over the femur was cut and removed from hip to the knee joint. The femur is then cut one end from the hip joint and the other from the knee. Twenty five gauge needle was then used to flush the bone marrow from the femur using L Cell Conditioned Media (LCM). Media containing cells were then place in a 15 ml tube and then centrifuged in a tabletop Beckman centrifuge for 5 minutes at 1000 rpm. The pellet were then resuspended in growth media (DMEM with 10% FCS and 1% penicillin-Streptomycin) and plated onto 10 cm tissue culture plastic dish for 2 days to remove unwanted cells and stroma which will adhere to the bottom of the dish. After 2 days, the suspended cells (macrophages) were plated in 10 cm petri plastic dish until they are confluent. Macrophages were then ready for stimulation using different reagents.

2.2.7.7 Splenocyte isolation and culture

Selected mice were sacrificed by CO_2 asphyxiation. Spleens were crushed between 2 frosted glass slides until suspension of cells were made. Suspension cells were then put in a 15 ml tubes for spinning down at 1000 rpm for 5 minutes. After spinning, the supernatant was removed and 5 ml of Red cell lysis buffer was added to remove red blood cells. Cells were then spinned down for 5 minutes at 1000 rpm. The supernatant was removed and the cells were re-suspended in 10 ml RPMI media containing 10% FCS and 1% Penicillin-Streptomycin. The cells were then allowed to grow in T-75 flask for further stimulation.

2.2.7.8 Tissue histology

Tissue histology of the descending colon was carried out. Both transverse and longitudinal section of the treated mice was done followed by Hematoxylin and Eosin staining using the animal histology core facility of the Alberta Diabetes Institute.

2.2.7.9 Subcutaneous injection of tumor cells

HCT116 colon cancer cells transiently transfected with the indicated expression constructs. After 48 h, cells were trypsinized and spun down at 1000 rpm for 5 min and resuspended in a 1:1 mix of media:matrigel (BD #354234, 10 mg/ml of LDEV-free matrix). Two hundred microlitres (containing ~ 3 X 10^6 cells) of this mixture was subcutaneously injected into the right and left flanks of athymic nude mice (Taconic Laboratories #NCRNU-M, CrTac:NCr-FoxN1Nu) in order to determine tumor promoting potential of the RASSF1A wild type and mutants. Mice were monitored weekly until tumors appear, and then twice a week thereafter. Once tumors exceed 20 mm diameter, mice were euthanized and tumors excised and measured.

2.2.7.10 NFκB electromobility shift assay (EMSA)

Briefly, duplex DNA specific for the NFκB binding site (underlined in TCAGAGGGGACTTTCC-GAGAGG) was end-labeled with [γ-^{32}P]ATP by using T4 polynucleotide kinase, purified using a G-50 sephadex column (Roche), and allowed to associate with nuclear extracts containing NFκB for 30 min at room temperature. DNA/protein complexes were then separated by non-denaturing gel electrophoresis, dried onto Whatman filter paper and autoradiographed. Nuclear extracts were prepared using hypotonic lysis followed by high salt extraction. Briefly, cell pellets from untreated or treated cells were dissolved in 200 μl of buffer

A/20 µl of cell pellet and incubated on ice for 20 min to lysis the cells with occasionally flicking of the tubes to aid in lysis. The suspension was spun down at 2500 rpm for 5 min and the supernatant removed as the cytoplasmic fraction. The pellet (nuclear fraction) was washed in buffer A without NP-40 once and then spun down as before. The pellet was resuspended in about 100µl volume of Buffer B/20 µl of original cell pellet and incubated on ice for 20 min with occasional flicking of the tube to aid in nuclear lysis. Samples were then spun down at 10 000 rpm for 10 min to pellet membranal fractions and the supernatant kept as the nuclear fraction. The nuclear fraction was then diluted in buffer C to dilute the salt used in the extraction. Samples can then be kept at – 80˚C until needed. For mouse tissues, cut tissues into short fragments and homogenize tissue in buffer A, ~ 20 mg tissue/1 ml if CE buffer. Spin down at 850 X g (about 1000 rpm) for 5 min. The supernant is kept as the cytoplasmic fraction and the pellet is the nuclear fraction that will be processed as described above. Buffer A (500 µl of 1M Hepes pH 7.6, 3 ml of 1M KCl, 100 µl of 0.5 M EDTA, 50 µl of 1M DTT, 0.2 % NP-40, 2 µl of 0.1M PMSF; 0.5 µl of aprotinin to 50 ml); Buffer B (1 ml of 1M Tris pH 8, 4.2 ml of 5M NaCl, 75 µl of 1M $MgCl_2$, 20 µl of 0.5 M EDTA, 12.5 ml of 100% glycerol, 2 µl of 0.1M PMSF; 0.5 µl of aprotinin to 50 ml); Buffer C (20 mM Tris, pH 7.6, 10 mM $MgCl_2$, 0.2 mM EDTA, 0.5 mM DTT).

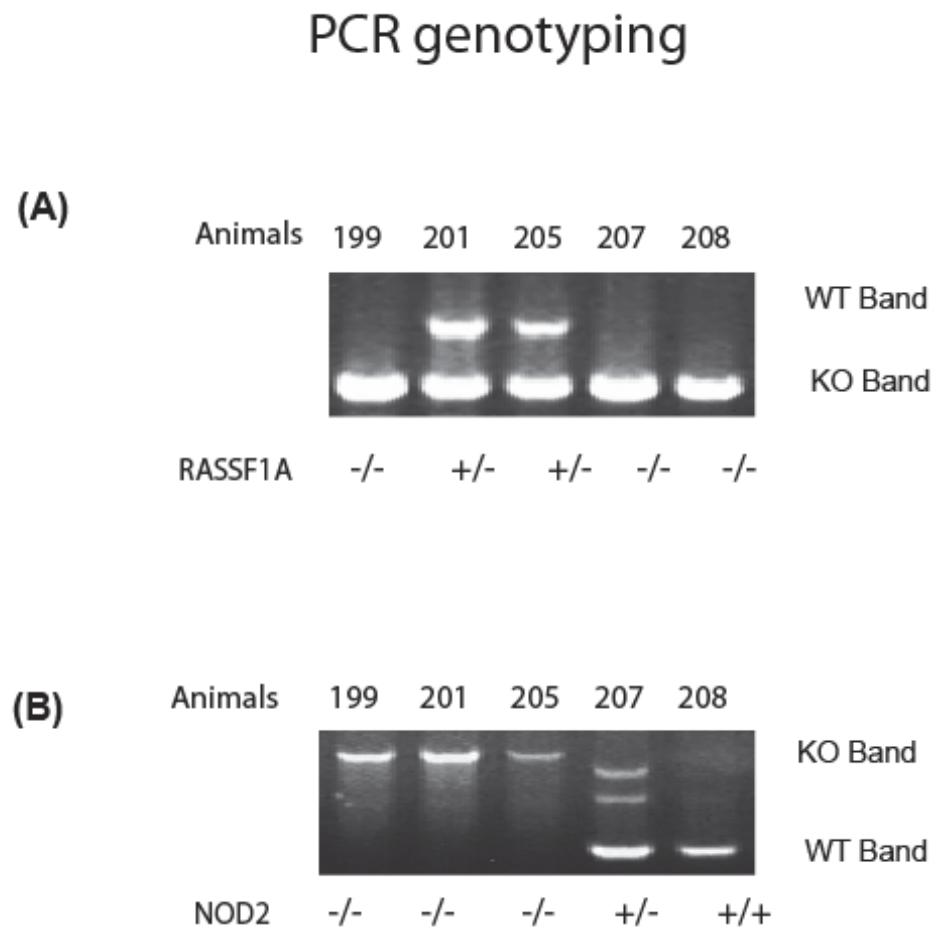

Figure 2.1: PCR genotyping of the indicated mice. (A) RASSF1A genotyping. The multiplex PCR produces a 520-bp band for the wild-type allele and a 380-bp band for the knockout allele and both for heterozygous mice. (B) NOD2 genotyping. The multiplex PCR produces a 370-bp band for the wild-type allele and a 1000-bp band for the knockout allele.

Chapter 3
RASSF1A and innate immunity

Inflammatory bowel disease has genetic linkages on several chromosomes including chromosome 1q32 (encoding for IL-10), 1p.31 (encoding the IL-23 receptor), chromosome 16q12 (encoding for the nucleotide-binding oligomerization domain-leucine-rich repeat protein 2 or NOD2), and uncharacterized linkages on 3p21 (the chromosomal location of RASSF1A). Some IBD genetic linkages have been characterized using mouse knockout models but they generally do not reflect the human disease.[22, 23, 171] RASSF1A can inhibit NFκB activity in HCT116 cells and we have observed associations of RASSF1A with TLR components (see chapter 5). These data would suggest that RASSF1A may negatively regulate NFκB and possibly NFκB-directed inflammation utilizing the TLR pathway. Therefore, we investigated the *in vivo* importance of RASSF1A in *Rassf1a*$^{-/-}$ mice. Currently, it is known that *Rassf1A*$^{-/-}$ mice do not have an overt phenotype. They demonstrate no altered cell cycle parameters or increased sensitivity to DNA-damaging agents and show no signs of gross genomic instability.[94, 95] They, however, develop tumours in response to chemical carcinogens[94] and spontaneous tumors by 18 months of age that are predominantly in the gastrointestinal tract and B cells (lymphomas). They also do not develop spontaneous colitis as far as 6 months post-birth (data not shown). We began to explore the importance of RASSF1A for inflammation using our *Rassf1a*$^{-/-}$ mice.

3.1 Survival of wild type and Rassf1a$^{-/-}$ *mice following LPS treatment*

Rassf1a$^{+/+}$ and *Rassf1a*$^{-/-}$ mice were injected intraperitoneally (IP) with 15 μg/g body weight of LPS (a stimulant of TLR4 function; reagent was obtained from Sigma, E. coli strain 0111:B4). Survival was followed over a course of 14 days and severity of disease was monitored by signs of piloerection, tremors, bloatedness, pussy eyes and slow movement. The majority of the *Rassf1A*$^{-/-}$ mice became sick showing the aforementioned signs within the first 48 h of IP

injection, whereas 75% of the wild type mice survived and showed no signs of disease (Fig. 3.1). These data suggest a role for RASSF1A as a survival element for LPS induced inflammation.

3.2 Cytokine Production after LPS treatment

We next investigated cytokine production in the peripheral blood of the treated mice to confirm what we observed in the survival curve. *Rassf1a*$^{+/+}$ and *Rassf1a*$^{-/-}$ mice were injected intraperitoneally (IP) with 10 μg/g body weight of LPS. Cytokine analysis after 24 hours revealed elevated production of NFκB regulated cytokines in *Rassf1A*$^{-/-}$ mice versus wild type mice (IL-6, IL-12, IL-10 and IFN-γ). There was also increased production of one chemokine, IL-8 (Fig.3.2). Together from data in fig. 3.1 and fig 3.2, these observations suggest that the loss of RASSF1A in the *Rassf1a*$^{-/-}$ mice resulted in an unregulated production of NFκB related cytokines. The elevated production of NFκB targeted cytokines most likely resulted in the reduced survival of *Rassf1a*$^{-/-}$ animals following LPS treatment. This would suggest a role for RASSF1A as a factor restricting the duration of NFκB activity and the inflammatory response.

In order to confirm our hypothesis that LPS-treated *Rassf1a*$^{-/-}$ mice have elevated levels of NFκB activity, we isolated nuclear extracts from bone marrow derived macrophages after LPS treatment and measured their NFκB DNA binding activity by EMSA analysis. Nuclear extracts from *Rassf1A*$^{-/-}$ mice revealed a much higher level of NFκB DNA binding activity when compared to the wild type animals (Fig. 3.1) confirming that NFκB activity was elevated in LPS-treated mice missing RASSF1A. The increased level of NFκB activity in the *Rassf1A*$^{-/-}$ mice is mostly likely the cause of the increased production of NFκB regulated cytokines and poor survival following LPS-treatment in the *Rassf1A*$^{-/-}$ mice.

3.3 Survival of wild type and Rassf1a$^{-/-}$ mice following Dextran Sulphate (DSS) treatment

3.3.1 Acute sustained Dextran Sulphate treatment

We had compelling results from the LPS experiments to suggest that RASSF1A may be an important modulator of inflammation. We then treated our wild type and *Rassf1a*$^{-/-}$ mice with 3% DSS in the drinking water, a chemical inducer of ulcerative colitis resulting from chemical irritation of the colonic mucosa. Mice develop symptoms that are identical to chronic colitis, such as (in increasing order of severity) piloerection, weight loss, bloatedness, tremors, rectal bleeding and slow movement. They were euthanized once rectal bleeding is severe (usually about 3 - 4 on a scale of 1 – 5 with 5 being the most severe). Similar to the LPS experiment, a significant proportion of the *Rassf1A*$^{-/-}$ mice because sick within 8 - 11 days of continuous DSS treatment, while about 40% of the wild type animals survived until day 18 during the experiment (Fig. 3.3.1).

3.3.2 Acute unsustained Dextran Sulphate (DSS) treatment

Wild type and *Rassf1a*$^{-/-}$ mice were treated with dextran sodium sulphate (DSS) in the drinking water for only 7 days followed by normal water for the rest of experiment. Survival was followed for 15 days for the same signs of colitis as above. The majority of the *Rassf1a*$^{-/-}$ mice became very sick whereas 100% of the wild type mice survived and showed no signs of disease (Fig. 3.3.2). Severity index at day 9 shows that *Rassf1a*$^{-/-}$ mice become rapidly sick showing severe signs of colitis (as mentioned before) when compared to the wild type animals. This supports our data on the survival of the *Rassf1a*$^{-/-}$ mice upon DSS treatment whereby majority of the *Rassf1a*$^{-/-}$ mice became sick and were not able to shut the inflammatory response (Fig. 3.3.2).

3.3.3 Chronic Dextran Sulphate (DSS) treatment

We then proceeded to investigate how wild type and *Rassf1a*$^{-/-}$ mice may behave during chronic DSS treatment, a situation that most likely may occur when human patients undergo short and repeated periods of inflammation. The outcome of these repeated episodes may depend upon how efficient one can fight against the inflammation. Chronic intermittent course of DSS in the drinking water was given to the wild type and *Rassf1a*$^{-/-}$ mice. DSS was given for 5 days followed by 10 day of normal water then 3% DSS was given for another 3 days followed by 7 days normal water then DSS was given until the end of the experiment. Survival was followed for 35 days for signs of colitis. More than 60% of the *Rassf1a*$^{-/-}$ mice became very sick whereas 100% of the wild type mice survived and showed no signs of disease (Fig. 3.3.3). Taken together our acute and chronic DSS treatments suggest a role for RASSF1A as a negative regulator of inflammation and the inability to shut down the inflammatory response.

3.4 Cytokine Production after DSS treatment

Cytokine analysis in the peripheral blood at day 9 of the experiment revealed a large amount IL-6, IL-12 and IL-10 cytokine production and elevated production of one chemokine (IL-8) in the DSS-treated *Rassf1a*$^{-/-}$ mice when comparison to wild type mice. However, we observed no difference in the production of IL-23 and IL-2 in the DSS-treated *Rassf1a*$^{-/-}$ mice when compared to DSS-treated wild type mice (Fig. 3.4). These data suggest that the loss of RASSF1A resulted in the uncontrolled production of cytokines and chemokines (all NFκB targeted genes). This would suggest a role for RASSF1A in the negative regulation of NFκB activity.

Similar to LPS treatment, we investigated the DNA binding activity of NFκB activity in nuclear extracts in bone marrow derived macrophages following 3% DSS treatment by EMSA. We observed a significant increase in the NFκB activity in bone marrow derived macrophages from *Rassf1A*$^{-/-}$ mice when compared to wild type mice (Fig. 3.3). The increased level of NFκB activity in the *Rassf1A*$^{-/-}$ mice is mostly likely the cause of the increased production of NFκB regulated cytokines and poor survival following DSS-treatment in the *Rassf1A*$^{-/-}$ mice in a similar manner to LPS-treated *Rassf1A*$^{-/-}$ mice. Taken together, these data would again suggest a role for RASSF1A as a factor restricting the duration of NFκB activity and the inflammatory response and most likely behaving as a negative modulator of NFκB activity.

3.5 Tissue histology after DSS treatment

Longitudinal section of the descending colon at day 9 revealed a severely disrupted colonic architecture in *Rassf1a*$^{-/-}$ mice following hematoxylin and eosin staining (H&E). H&E staining was used to nonspecifically stain the colonic tissue. Moreover, we observed massive infiltration of inflammatory cells (as represented by blue dots in Figure 3.6) in DSS treated *Rassf1a*$^{-/-}$ colonic tissue which can be observed all over the colonic wall while treated wild type mice showed normal colonic morphology and very little infiltration of inflammatory cells that was similar to untreated wild type animals (Fig. 3.6) Taken together our observations of low survival of *Rassf1a*$^{-/-}$ mice following challenge with either LPS or DSS treatment, increased production of NFκB regulated cytokines in *Rassf1a*$^{-/-}$ mice and loss of colonic architecture in *Rassf1a*$^{-/-}$ mice suggest a role for RASSF1A as a negative regulator of inflammation. Therefore, *Rassf1a*$^{-/-}$ mice might be a good model for what human patients experience as they also reveal elevated production of NFκB regulated cytokines when challenged with bacterial components.

3.6 Ex vivo analysis of macrophages and splenocytes from wild type and Rassf1a$^{-/-}$ mice

In support of our data using LPS or DSS treatment of *Rassf1a*$^{-/-}$ mice, we isolated bone marrow derived macrophages and splenocytes from untreated wild type and *Rassf1a*$^{-/-}$ mice, cultured them *ex vivo*, stimulated them with various TLR activators and quantified secreted cytokine production. Cells derived from *Rassf1a*$^{-/-}$ mice produced significantly more cytokines in response to TLR9 and TLR4, but not with TLR3 stimulants (Fig. 3.5). We observed elevated production of TNF-α, IL-6, IL-12 and modest increase in IL-8 production (a chemokine) in bone marrow derived macrophages derived from *Rassf1a*$^{-/-}$ mice when compared to the wild type animals following TLR4 stimulation with LPS (Fig. 3.5A and 3.5B). Splenocytes derived from *Rassf1a*$^{-/-}$ mice also showed a similar increase production of TNF-α following TLR4 stimulation (Fig. 3.5A). Moreover, we can also observe elevated production of TNF-α in both bone marrow derived macrophages and splenocytes derived from *Rassf1a*$^{-/-}$ mice following TLR9 stimulation with CpG DNA (Fig. 3.5C).

These data confirm our *in vivo* experiments that cells from *Rassf1a*$^{-/-}$ mice have dysregulated NFκB activities resulting in the uncontrolled production of cytokines (and chemokines) most likely as a result of increased NFκB activity. Our *ex vivo* data suggest that the importance of RASSF1A may be restricted to non-TLR3 responses as we do not observe significant elevation in cytokine production of IL-6 and TNF-α (Fig. 3.5D) and only a modest 1.4 fold increase in IL-8 chemokine production [data not shown]) when bone marrow derived macrophages are stimulated with poly (dI:C), a stimulant of the TLR3 pathway.[172] However, we do observe a significant increase in IL-12 production suggesting that RASSF1A may modulate some aspect of the TLR3 signaling pathway. This will require further analysis. In addition, no change in cytokine productin of IL-10 and IFNγ was observed in bone marrow derived

macrophages and splenocytes from wild type and *Rassf1a*$^{-/-}$ animals following TLR4, LR3, or TLR9 stimulation. TLR2 stimulation produced irreproducible results and requires further analysis.

As mentioned earlier, numerous mouse models have been established that have either deletions or mutations in key regulatory elements involved in NFκB activation and TLR function. To varying degrees, these models are useful in understanding the pathogenesis of IBD since CD and UC have multifactorial etiologies. An underlying hallmark of IBD is enhanced NFκB activation and elevated production of NFκB regulated cytokines. In our current study, we have explored the use of *Rassf1a*$^{-/-}$ mice to model IBD in mice. Following challenge with either components of the bacterial cell wall (LPS) or with a chemical irritant of the colonic mucosa (DSS), we have observed low survival of *Rassf1a*$^{-/-}$ mice, elevated production of NFκB regulated cytokines, and destruction of the colonic architecture which most properly result from increased NFκB activation. These are similar to the situation that exists with human IBD. Furthermore, since treated *Rassf1a*$^{-/-}$ mice reveal the similar clinical signs of IBD, we can use these mice to test new therapies in the treatment of IBD. We speculate that RASSF1A is a new and novel susceptible gene for IBD on chromosome 3p21 and understanding the molecular mechanisms involved in RASSF1A-dependent modulation of NFκB is greatly needed in understanding the pathogenesis of IBD and how the duration of the inflammatory response is regulated.

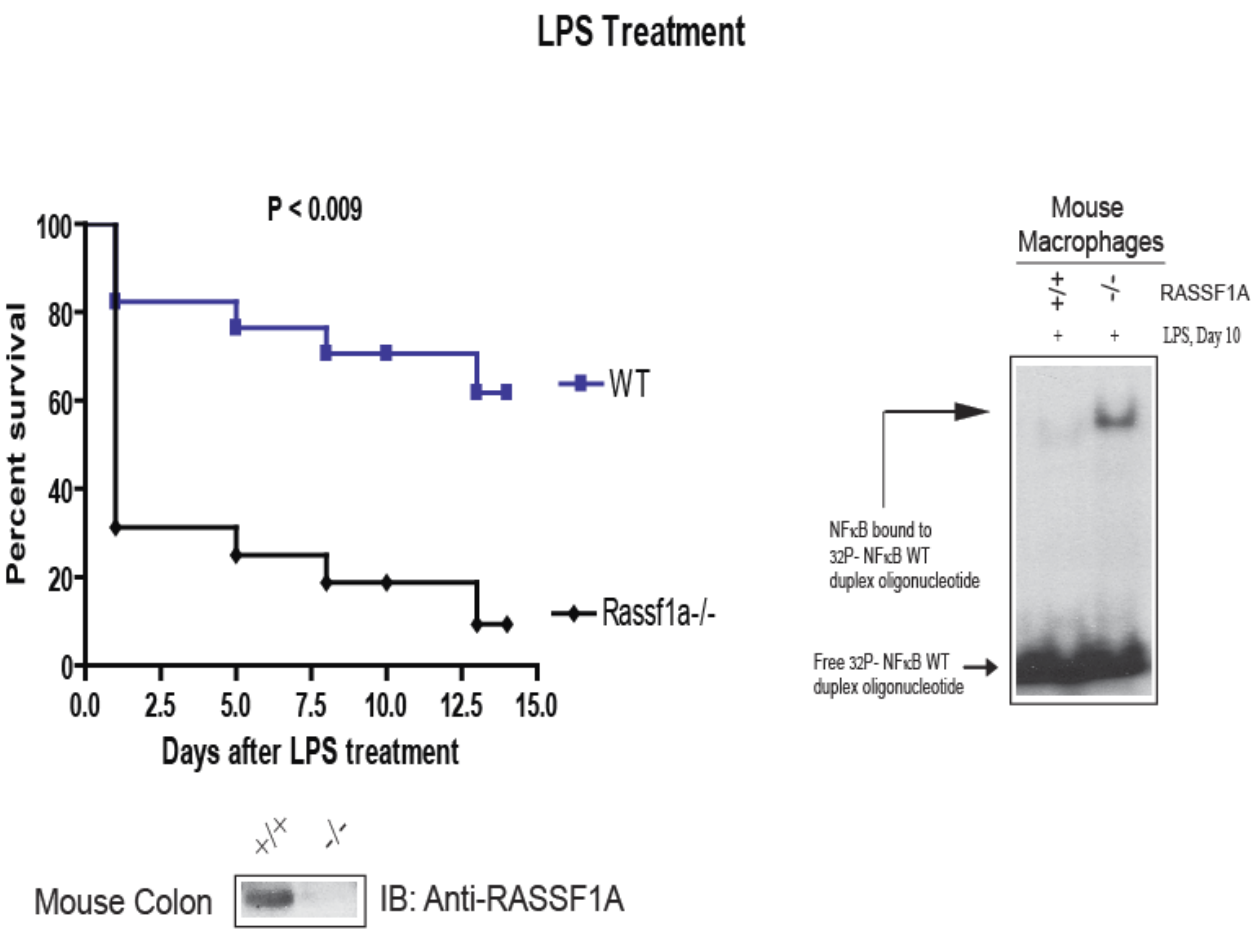

Figure 3.1: *Rassf1a*$^{-/-}$ animals are senstitive to LPS treatment. Lipopolysaccharide (LPS, 15 µg/g body weight) was intraperitoneally (IP) injected into the indicated RASSF1A animals and % survival was monitored following treatment. In bottom panel is immunostaining for endogenous RASSF1A in mouse colon from wild type and *Rassf1a*$^{-/-}$ illustrating the loss of RASSF1A in *Rassf1a*$^{-/-}$ mice. n = 16 for each genotype. On the right panel, Electrophoretic mobility shift assay (EMSA) showing increased NFκB activity in LPS treated *Rassf1a*$^{-/-}$ mice when compared to the WT animals.

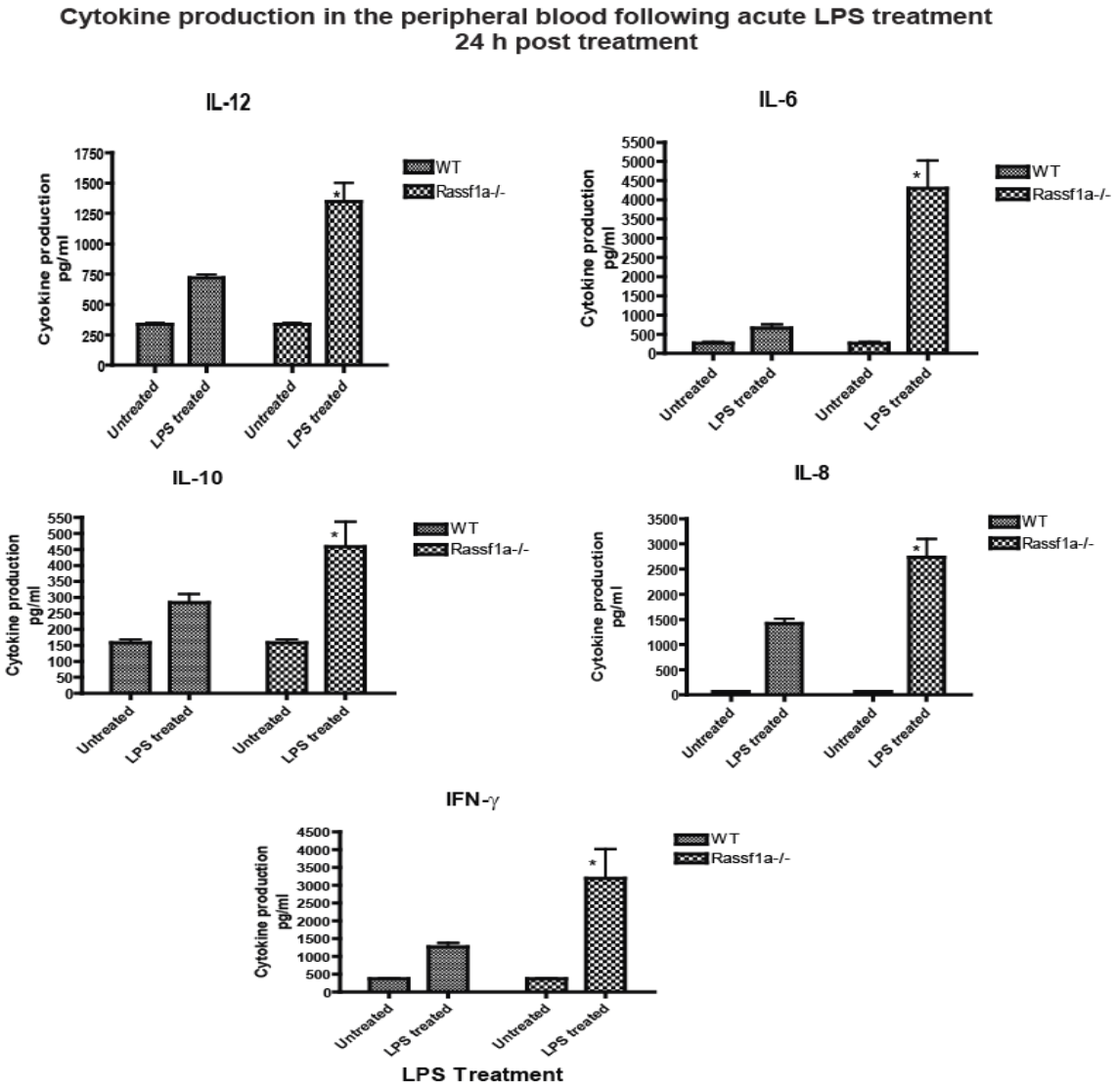

Figure 3.2: *Rassf1a*$^{-/-}$ animals show higher cytokine production after LPS treatment. Lipopolysaccharide (LPS, 10 µg/g body weight) was intraperitoneally (IP) injected into the indicated RASSF1A animals. Cytokine analysis 24 hour following treatment show high production of IL-6, IL-12, IL-8, IL-10 and IFN-γ in *Rassf1a*$^{-/-}$ mice when compared to WT mice. (*) means significance p value. For IL-6, IL-12, IL-8, IL-10 and IFN-γ, p value is <0.01, <0.01, <0.001, <0.05 and <0.05 respectively between treated *Rassf1a*$^{-/-}$ and treated WT mice. n = 6

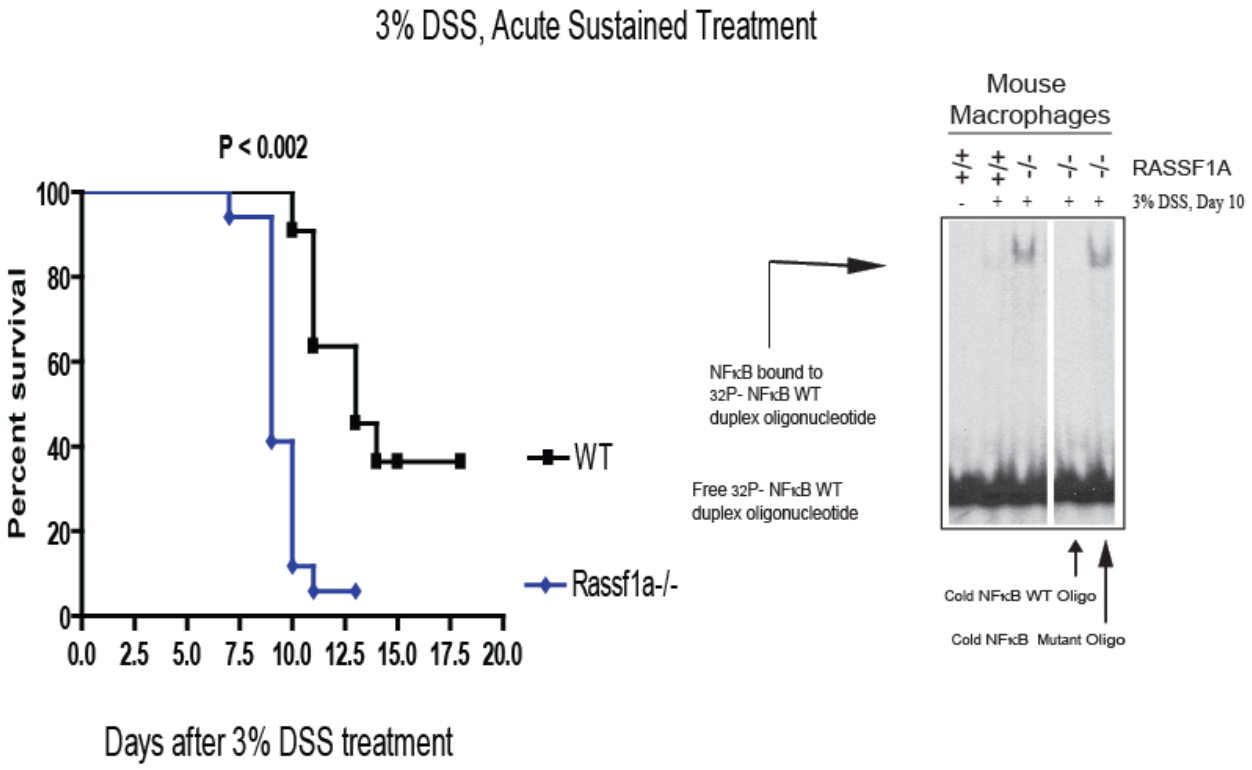

Figure 3.3: *Rassf1a*$^{-/-}$ animals are sensitive to Dextran Sulphate (DSS) treatment. 3% DSS was added to the drinking water for the duration of the experiment and % survival were monitored following treatment. n = 11 for each genotype. On the right panel, Electrophoretic mobility shift assay (EMSA) showing increased NFκB activity in DSS treated *Rassf1a*$^{-/-}$ mice when compared to the WT animals.

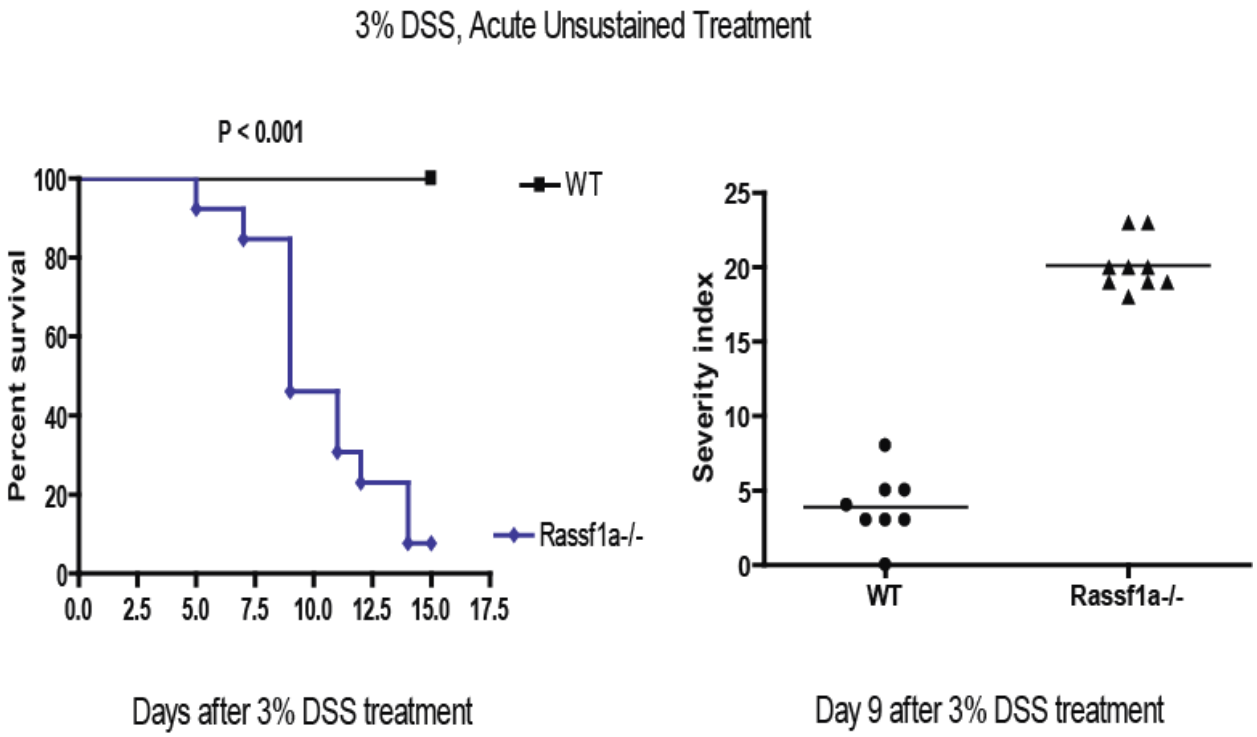

Figure 3.4: *Rassf1a*$^{-/-}$ animals are senstitive to Dextran Sulphate (DSS) treatment. Left panel, 3% DSS was added to the drinking water of the animals for 7 days and % survival were monitored following treatment. n = 12 for each genotype. On the right panel *Rassf1a*$^{-/-}$ mice show high severity index when compared to the WT animals. n=9, $p<0.001$ between the 2 groups.

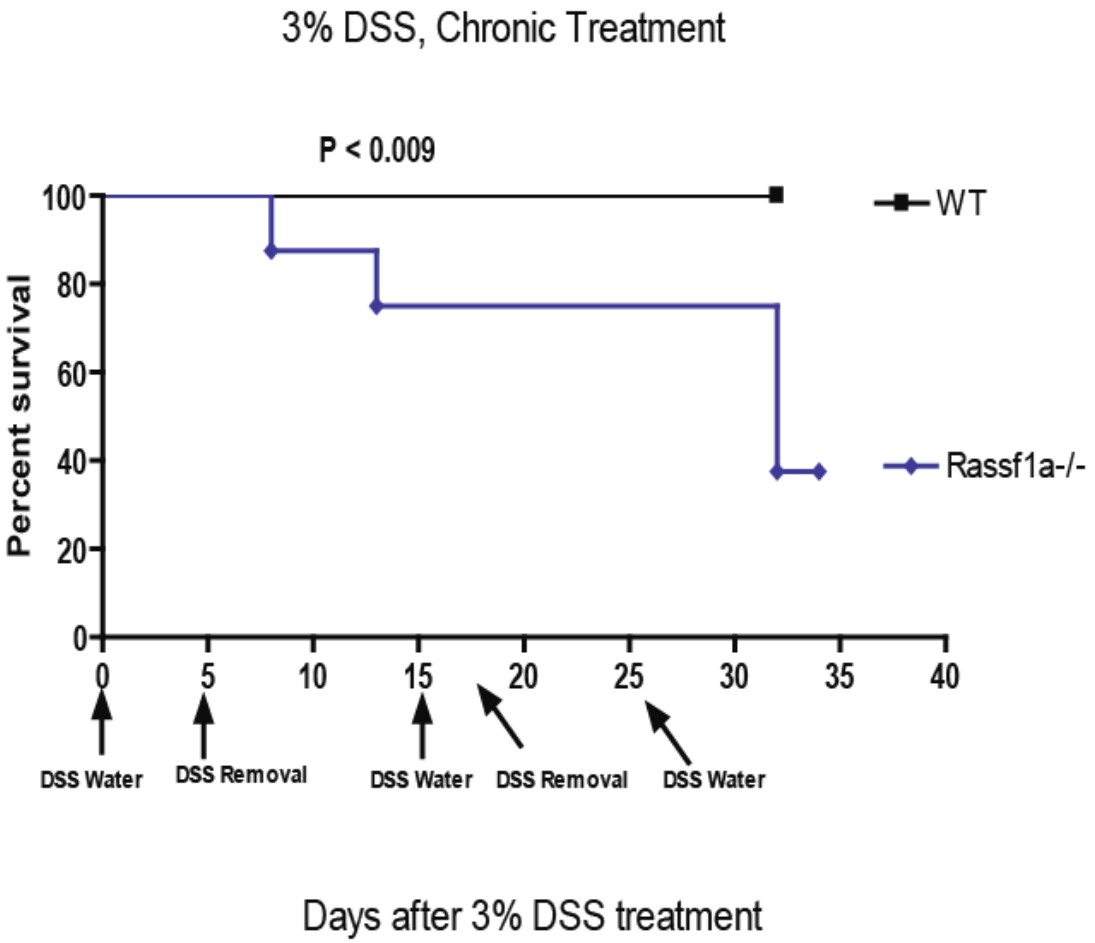

Figure 3.5: *Rassf1a*$^{-/-}$ animals are sensitive to Dextran Sulphate (DSS) treatment. 3% DSS was added to the drinking water of the animals as indicated in the graph and % survival were monitored following treatment. n = 8 for each genotype.

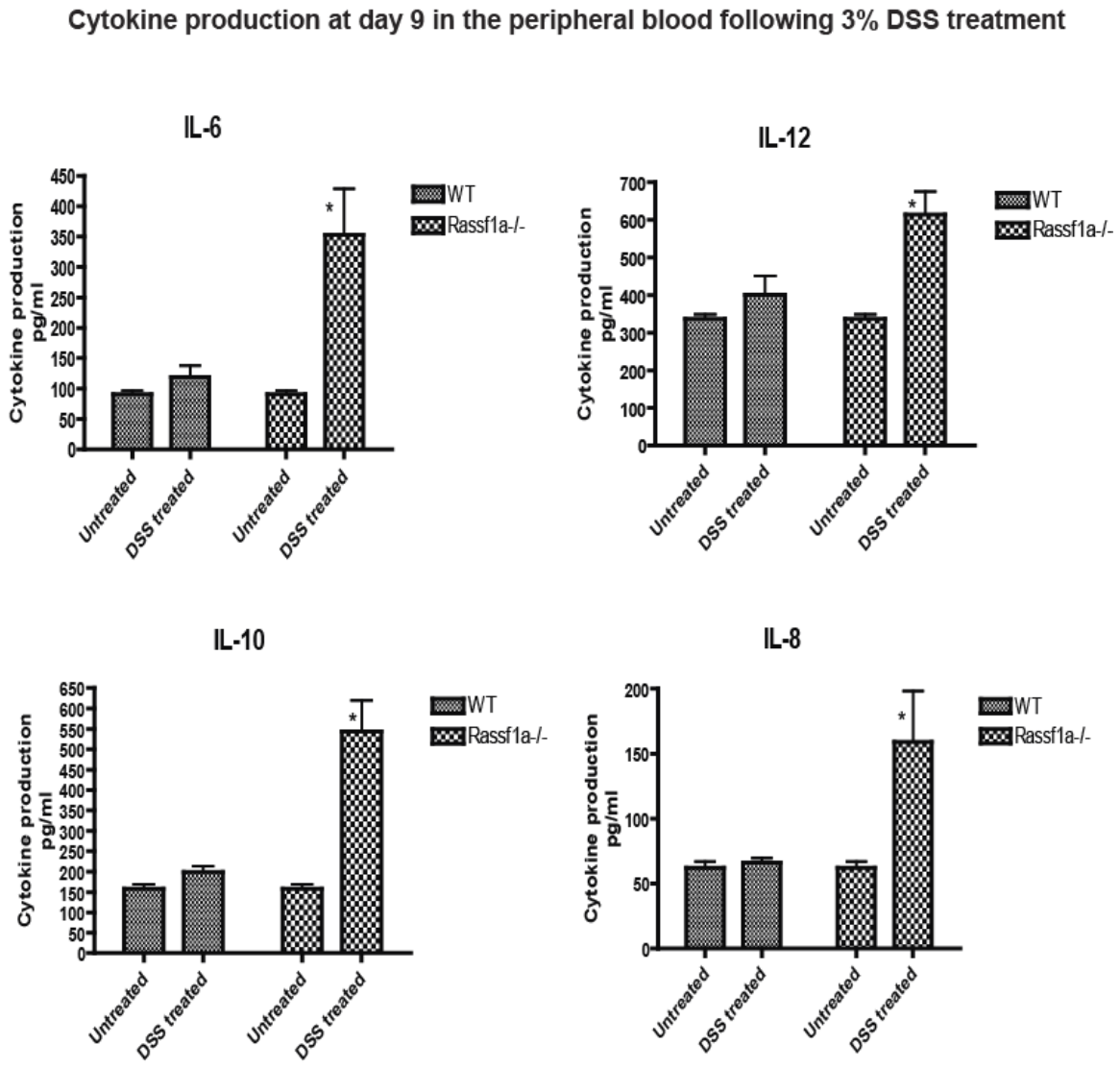

Figure 3.6: *Rassf1a*$^{-/-}$ animals show higher cytokine production after DSS treatment. Cytokine analysis at day 9 after 3% DSS treatment show high production of IL-6, IL-10, IL-12 and IL-8 in Rassf1a-/- mice when compared to WT mice. There was no increase in IL-23 or IL-2 production. (*) means significance p value. For IL-6, IL-10, IL-12 and IL-8, p value is <0.01, <0.001, <0.01, <0.05 respectively between treated *Rassf1a*$^{-/-}$ and treated WT mice. n = 6

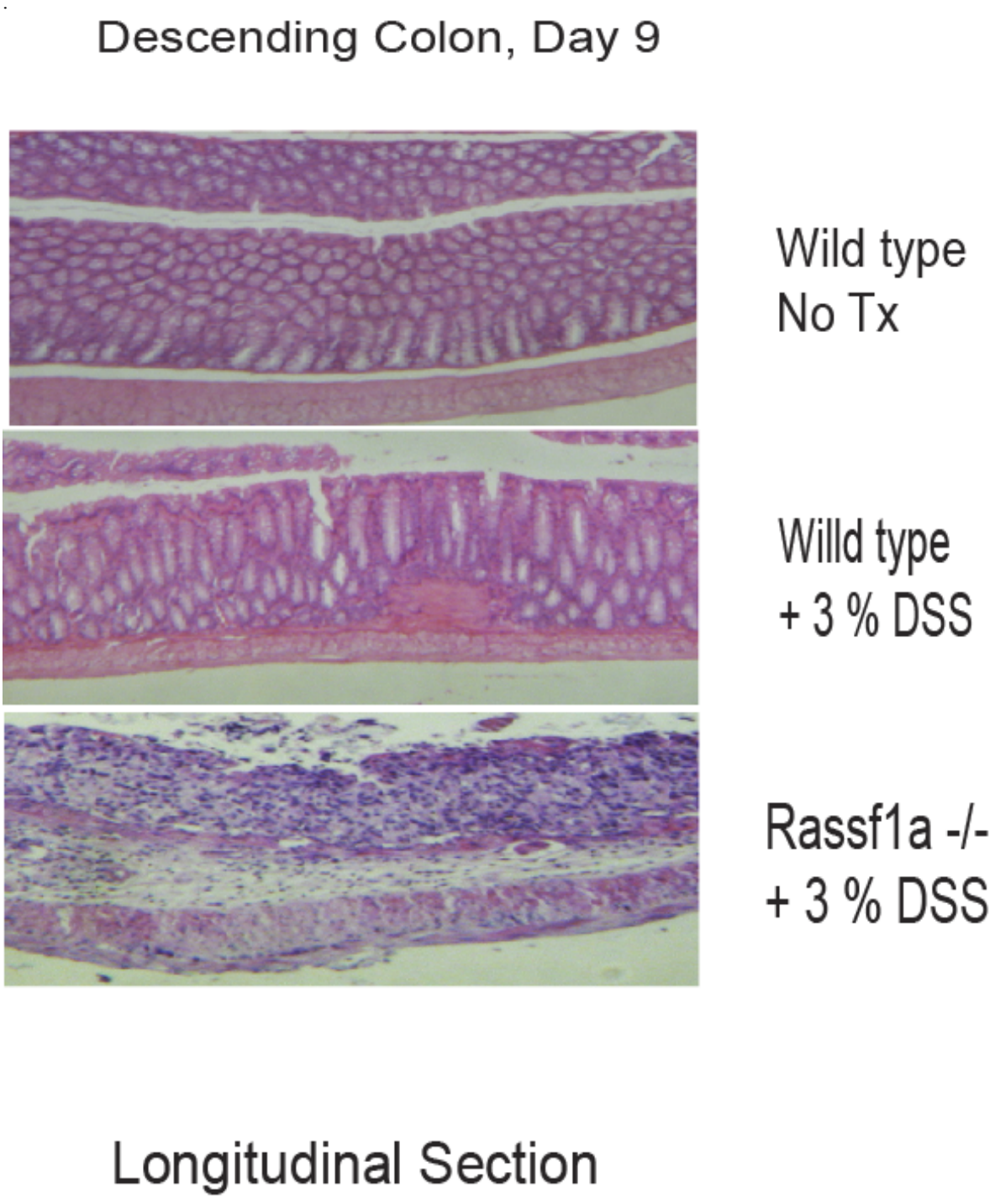

Figure 3.7: Longitudinal cross-sectional picture of the descending colon stained with H&E. Colon of DSS treated *Rassf1a*$^{-/-}$ mice reveal loss of architecture and massive infiltration of the immune cells (blue dots) that are not present in either untreated or wild type treated animals.

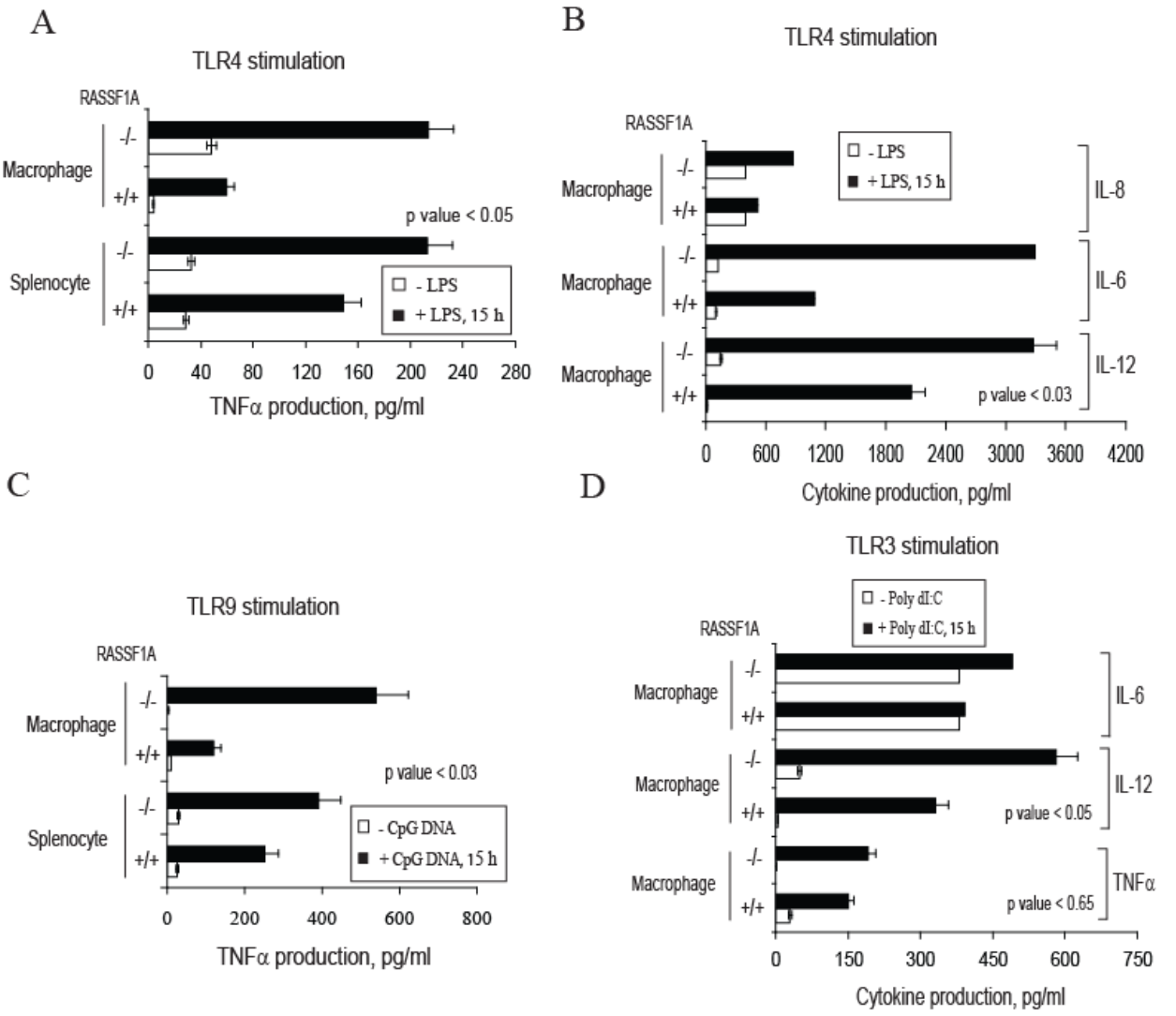

Figure 3.8: Rassf1a-/- animals have unregulated cytokine production following treatment with specific TLR agonists - CpG DNA (unmethylated bacterial DNA containing dinucleotides for TLR9); LPS, lipopolysaccharide, a bacterial cell wall component (for TLR4); and Poly (dI:C) (double stranded DNA for TLR3). Bone marrow derived macrophages and splenocytes were cultured *ex vivo* and then stimulated with the TLR agonists for the indicated times. Supernatants were harvested and the amount of the indicated cytokines quantified by ELISA; n = 3. For (A) and (C), p values between wild type and *Rassf1a*$^{-/-}$ animals was < 0.05 and < 0.03, respectively for both macrophage and splenocyte cells; for (B) and (D) p values between wild type and *Rassf1a*$^{-/-}$ animals are indicated. For (B), we observed a two fold increase in IL-6 production in bone marrow derived macrophages from *Rassf1a*$^{-/-}$ animals when compared to wild type animals but there was no p value as the experiment was done once. For (D) TLR3 stimulation did not result in significance increase in cytokine production except for IL-12.

Chapter 4

NOD2 and innate immunity

Inflammatory bowel disease has multiple susceptibility loci on several chromosomes. NOD2 (nucleotide-binding oligomerization domain containing 2) is one the susceptibility genes located on chromosome 16q12. Structurally, NOD2 contains two N terminus, CARD (caspase activation recruitment) domains, a central nucleotide oligomerization domain and a C terminus Leucine rich repeat LRR) domain that can function as intracellular sensor of bacterial infection.[173, 174] NOD2 protein is expressed by monocytes, granulocytes, dendritic cells and epithelial cells.[175] Initially, LPS was thought to be the bacterial component that is recognized by NOD2 protein, but recently it has been shown that it is in fact, muramyl dipeptide, a component of peptidoglycan that found with various bacteria and frequently contaminates LPS preparations.[176] Activation of NOD2 results in activation of multiple signaling pathways, including the NFκB and MAPK (mitogen-activated protein kinases) pathways, and ultimately leads to a variety of immune responses.[177]

Many groups have identified mutations within the Nod2 gene on chromosome 16 as being associated to CD, but not UC (Please see more details in Familial and Genetic Factors in chapter 1).[29, 84] However, Nod2 deficient mice do not have spontaneous intestinal inflammation[85, 86] Furthermore, colonic inflammation is of the same as wild type mice upon challenge with an agent leading to acute colitis.[86] on the other hand, mouse Nod2 activates NFκB and confers responsiveness to LPS and PGN when wild type Nod2 was transfected in HEK293T cells.[178] Multiple genes may be affected in IBD patients that result in the enhanced inflammation experienced by these patients. Since both NOD2 and RASSF1A are genetic susceptibility loci for IBD, we used the *Nod2*$^{-/-}$ mice and generated the *Rassf1a*$^{-/-}$*Nod2*$^{-/-}$ mice to explore how the loss of multiple susceptibility genes may promote NFκB dysregulation and enhance inflammation. All of these mice are viable and fertile and do not reveal an overt phenotype

(including the occurrence of spontaneous colitis). We therefore used both the *Nod2*$^{-/-}$ and *Rassf1a*$^{-/-}$*Nod2*$^{-/-}$ mice in LPS and DSS experiments in order to compare to the functional importance influence of NOD2 and RASSF1A to innate immunity and inflammation.

4.1 Survival of Nod2$^{-/-}$ *and Rassf1a*$^{-/-}$*Nod2*$^{-/-}$ *following LPS treatment*

Nod2$^{-/-}$ and *Rassf1a*$^{-/-}$*Nod2*$^{-/-}$ were injected IP with 15 μg/g body weight of LPS (a stimulant of TLR4 function; reagent was obtained from Sigma, E. coli strain 0111:B4). Survival was followed over a course of 14 days and severity of disease was monitored by signs of piloerection, tremors, bloatedness, pussy eyes and slow movement. *Nod2*$^{-/-}$ and *Rassf1a*$^{-/-}$*Nod2*$^{-/-}$ mice show better survival (70% and 100% respectively) following LPS treatment when compared to *Rassf1a*$^{-/-}$ mice (Fig. 4.1). We have carried out this experiment twice with a total of 8 animals and we have always observed better survival for the *Rassf1a*$^{-/-}$*Nod2*$^{-/-}$ mice. Further analysis may be required to confirm this observation.

4.2 Cytokine production after LPS treatment

Nod2$^{-/-}$ and *Rassf1a*$^{-/-}$*Nod2*$^{-/-}$ mice were injected intraperitoneally (IP) with 10 μg/g body weight of LPS. Cytokine analysis after 24 hours revealed the same level in the cytokine production in *Nod2*$^{-/-}$ and *Rassf1a*$^{-/-}$*Nod2*$^{-/-}$ mice when compared to the wild type animals for IL-6, IL-12, IL-8, IL-10 and IFN-γ (Fig. 4.2 and data not shown for IL-12). There is no statistical difference in the cytokine production between *Nod2*$^{-/-}$ and *Rassf1a*$^{-/-}$*Nod2*$^{-/-}$ mice for IL-6, IL-8, IL-10 and IFN-γ (Fig. 4.2). This suggests that NOD2 may be dispensable for LPS-induced inflammation whereas RASSF1A may be required to protect from LPS-induced inflammation. We speculate that following LPS-induced inflammation *Rassf1a*$^{-/-}$ animals can mount an immune

response but can not properly shut it down resulting in increased production NFκB activity, increased production of NFκB targeted cytokines, and decreased survival (Fig. 4.1 and 4.2).

4.3 Survival of Nod2$^{-/-}$ and Rassf1a$^{-/-}$Nod2$^{-/-}$ following DSS treatment

Nod2$^{-/-}$ and *Rassf1a*$^{-/-}$*Nod2*$^{-/-}$ mice were treated with dextran sodium sulphate (DSS) in the drinking water for only 7 days followed by removal and the addition of regular drinking water. Survival was followed for 15 days for the same signs of colitis. *Nod2*$^{-/-}$ mice appear to be more sensitive to DSS treatment than *Rassf1a*$^{-/-}$*Nod2*$^{-/-}$ but there is no statistically difference between the two groups (Fig 4.3) and each group had significantly greater survival when compared to *Rassf1a*$^{-/-}$ mice (compare with Fig. 3.3.2). In addition, we observed very little NFκB DNA binding activity by EMSA in nuclear extracts from macrophages of DSS-treated *Nod2*$^{-/-}$ and *Rassf1a*$^{-/-}$*Nod2*$^{-/-}$ mice (data not shown) in contrast to what we observed for DSS-treated *Rassf1a*$^{-/-}$ mice (Fig. 3.3). This is in support of the greater survival of both *Nod2*$^{-/-}$ and *Rassf1a*$^{-/-}$*Nod2*$^{-/-}$ mice when compared to *Rassf1a*$^{-/-}$ mice. Moreover, severity index at day 9 following 3% DSS shows no significance difference between the wild type, *Nod2*$^{-/-}$ and *Rassf1a*$^{-/-}$*Nod2*$^{-/-}$ mice (fig.4.3).

4.4 Cytokine production after DSS treatment

Cytokine analysis in the peripheral blood at day 9 of the experiment revealed the same level of IL-6, IL-8 and IL-10 production by both *Nod2*$^{-/-}$ and *Rassf1a*$^{-/-}$*Nod2*$^{-/-}$ mice when compared to type wild type mice. There is no statistical difference in the cytokine production between *Nod2*$^{-/-}$ and *Rassf1a*$^{-/-}$*Nod2*$^{-/-}$ mice for IL-6, IL-8 and IL-10 (Fig. 4.4). Together with

data in Fig. 4.2, our data suggest that *Nod2*$^{-/-}$ mice may be dispensable for DSS-induced inflammation.

.

4.5 Tissue histology after DSS treatment

Longitudinal section of the descending colon at day 9 for the *Nod2*$^{-/-}$ and *Rassf1a*$^{-/-}$*Nod2*$^{-/-}$ mice revealed normal colonic morphology and very almost no infiltration of inflammatory cells that was mostly similar to untreated wild type animals (fig. 4.5). Together with the survival and cytokine production data, both *Nod2*$^{-/-}$ and *Rassf1a*$^{-/-}$*Nod2*$^{-/-}$ mice behave the same like the wild type animals. Therefore, NOD2 may be dispensable for DSS or LPS induced inflammation whereas RASSF1A may be required to protect the animals from DSS or LPS-induced inflammation. These data support our observation of the role of RASSF1A as a negative modulator of immune response and inflammation as we had observed low survival, high production of cytokines and disturbed colonic architecture in the *Rassf1a*$^{-/-}$ mice when compared to the *Nod2*$^{-/-}$ mice.

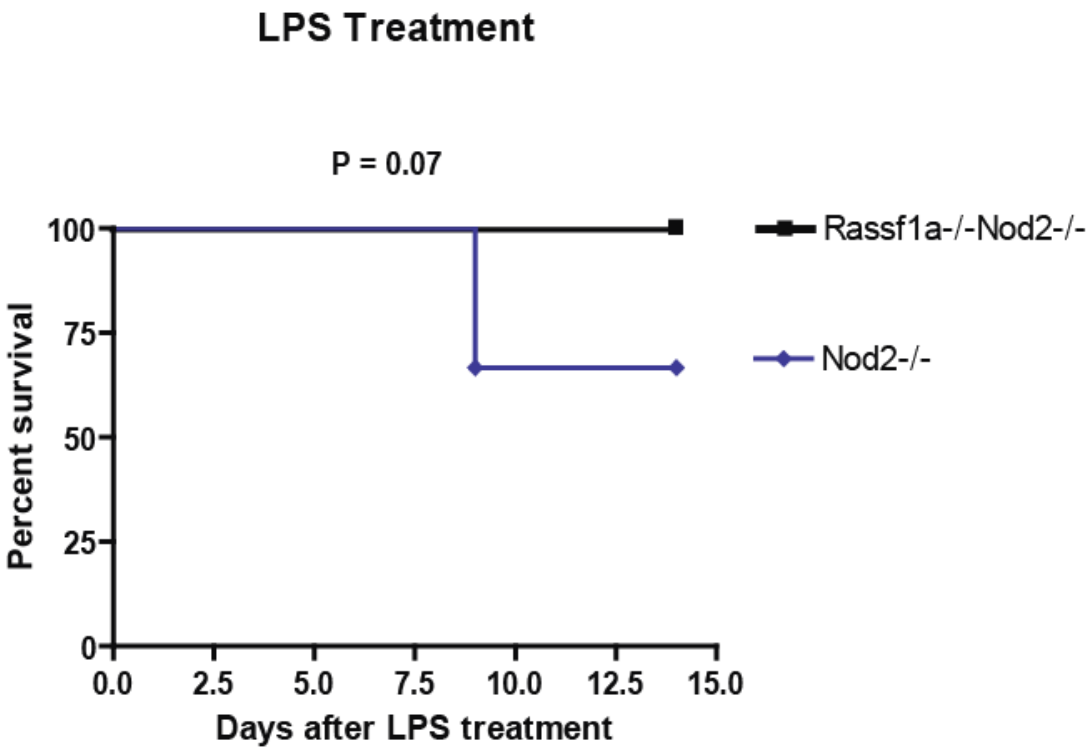

Figure 4.1: *Nod2*$^{-/-}$ animals are more sensitive to LPS treatment than *Rassf1a*$^{-/-}$*Nod2*$^{-/-}$ but there is no statistical difference between the two groups and both animal groups reveal significantly more survival than *Rassf1a*$^{-/-}$ animals following LPS treatment (compare to figure 3.1). Lipopolysaccharide (LPS, 15 µg/g body weight) was intraperitoneally (IP) injected into the indicated animals and % survival was monitored following treatment. n = 8.

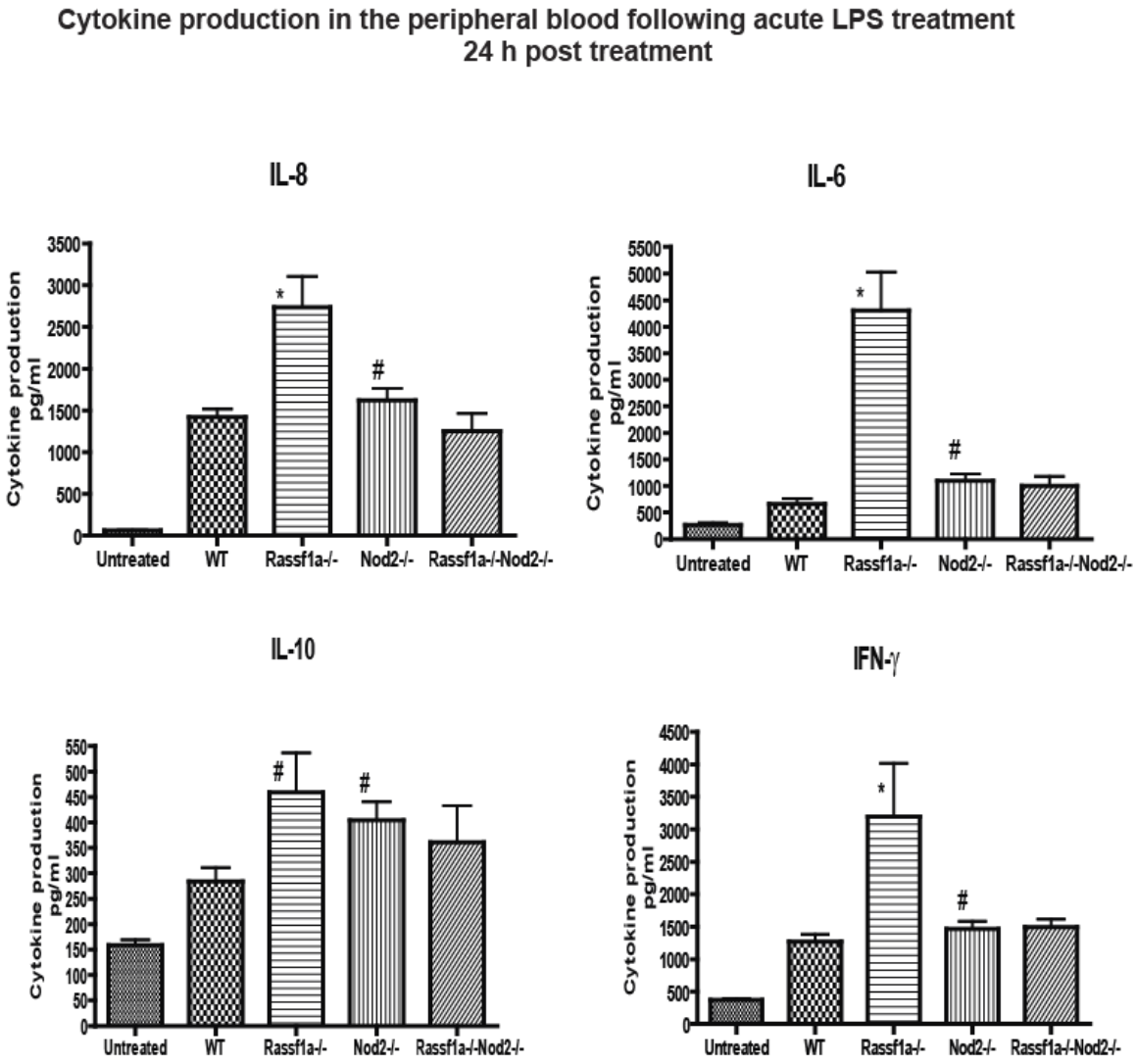

Figure 4.2: *Nod2*$^{-/-}$ and *Rassf1a*$^{-/-}$*Nod2*$^{-/-}$ animals show low cytokine production after LPS treatment. Lipopolysaccharide (LPS, 10 µg/g body weight) was intraperitoneally (IP) injected into the indicated animals. Cytokine analysis 24 hour following treatment show low production of IL-6, IL-8, IL-10 and IFN-γ in *Nod2*$^{-/-}$ and *Rassf1a*$^{-/-}$*Nod2*$^{-/-}$ mice when compared to *Rassf1a*$^{-/-}$ mice. (*) means significance p value. (#) means insignificance p value. For IL-6, IL-8 and IFN-γ, p value is <0.01, <0.01, <0.05 respectively between treated *Rassf1a*$^{-/-}$ and both treated *Nod2*$^{-/-}$, *Rassf1a*$^{-/-}$*Nod2*$^{-/-}$ mice. For IL-10, p value is >0.05 between treated *Rassf1a*$^{-/-}$ and both treated *Nod2*$^{-/-}$, *Rassf1a*$^{-/-}$*Nod2*$^{-/-}$. For all shown cytokines, there are no significant differences between treated *Nod2*$^{-/-}$ and treated *Rassf1a*$^{-/-}$*Nod2*$^{-/-}$ mice. n = 6

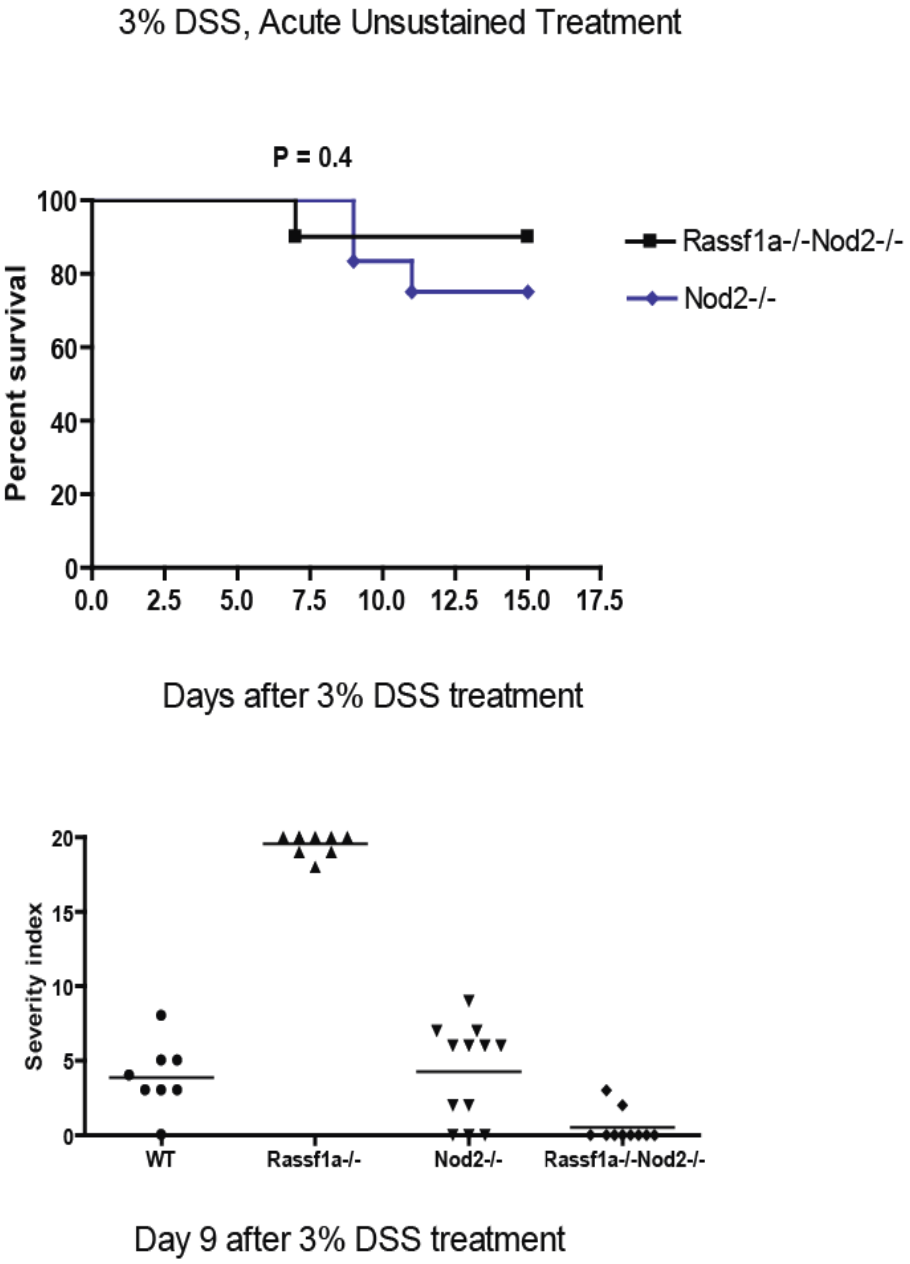

Figure 4.3: *Nod2*$^{-/-}$ animals are sensitive to Dextran Sulphate (DSS) treatment more than *Rassf1a*$^{-/-}$*Nod2*$^{-/-}$ mice but there is no statistical difference between the two groups. Upper panel, 3% DSS was added to the drinking water of the animals for 7 days and then replaced by normal drinking water. Percent survival was monitored following treatment. n = 12 for each genotype. In the lower panel *Nod2*$^{-/-}$ and *Rassf1a*$^{-/-}$*Nod2*$^{-/-}$ mice show similar severity index to the WT mice but less severity when compared to the *Rassf1a*$^{-/-}$ mice. n=8, p value is >0.05 between WT, *Nod2*$^{-/-}$ and *Rassf1a*$^{-/-}$*Nod2*$^{-/-}$ mice.

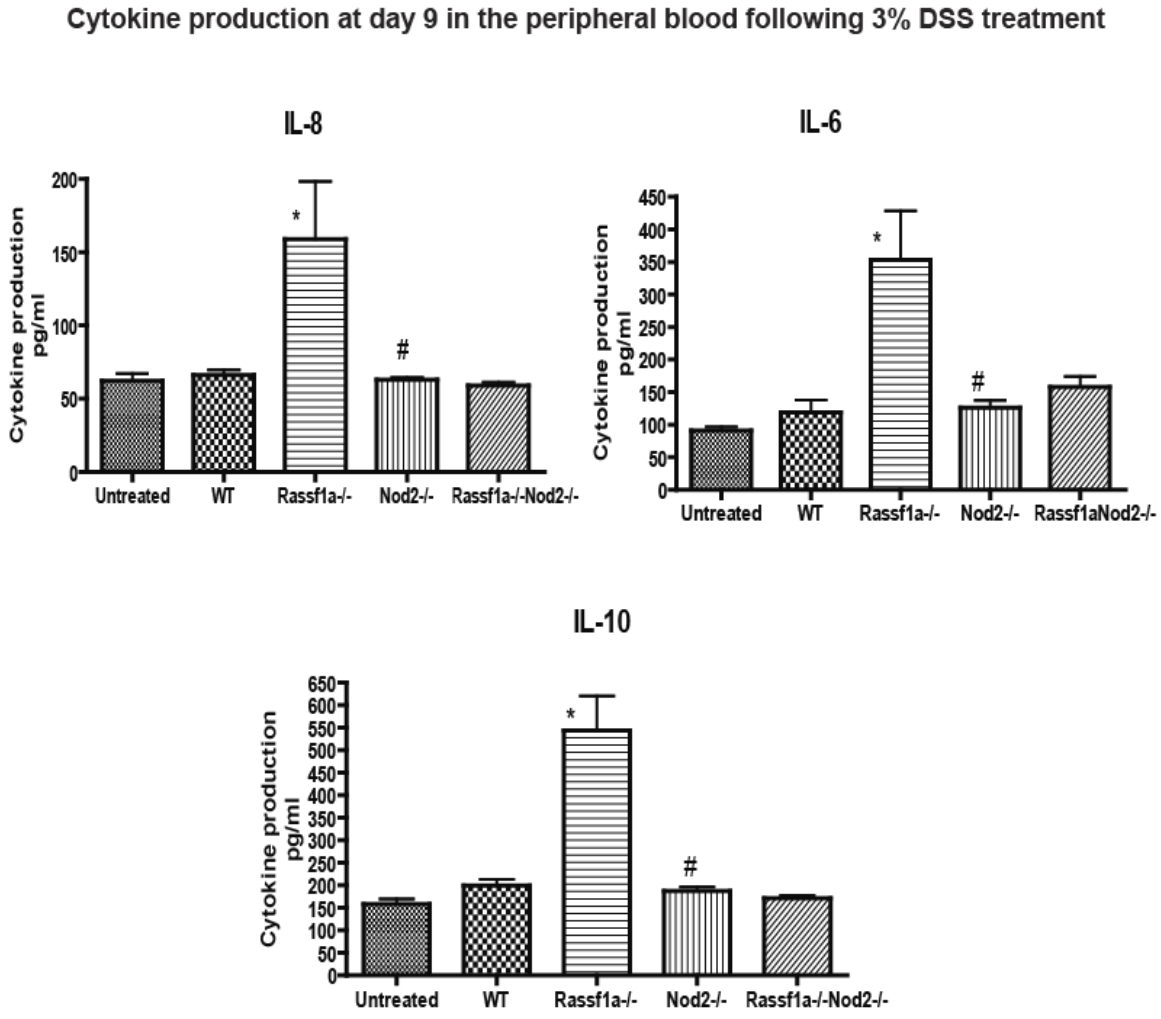

Figure 4.4: *Nod2*$^{-/-}$ and *Rassf1a*$^{-/-}$*Nod2*$^{-/-}$ animals show low cytokine production after DSS treatment. Cytokine analysis at day 9 after 3% DSS treatment show low production of IL-6, IL-18 and IL-10 in both *Nod2*$^{-/-}$ and *Rassf1a*$^{-/-}$*Nod2*$^{-/-}$ mice (similar to the untreated mice) when compared to *Rassf1a*$^{-/-}$ mice. (*) means significance p value. (#) means insignificance p value. For IL-6, IL-10 and IL-8, p value is <0.01, <0.001, <0.01 respectively between treated *Rassf1a*$^{-/-}$ and both treated *Nod2*$^{-/-}$, *Rassf1a*$^{-/-}$*Nod2*$^{-/-}$ mice. For all shown cytokines, there are no significant differences between treated *Nod2*$^{-/-}$ and treated *Rassf1a*$^{-/-}$*Nod2*$^{-/-}$ mice. n = 6

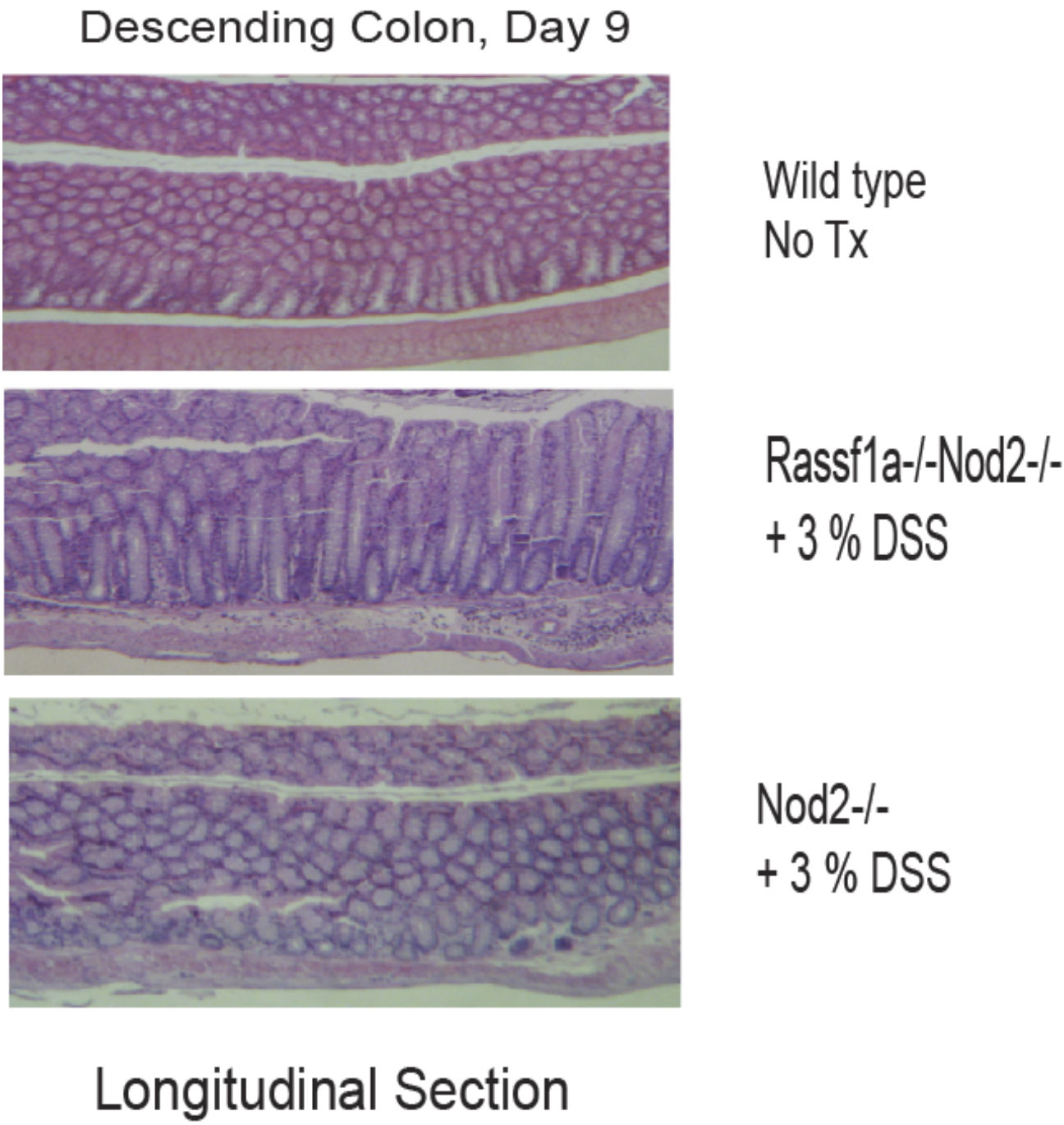

Figure 4.5: Longitudinal crosssectional picture of the descending colon stained with H&E. Colon of DSS treated *Nod2*$^{-/-}$ or *Rassf1a*$^{-/-}$*Nod2*$^{-/-}$ mice reveal preserved colonic architecture and no infiltration of the immune cells (blue dots) when compared to DSS treated *Rassf1a*$^{-/-}$ animals (compared to the bottom panel of Fig. 3.8).

Chapter 5

RASSF1A and TLR pathway

The RASSF1A pro-apoptotic pathway utilizes the TNF-R1 receptor following TNFα-stimulation to activate Bax, a key modulator of mitochondrial driven apoptosis (Fig 1.5). RASSF1A functions to conformationally change MOAP-1 to allow it to activate Bax and then cell death. However, TNFα-stimulation can also activate NFκB. Preliminary results from our research group revealed that RASSF1A does not associate with TNF-R1 pathway components linking to NFkB activation (unpublished observations). We next investigated associations with other key activators of NFκB, such as the Toll receptors, the TLRs. Using an NFκB gene reporter assay, RASSF1A can inhibit LPS induced activation of NFκB (Baksh et al. unpublished data) suggesting that RASSF1A is an inhibitor of NFκB activation following TLR stimulation. Therefore, we began to explore the association of RASSF1A with different components of TLR pathway.

5.1 Association of RASSF1A with TLR3 and TLR4

HCT116 cells are a colon cancer epithelial cell line. They were chosen for our experiments as they may represent the cells of the gastrointestinal tract where these receptors would have an important function in normal (microbial infections) and diseased (IBD patients) states. Moreover, these cells can be easily transfected with PEI, they grow very well, and can also respond to different TLR stimuli. RASSF1A was observed to associate with TLR4 in response to LPS stimulation in HCT116 cells (Fig. 5.1A). Association was stimulus and time dependent with strong association at approximately 3 hours for TLR4 (Fig. 5.1A). Similar associations of RASSF1A were observed with TLR2 and TLR9 suggesting in response to their respective stimuli (data not shown). We have observed that RASSF1A was not able to associate with TLR3 (Fig 5.1B) however, RASSF1A may still associate with TRIF or TRAF6 following

Poly I/C stimulation and then can still regulate NFκB activity. This has not been investigated this time. Associations with several TLRs suggested a universal role for RASSF1A in modulating TLR function and NFκB activation, most likely utilizing a common downstream target for the TLRs, such as MyD88, IRAK1/4 or TRAF6 (Fig. 1.1). Most TLRs utilized MyD88 except for TLR3 that relies on TRIF (TIR domain containing adapter inducing IFNβ) and TRAF6 to directly activate IKK. RASSF1A may modulate NFκB activity through associations with the TLR4 pathway most likely through MyD88.

5.2 Association of RASSF1A with MyD88, a downstream effector of the TLRs pathway

Since we have observed association with numerous TLRs, we speculated that this most likely occurs by utilizing a common downstream element for TLR2, 4 and 9 such as MyD88, IRAK1/4 or TRAF6 (Fig. 1.1). RASSF1A revealed basal association and stimulus dependent release following LPS stimulation (Fig. 5.2). This would suggest that RASSF1A may restrict the function of MyD88 until needed. Following TLR activation, MyD88 can no longer associate with RASSF1A and MyD88 is free to associate with downstream protein complexes. Once activation of NFκB occurs and inflammation proceeds, RASSF1A may play a role to downmodulate the activity of NFκB by re-association with MyD88. Moreover, our research group has observed basal and time dependent release associations with TRAF6 and IRAK similar to MyD88. Therefore, RASSF1A may associate with IRAK/TRAF6/Myd88 complex to restrict it from activating NFκB following stimulus addition.

Taken together these data suggest that RASSF1A could be a novel negative regulator of NFκB directed inflammation originating with TLR pathway and may function to restrict the formation of complexes that would lead to the activation of IKK and NFκB.

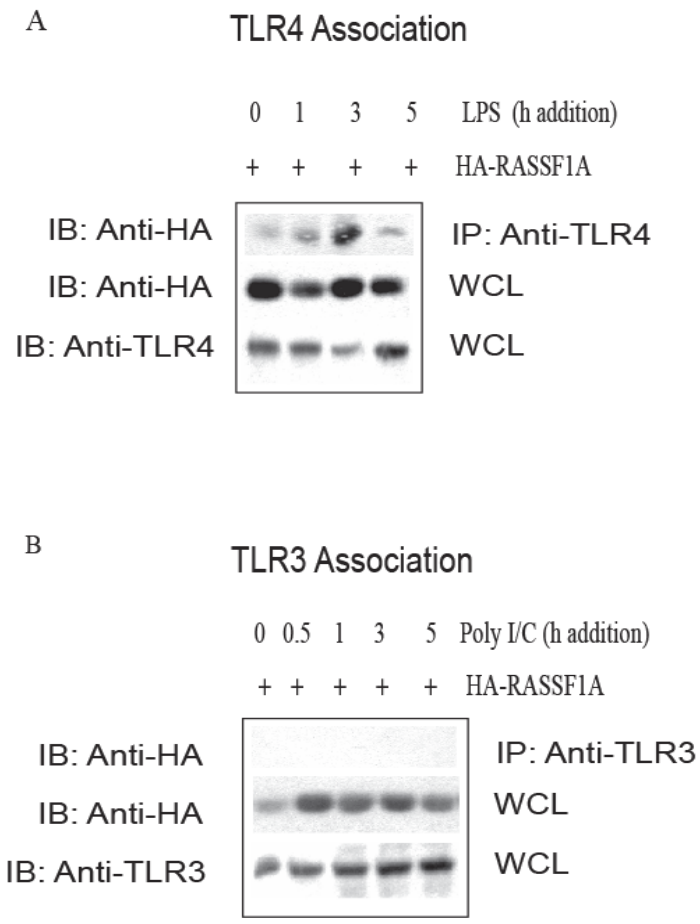

Figure 5.1: HCT116 cells transiently expressing HA-tagged RASSF1A were stimulated with the respective TLR ligand, lysed and immunoprecipitation experiments (IP) with TLR4 (A), TLR3 (B) was carried out. Associated proteins were separated by SDS-PAGE, transfered to PVDF membrane, and immunoblotted (IB) against the indicated antibodies.

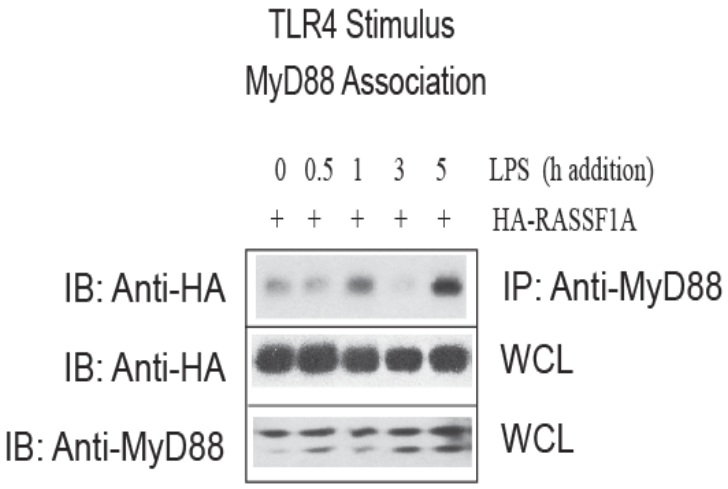

Figure 5.2: HCT116 cells transiently expressing HA-tagged RASSF1A were stimulated with the respective TLR ligand, lysed and immunoprecipitation experiments (IP) with MyD88 was carried out. Associated proteins were separated by SDS-PAGE, transfered to PVDF membrane, and immunoblotted (IB) against the indicated antibodies.

Chapter 6

Functional Importance of RASSF1A Microtubule localization and Polymorphism

The appearance of cancer is defined by many dynamic changes in the genome. These changes were defined by Hanahan and Weinberg in 2000 as the "hallmarks of cancer".[179] They include nucleotide changes (polymorphisms) possibly leading to point mutations, gene amplifications and deletions, chromosomal translocations, and epigenetic changes. It is now widely accepted that tumor suppressor proteins, such as retinoblastoma protein (pRb), p53, p73, and PTEN to mention a few are all targets for genetic changes.[180] The RASSF1A tumor suppressor gene is no exception as it is one of the most heavily methylated genes in human cancers.[100, 101] In addition, polymorphisms to RASSF1A are present in some cancers that may lead to the loss of function of RASSF1A[181] (Figure 6.6a).

It is now well established that RASSF1A is a microtubule protein that co-localizes with tubulin and can stabilize microtubules in a paclitaxel (taxol)-like manner. It can associate with α-, γ-, and β-tubulins[124, 125] and with microtubule binding proteins, such as microtubule binding protein 1B (MAP1B)[125] and the MAP1B homolog C19ORF5/RASSF1A-binding protein 1 (RABP1).[131, 132] These associations are speculated to function to stabilize tubulin and allow microtubules to carry out their role during mitosis to allow sister chromatid segregation. Important to the latter is the role of the microtubules within the spindle complex, the single most important complex underlying chromosomal segregation during cell division.[182] The microtubule spindle complex is regulated by numerous factors and if not formed properly cell death proceeds to prevent inheritable aneuploidy due to chromosome missegregation. If inheritable aneuploidy proceeds it can be detrimental, especially if a genetic change is transferred during chromosomal missegregation. Once one or more of these missegregation events occurred, malignancy leading to cancer can arise. Therefore, it is imperative that we understand what may indirectly or directly affect the stability of microtubules, especially during mitosis.

RASSF1A, 1C, 5, and 7 have been demonstrated to associate with the microtubular network.[127, 183-186] All have been shown to associate with centrosomal elements and, in the case of RASSF1A, with α-, γ, and β-tubulins. Several groups have observed mitotic specific associations of RASSF1A with γ-tubulin within centromeres near to the region of the microtubule organizing center (MTOC). The MTOC is a region whereby microtubules emerge and is a site of microtubule nucleation and an abundance of γ-tubulin.[118, 127, 187] RASSF1A localizes to spindle poles and centromeric areas during metaphase and anaphase, most likely in association with γ-tubulin.

What is currently known about the involvement of RASSF1A during mitosis is that RASSF1A, but not RASSF1C, may function to protect the polymerization state of tubulin during mitosis. This allowed for sister chromatid separation by stabilizing microtubules comparatively to the level of paclitaxel/taxol addition.[123, 124, 188] Tubulin depolymerization can be induced by the addition of the M-phase arresting agent nocodazole. In the presence of RASSF1A, tubulin polymerization is stable and tubulins are acetylated.[125] In the absence of RASSF1A [as found in the mouse embryonic fibroblasts from *Rassf1a*$^{-/-}$ mice[121, 123]], cells more sensitive to nocodazole-induced depolymerization of microtubule resulting in tubulin de-acetylation and destabilization. Destabilized tubulin results in inadequate formation of mitotic spindles, possible chromosome missegregation, inheritable aneuploidy and cancer.

RASSF1A has been demonstrated to associate with the MAP1B homolog C19ORF5/RASSF1A-binding protein 1 (RABP1) by yeast two hybrid and direct immunoprecipitation analysis.[129, 131, 132] C19ORF5 is widely expressed in tissues with a cytosolic localization not associated with microtubules[188], in contrast to RASSF1A that has a cytosolic localized but is associated with microtubules. It has been demonstrated that C19ORF5 is

recruited specifically to microtubules upon paclitaxel/taxol treatment or RASSF1A ovexpression.[132, 188] Dallol et al.[132] suggested a novel role for C19ORF5 was to anchor α- and γ-tubulin to the centrosomes during microtubule nucleation and regrowth, most likely in association with RASSF1A. However, RASSF1A does not require C19ORF5 for its localization to microtubules and C19ORF5 does not appear to protect microtubules from depolymerization upon nocodazole treatment. Therefore, it appears that the RASSF1A-C19ORF5 interaction may be an intriguing link between the microtubules, cell cycle control, and apoptosis. The disruption of this pathway may have a large effect on the process of tumorigenesis.

Several groups have tried to identify the minimal region required for RASSF1A microtubule localization. These reports vary considerably identifying regions important for microtubule localization, such as amino acids 120-185[124], amino acids 163-257 containing 28% basic charges[123], amino acids 289-340[121], and amino acids 125-138 and 167-186.[131] Once RASSF1A loses its microtubule localization it appears to be associated within the nucleus. So far, the only functional consequence of these cellular changes with these RASSF1A deletion mutants is modulation of tubulin depolymerization and stability. In this report, we demonstrate mitotic specific associations of RASSF1A with both α- and γ-tubulin and detail specific amino acid requirements for the microtubule localization of RASSF1A. Lack of RASSF1A microtubule association results in the loss of tubulin acetylation and complete loss of tumor suppressor properties. Furthermore, polymorphisms to RASSF1A also modulate microtubule association and possible tumor suppressor properties.

6.1 RASSF1A microtubule localization required two regions within the primary sequence

RASSF1A is a microtubule associated protein that co-localizes with tubulin (Figure 6.1a). Overexpression of RASSF1A in U2OS cells resulted in a distinct microtubular like appearance that enveloped the cell (Figure 6.1a, *left panel*). Interestingly, RASSF1A staining was also concentrated in the perinuclear area of the cell (Figure 6.1a, *middle panel*) and was bundled into distinct structures surrounding the nucleus but not in the nucleus (Figure 6.1a, *right panel*). Deletion analysis revealed that both amino (N)- and carboxy (C)-terminal regions of RASSF1A were required for the microtubule localization of RASSF1A (as observed for expression constructs 139 – 340 and for 1 – 300). Detailed five amino acid deletions revealed the sequences ^{131}SQAEI and ^{300}ELHNFL were required for microtubule localization (Figure 6.1b). Interestingly, ^{131}SQAEI is the ATM phosphorylation site on RASSF1A^{181} and ^{300}ELHNFL is just downstream of the site of association with the only known downstream effector of RASSF1A-mediated cell death, the modulator of apoptosis 1 (MOAP-1 at amino acid ^{311}REEEEHL).[7, 110] These results are similar to some of the published observations that suggest that both N- and C-terminal regions of RASSF1A determine microtubule localization.

6.2 Loss of RASSF1A-mediated apoptosis in the presence of the δMT mutant of RASSF1A

RASSF1A promotes death receptor-mediated apoptosis modulated by direct associations with tumor necrosis factor α receptor R1 (TNF-R1) and with TNFα related apoptosis inducing ligand R1 (TRAIL-R1, but not Fas receptor (CD95) [Figure 6.2a and Figure 6.2b and[7], respectively]. In U2OS cells, we have observed a robust stimulus dependent association of RASSF1A with both TNF-R1 and TRAIL (Figure 6.2a). However, unlike the wild type, RASSF1A microtubule defective mutant (δMT) significantly lost its ability to associate with both TNF-R1 and TRAIL-

R1 (Figure 6.2a and b), suggesting that microtubule localization is required for death receptor association.

Furthermore, in support of our data in Figure 6.2, analysis of cell death by either Annexin V staining (to determine early to mid stages of apoptosis, Figure 6.3a and b), poly (ADP-ribose) polymerase (PARP) cleavage analysis (in order to determine the levels of caspase activity, Fig. 6.3c), and the rate of internalization of the TNF-R1 (in order to determine how effectively apoptotic stimuli drives the activation of TNF-R1, Figure 6.3d) were carried out. These studies revealed that the lack of RASSF1A microtubule localization resulted in a significant loss of its ability to promote RASSF1A-driven cell death as observed by reduced Annexin V staining (Figure 6.3a and b) and reduced PARP cleavage from the 126 kDa form to the p85 kDa form (Figure 6.3c) in cells containing the δMT mutant of RASSF1A. Interestingly, the loss of microtubule localization significantly reduced the rate of TNF-R1 internalization in U2OS cells (Figure 6.3d), suggesting that RASSF1A may be an integral component of how TNF-R1 becomes internalized and interacts with signaling components. These observations validate the role of RASSF1A in cell death and the biological importance for RASSF1A to be tethered to microtubules.

6.3 The δMT mutant of RASSF1A does not lose its ability to self associate suggesting that it maintains a proper tertiary structure

As the association site for microtubule association is juxtaposed to the association site for MOAP-1, we investigated MOAP-1 association with wild type and δMT mutant of RASSF1A. MOAP-1 can associate with both wild type and the δMT mutant of RASSF1A in a time dependent manner as previously observed [data now shown and[7]]. Similarly, RASSF1A self

association was preserved in the δMT mutant of RASSF1A in a similar way to wild type self association (Figure 6.4a). This self association is required prior to RASSF1A recruitment to death receptors.[110] These data suggest that the δMT mutant of RASSF1A still maintained a tertiary structure to allow for both self and MOAP-1 association but not death receptor association.

6.4 Cell cycle dependent associations of RASSF1A with - and γ-tubulin

Several groups have demonstrated association of RASSF1A with α-,β- and γ-tubulin.[123-125] However, a comprehensive analysis of how RASSF1A can associate with tubulin has not been carried out. We proceeded to test the association of RASSF1A with α- and γ-tubulin under asynchronous conditions, S phase arrest (+ hydroxyurea treatment) or M phase arrest (+ nocodazole) (Figure 6.4). Confirming the importance of RASSF1A in mitosis, robust associations with RASSF1A was only observed under M phase arrest with 2 μM nocodazole treatment (compare lanes 1, 3, and 5 of Figure 6.4b, left and right panels). Not surprisingly, the δMT mutant of RASSF1A did not significantly associate with α- and γ-tubulin (compare lanes 2, 4, and 6 of Figure 6.4b, left and right panels). In order to further confirm mitotic specific association of RASSF1A with tubulin, we carried out cell cycle arrest in S phase with the addition of hydroxyurea overnight followed by release from S phase arrest by removing the media and adding fresh media for the indicated times after release. RASSF1A associated with γ-tubulin at 3 h after release from S-phase arrest, a time when majority of the cells were in M phase (cell cycle profiles were confirmed by FACS analysis, Figure 6.8). By 6 h and 9 h after release from hydroxyurea association with γ-tubulin was lost. These data suggest that

RASSF1A/tubulin association is cell cycle dependent with specific and robust association during M phase.

6.5 RASSF1A regulation of tubulin stability

Several groups have also demonstrated that RASSF1A can stabilize microtubules by affecting both their polymerization and acetylation states (as described for β-tubulin). The polymerization of tubulin was affected by overexpression of RASSF1A or by the specific loss of RASSF1A using siRNA knockdown[132] or in cells from *Rassf1a*$^{-/-}$ mice.[95, 121] In this study, we specifically addressed whether the loss of microtubule association (as observed for the δMT mutant of RASSF1A) may interfere with the stability of tubulin via modulation of tubulin acetylation. The more α-tubulin is acetylated the more stable it is. U2OS cells were transfected with the indicated constructs, harvested, lysed in RIPA buffer and western blotted with the indicated antibodies. Paclitaxel (Taxol) treatment of the cells resulted in the stabilization of tubulin, especially in the presence of overexpressed wild type RASSF1A (Figure 6.5*a,* middle panel). The presence of the microtubule destabilizing agents nocodazole and colchine abolished the acetylated state of α-tubulin in vector control cells and cells overexpressing the δMT mutant of RASSF1A (Figure 5a, top and bottom panels, respectively), but not in cells expression RASSF1A WT (Figure 6.5a, middle panel). Surprisingly, cells overexpressing RASSF1C also revealed a loss of acetylation of α-tubulin (Figure 6.5b, bottom panel). These data would suggest an important role for the microtubule localization of RASSF1A and the importance of 1A (and not IC isoform) of the RASSF1 gene family in maintaining tubulin stability by modulating the acetylation status of α-tubulin.

6.6 Polymorphisms to RASSF1A have reduced ability to associate with and stabilize microtubules

Numerous polymorphisms to RASSF1A have been identified. They have not been well characterized and it is currently not known if they have an impact on the physiological role for RASSF1A in cell death, microtubule stability, and/or its tumor suppressor properties. We have begun to explore the role(s) for three polymorphisms of RASSF1A: C65R (in close proximity to the C1 domain zinc finger), A133S (part of the ATM phosphorylation site), and E246K (part of the Ras binding domain)[181] (Figure 6.6a). Confocal imaging revealed that similar to wild type RASSF1A, the A133S and E246K polymorphic forms of RASSF1A localized to microtubules with < 20 % having a nuclear localization (Figure 6.6b and Figure6.9a). In contrast, the C65R polymorphic form or the δMT mutant of RASSF1A had > 80% of cells revealing a nuclear localization and predominantly did not localize to microtubules (Figure 6.6b and Figure 6.9a). Both C65R and A133S significantly lost their ability to associate with both γ-tubulin (Figure 6.6c) and α-tubulin (Figure 6.6d), whereas the E246K polymorphisms maintained the ability to associate with both γ-tubulin and α-tubulin. In addition, both C65R and A133S could not promote tubulin acetylation as efficiently as the E246K or WT RASSF1A (Figure 6.6e), confirming the reduced ability of both C65R and A133S to associate with tubulin. The lack of cytoskeletal localization of both the C65R and the δMT mutant of RASSF1 most likely explained why these two constructs lacked association with α-tubulin and the inability to promote acetylation of α-tubulin. However, it is not entirely clear why the A133S polymorphism, which maintained wild type localization, lacked the ability to associate with γ-tubulin and α-tubulin and promoted a reduced level of tubulin acetylation similar to the C65R polymorphisms (Figure 6.6f). This irregularity prompted us to explore associations with β-

tubulin, a protein known to stabilize microtubules by bridging between α-tubulin and β-tubulin dimers. To our surprise (in both U2OS and HCT116 cells), the C65R and E246K mutants did not associate with β-tubulin (Figure 6.6e) whereas wild type RASSF1A associated very weakly with β-tubulin. Interestingly, the A133S mutant robustly associated with β-tubulin suggesting a unique gain of function for this polymorphism of RASSF1A (Figure 6.6e).

We further explored how RASSF1A polymorphisms may affect the ability to promote cell death. Two key elements appear to govern the initiation of RASSF1A dependent cell death: the loss of self association[110] and the loss of association with 14-3-3 (Abu Ghazaleh et al., unpublished results). If left unchecked (by either self associations or associations with 14-3-3), RASSF1A may promote uncontrolled cell death or be involved in abnormal growth control mechanisms. As suspected, RASSF1A self association was retained in the presence of these mutants (Figure 6.9b) as well as association with 14-3-3 (Supplemental Figure 6.9c) suggesting that these polymorphisms have maintained the proper tertiary structure of RASSF1A in these associations. Furthermore, the C65R polymorphisms lacked the ability to efficiently promote PARP cleavage in the presence of TNFα (Figure 6.9e*)* whereas A133S and E246K can efficiently promoter PARP cleavage (data not shown). The loss of association with tubulin is, therefore, a direct loss of protein-protein interaction not explained by a loss or disturbance of RASSF1A tertiary structure. Interestingly, the δMT mutant of RASSF1A lacked the ability to associate with 14-3-3 suggesting that 14-3-3 associations may depend upon tethering to the cytoskeleton in a similar manner to other pro-apoptotic activators, such as Bad.[189]

6.7 The tumor suppressor property of RASSF1A is inhibited in the presence of the δMT mutant of RASSF1A and by RASSF1A polymorphisms

We next investigated how the δMT mutant of RASSF1A and these polymorphic changes of RASSF1A might affect the primary role for RASSF1A in preventing tumor formation. Using a xenograft model in athymic nude mice, HCT116 colon cancer cells (containing the indicated expression constructs) were subcutaneously injected into the flanks of the nude mice and the resulting tumors were monitored for 35 days post injection. Cells containing wild type RASSF1A were effective in significantly reducing tumor burden in these mice when compared to animals injected without RASSF1A (Figure 6.7a, compare "HA1A WT" with "Vector"). However, cells containing the δMT mutant of RASSF1A were not effective at reducing tumor burden and, additionally, contained a large population of tumors that were multi-nodal (Figure 6.7a). This suggested that if RASSF1A cannot localize to microtubules it may be ineffective as tumor suppressor protein, and, may actually function as an oncogene promoting the accelerated appearance of tumors.

We next proceeded to investigate the tumor suppressing function of the RASSF1A polymorphisms characterized in the previous section. Surprisingly, the C65R mutant of RASSF1A (localizing predominantly to the nucleus) lost its ability to prevent tumor growth and produced a large population of tumors similar to the δMT mutant of RASSF1A (compare Figure 6.7a with Figure 6.7b). Cells containing the A133S or the E248K mutant of RASSF1A promoted tumor formation significantly above that found in vector control cells and wild type RASSF1A suggesting that some tumor suppressor property was lost in the presence of these polymorphisms (Figure 6.7b). Additionally, we carried out two more controls for cysteine changes within the C1 domain of RASSF1A, a C98A and C101A/C102A change (Figure 6.9f).

C98 is not part of the C1 domain zinc finger of RASSF1A and does not perturb associations with death receptors[110] and can effectively inhibit tumour formation (Figure 6.9f). However, a C101A/C102A change was found within the C1 domain zinc finger of RASSF1A and was found to lack the ability to associate with death receptors.[110] Not surprisingly, cells containing the C101A/C102A expression construct lacked the ability to promote cell death[110] and lacked the ability to inhibit tumour formation in a xenograft model in nude mice (Figure 6.9f). These results confirm the role for RASSF1A as a tumor suppressor protein and the importance of microtubule localization. All experiments were carried out by transient transfections in HCT116 cells. We can obtain > 60% of the cells expressing the indicated construct in HCT116 cells until day 9 after transfection in tissue culture (Figure 6.10a). However, analysis of HA expression by day 35 indicated that protein expression is lost (or not detected using our anti-HA antibody). We speculate that expression exists at the beginning of the tumour assay that may be sustained for up to 6 days after subcutaneous injection and this early expression drives the growth profile of the cells towards their respective outcomes. We can observe tumour growth between day 7 and 14 for most of the expression constructs suggesting that the indicated expression constructs can drive tumour formation and commit the cell to a defined growth phenotype after day 7 even though protein expression may be lost shortly after day 7.

RASSF1A is a tumor suppressor protein that is frequently inactivated in most human cancers. In addition to inactivation by promoter specific methylation, RASSF1A polymorphisms exist that may affect the function for the protein. In this study, we demonstrate microtubule localization and amino acid requirements for this localization. Both N- and C-terminal regions are required for RASSF1A microtubule localization as a mutant missing both of these regions displayed localization to the nucleus (the δMT mutant of RASSF1A, Figure 6.1b). RASSF1A

δMT significantly lost its ability to associate with death receptors, tubulin, and lacked the ability to stabilize tubulin acetylation. In addition, there was a significant loss of pro-apoptotic activity associated with the RASSF1A δMT and a significant increase in tumor burden when cells containing the RASSF1A δMT mutant of RASSF1A were subcutaneously injected into nude mice (Figure 6.7a). These observations would suggest that the microtubule association is directly connected to the role for RASSF1A as a tumor suppressor protein.

Numerous tumor suppressor proteins have been observed to interact with microtubule proteins and function to regulate microtubule stabilization, such as BRCA1[190], VHL[191], Adenomatous Polyposis Coli (APC1)[192], and others.[193, 194] RASSF1A now joins the growing list of tumor suppressor proteins that can modulate microtubule dynamics. In addition, RASSF1A can cooperate with some of these tumor suppressor proteins, such as APC1, to modulate intestinal homeostasis[195] Inactivation of RASSF1A and deletions in the APC1 gene are common in human colorectal cancers and may contribute to chromosomal instability in cancer cells. The effect of RASSF1A on chromosomal segregation is well documented and functions to maintain the polymerized tubular structure of tubulin within mitosis even in the presence of the microtubule depolymerization agent such as nocodazole.[121, 132] The stabilizing effect of RASSF1A is specific and does not appear to be shared with RASSF1C (Figure 6.5b), the other major splice variant of the RASSF gene family. It appears that the microtubule localization of RASSF1A is fundamental to its role as a tumor suppressor protein and a mediator of death receptor dependent apoptosis.

We have extensively described how RASSF1A can function as a pro-apoptotic modulator of death receptor signalling.[7, 110] In the present study, we additionally describe how the presence of RASSF1A on microtubules may influence death receptor associations (Figure 6.2*a* and *b*), and

endocytosis (Figure 6.3d), the stability of α-tubulin (Figure 6.5), and tumor inhibition (Figure 6.7a). All are affected by the loss of microtubule localization supporting a role for RASSF1A as a paclitaxel-like microtubule stabilizer and promoter of cell death. In addition, preliminary data demonstrated that the δMT mutant of RASSF1A promoted a faster rate of migration of cells following wounding when compared to wild type cells (Figure 6.10b). This observation is in line with high oncogenic properties of the δMT mutant of RASSF1A and it highlights the important of microtubule localization of RASSF1A in not only preventing tumor formation but, possibly, inhibiting metastasis.

Recently, RASSF1A has been demonstrated to associate with the MAP1B homolog C19ORF5/RASSF1A-binding protein 1 (RABP1)[129, 131, 132] and how RASSF1A may play a role in the localization of C19ORF5 to the mitochondria. Within the mitochondria, C19ORF5 was found in association with the leucine rich PPR-motif containing protein (LRPPRC)[128], a nucleic acid binding, mitochondria-associated protein. LRPPRC is involved in cytoskeletal dynamics, nucleocytosolic shuttling, and chromosome activity[196, 197], but does not associate directly with RASSF1A.[131, 188] Mutations in LRPPRC cause Leigh syndrome (French-Canadian type) that is characterized by a defect in oxidative metabolism related to abnormal mitochondrial cytochrome c oxidase activity.[198-200] It will be interesting to explore how the δMT mutant of RASSF1A (or RASSF1A polymorphisms) may perturb the RASSF1A/C19ORF5/LRPPRC complex and influence microtubule and mitochondrial dynamics.

If RASSF1A is not on microtubules, we and others have demonstrated that RASSF1A can be localized to the nucleus (Figure 6.1). A role of RASSF1A within the nucleus is currently unexplored. We have demonstrated association with $p120^{E4F}$, a zinc finger transcription factor that differentially regulates the adenovirus E4F gene in an E1Adependent manner.[201, 202] In

addition, $p120^{E4F}$ can also associate with $p14^{ARF}$, retinoblastoma, and $p53$[203-205] linking RASSF1A to other tumor suppressor proteins. The RASSF1A/$p120^{E4F}$ association was found to enhance G1 cell cycle arrest and S phase inhibition and promote the stabilization of cyclins.[201, 203] Within the primary sequence of RASSF1A, two potential nuclear export sequences (NES) can found that follow the consensus sequence, LxxxLxxL[206]: ^{10}LIELREL and ^{301}LHNFLRIL (numbers denote amino acid number within the primary sequence of human RASSF1A). Interestingly, 17/35 or 48% of the leucine residues within the primary sequence of RASSF1A are found within the last 100 amino acids. It is uncertain if these residues function as an NES and it is unknown how RASSF1A enters into the nucleus as it does not appear to have a nuclear localization signal as determined by the NucPre program of the Stockholm Bioinformatics center at http://www.sbc.su.se/~maccallr/nucpred/cgi-bin/single.cgi).[207]

Numerous polymorphisms to RASSF1A can be found in cancer patients (Figure 6.6a). In this study, we have begun to explore the role(s) for three polymorphisms of RASSF1A: C65R (in close proximity to the C1 domain zinc finger), A133S (part of the ATM phosphorylation site), and E246K (part of the Ras binding domain).[181] The E246K mutant of RASSF1A mimicked the properties of wild type RASSF1A. However, the C65R polymorphism was found to localize to the nucleus (Figure 6.6b), lacked the ability to associate with tubulin and promote tubulin stability in comparison to the wild type protein (Figure 6.6c-e), lacked the ability to regulate entrance into mitosis[125], and significantly promoted the appearance of tumors in nude mice suggesting oncogenic characteristics (Figure 6.7b). Interestingly, the A133S polymorphism was found to localize to microtubules (Figure 6.6b), lacked the ability to associate with α- and γ-tubulin but gained the ability to associate with β-tubulin (Figure 6.6c – e), and promoted tumour formation similar to the E246K in an accelerated manner when compared to wild type and vector

control cells. We speculate that under specific cellular conditions and/or settings these polymporhisms will behave differently to modulate biology. Our observations are in line with those by Dallol et al (2004)[125] suggesting importance to some of the RASSF1A polymorphisms. Based on our observations, there is a great need to explore how other polymorphisms of RASSF1A may influence its cellular localization, ability to stabilize tubulin, promote cell death and inhibit tumor formation. Our results strongly suggest that some polymorphic changes may be as devastating as the loss of RASSF1A expression and may directly influence the tumor suppressor properties of RASSF1A and play an important role tumourigenesis.

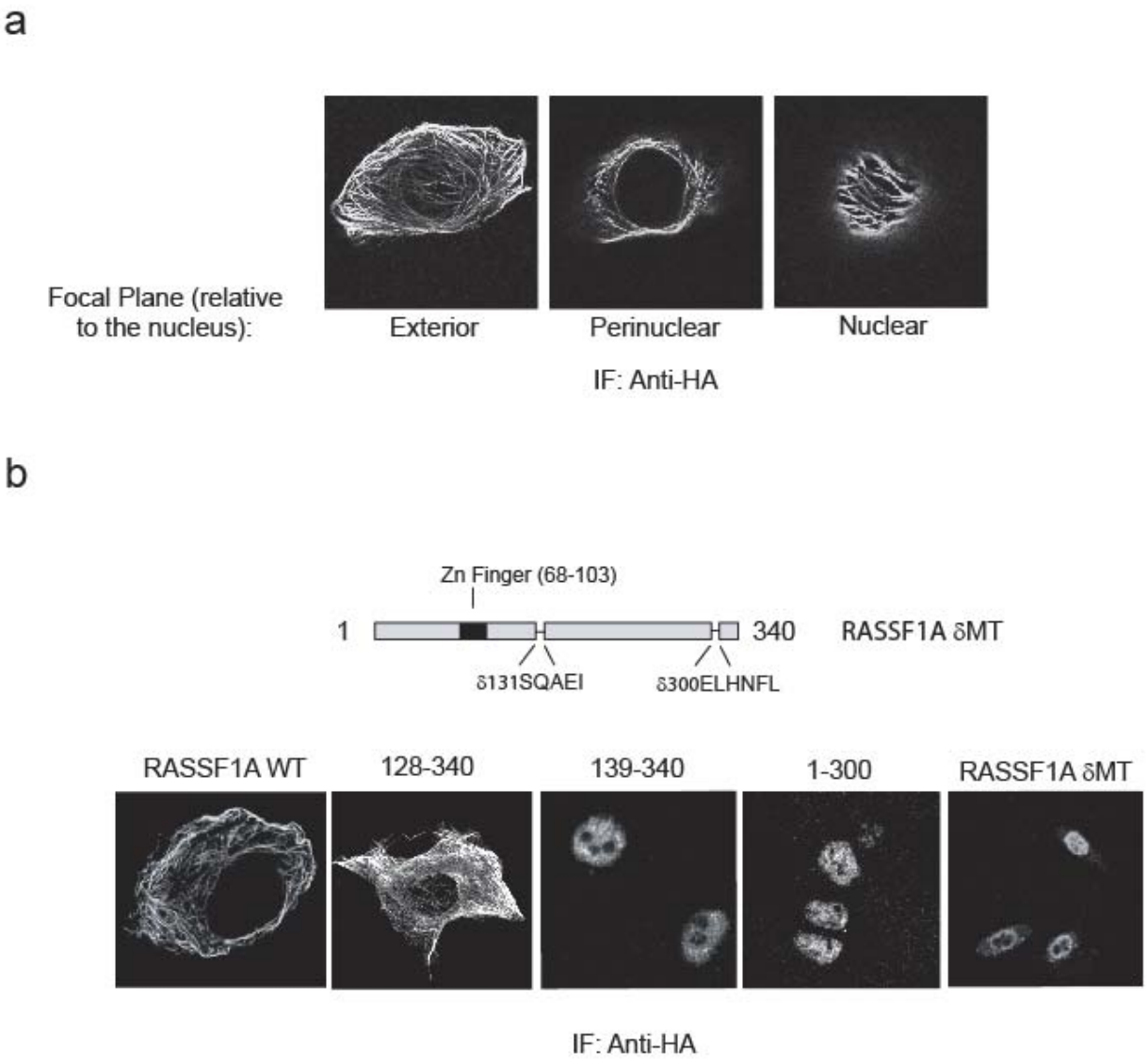

Figure 6.1: RASSF1A microtubule localization is modulated by two amino acid stretches within the primary sequence. U2OS cells were transfected onto square 12 cm X 12 cm coverslips with (a) wild type RASSF1A or (b) truncated mutants of RASSF1A using an HA expression construct. Fourty-eight hours after transfection cells were immunostained with mouse anti-HA antibody and rabbit anti-mouse Alexa 546 secondary antibody. Cellular localization of RASSF1A was visualized by confocal microscopy using a Zeiss microscope. Numbers refer to the amino acid location within the primary sequence of RASSF1A (accession number AF102770). IF, immunoflourescence.

a

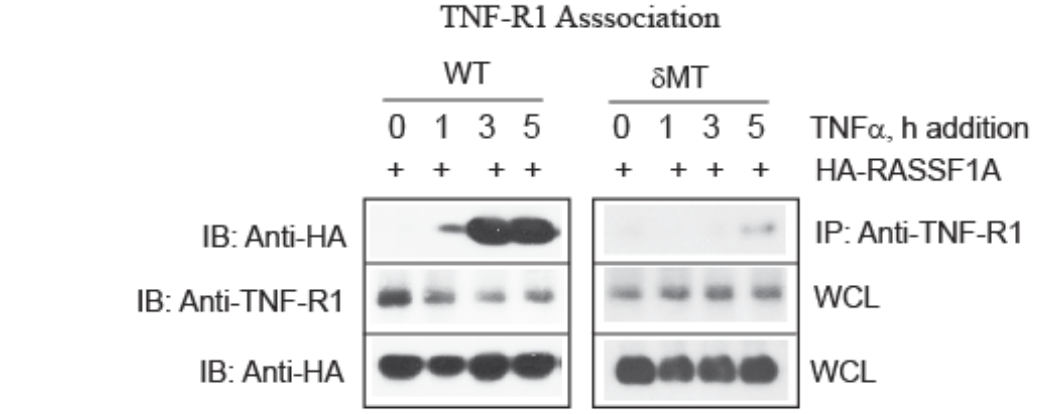

b

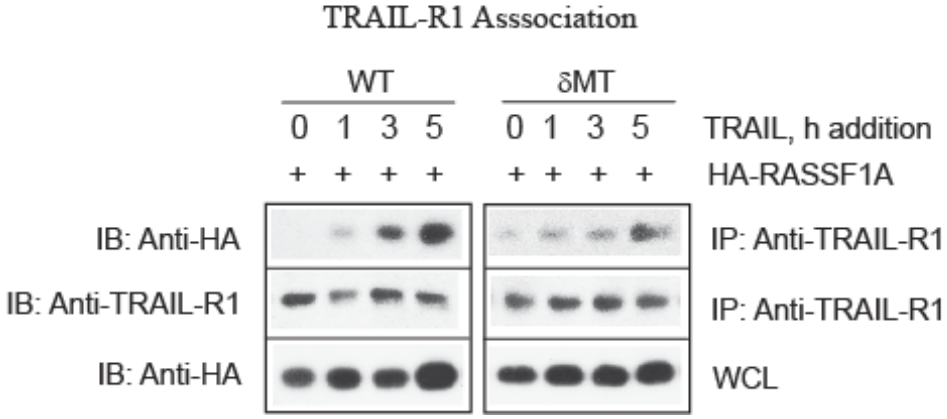

Figure 6.2: Loss of RASSF1A microtubule association results in the loss of death receptor association. HA tagged RASSF1A wild type (WT) or δMT proteins were ectopically expressed in U2OS cells. Following either TNFα (**a, c**) or TRAIL (**b**) stimulation, associated RASSF1A was recovered by immunoprecipitation (IP) with the respective death receptor antibody (**a, b**) or anti-HA antibody (**c**) and recovered proteins were separated by SDS-PAGE and immunoblotted (IB) with the indicated antibodies.

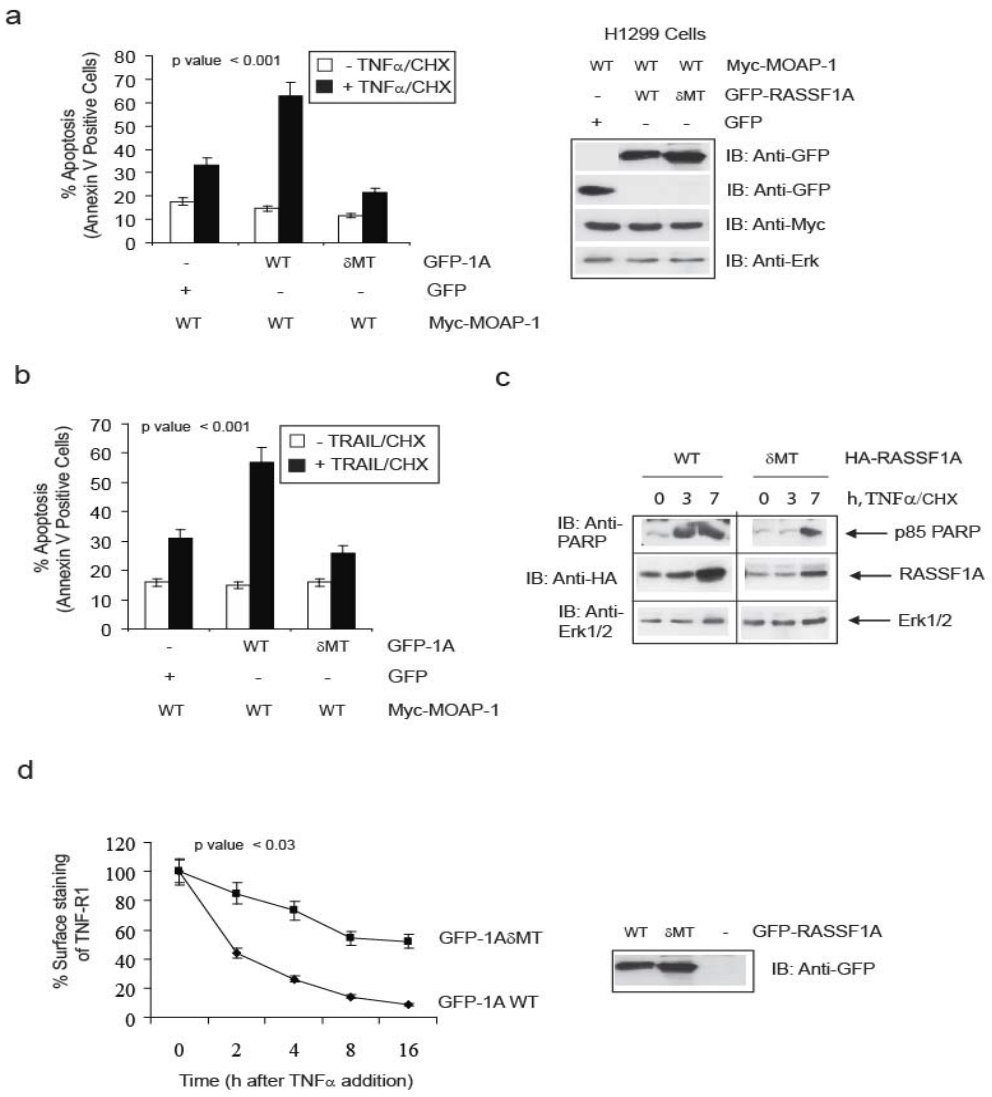

Figure 6.3: Loss of RASSF1A microtubule association results in decreased ability to induce cell death. (**a and b**) H1299 stable cells containing Myc-MOAP-1 were transiently transfected with GFP-RASSF1A WT or the δMT mutant of RASSF1A. Annexin V/Propidium iodide staining of TNFα/cyclohexamide (CHX) (**a**) and TRAIL/(CHX) (**b**) treated cells was carried out for 16 h. *Right panel to A*: expression of proteins used in Annexin V staining for both (**a**) and (**b**). Experiment was repeated 6 times and significance was evaluated by Student's T-test (two-tailed) with the indicated p value (*) < 0.001. CHX is a protein synthesis inhibitor that was used to inhibit survival signals and allow cell death to be observed in the cancer cells used in this study. All FASC analyses were carried out on GFP-positive cells. (**c**) HA-RASSF1A WT or δMT mutant were ectopically expressed in U2OS cells and associated TNFα/CHX-evoked PARP cleavage (see IB: Anti-PARP) was detected using an anti-PARP antibody in order to detect the cleaved form of PARP (p85 PARP). Also indicated are expression levels for HA-RASSF1A and anti-Erk1/2 expression as loading controls. (**d**) Stable cells containing either HA-RASSF1A WT or δMT mutant were generated and stimulated with TNFα for the indicated times and the amount of surface TNF-R1 determined by FACS analysis as described in Experimental Procedures. Experiment was repeated 5 times and significance was evaluated by Student's T-test (two-tailed) with the indicated p value. *Right panel to* (**d**): expression of proteins in the stable U2OS cells.

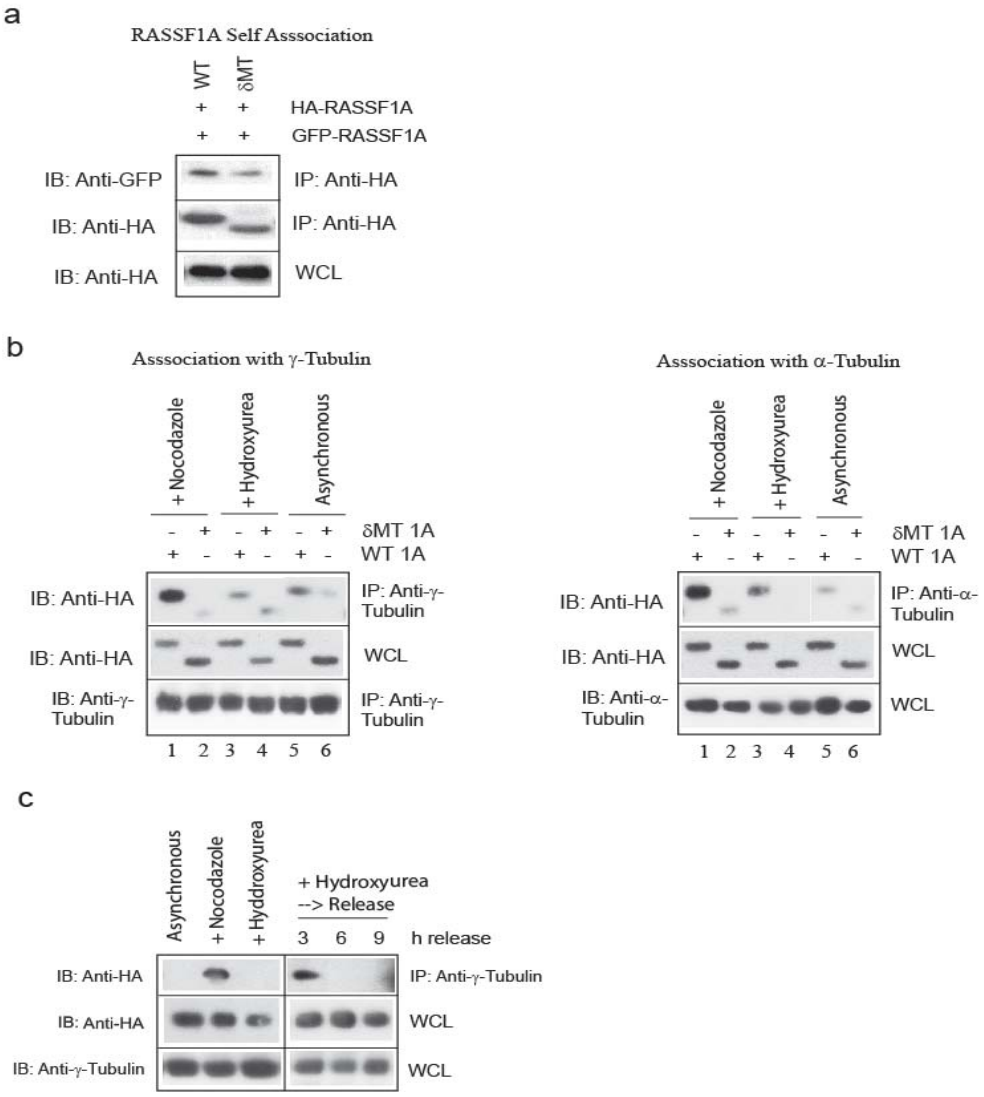

Figure 6.4: RASSF1A δMT mutant results in the loss of association α-tubulin and γ-tubulin association, but not self association. (**a**) GFP-RASSF1A was co-transfected with HA tagged RASSF1A WT or δMT proteins in U2OS cells. RASSF1A self association was determined by IP with anti-HA antibodies followed by immunoblotting (IB) with the indicated antibodies. (**b**) HA tagged RASSF1A WT or δMT proteins were ectopically expressed in U2OS cells followed by immunoprecipitation (IP) with either a γ-tubulin antibody (*left panel*) or an α-tubulin antibody (*right panel*) and recovered proteins were separated by SDS-PAGE and immunoblotted (IB) as indicated. Analysis was carried out using asynchronous/interphase, S-phase (+ Hydroxyurea), or M-phase (+ Nocodazole) arrested cells. C, HA tagged RASSF1A WT or δMT proteins were ectopically expressed in U2OS cells followed by immunoprecipitation (IP) with γ-tubulin antibody during interphase (asynchronous cells), S-phase (+ Hydroxyurea), M-phase arrest (+ Nocodazole), or release from S-phase arrest (+ Hydroxyurea → release). IP samples were recovered and proteins separated by SDS-PAGE and immunoblotted (IB) as indicated.

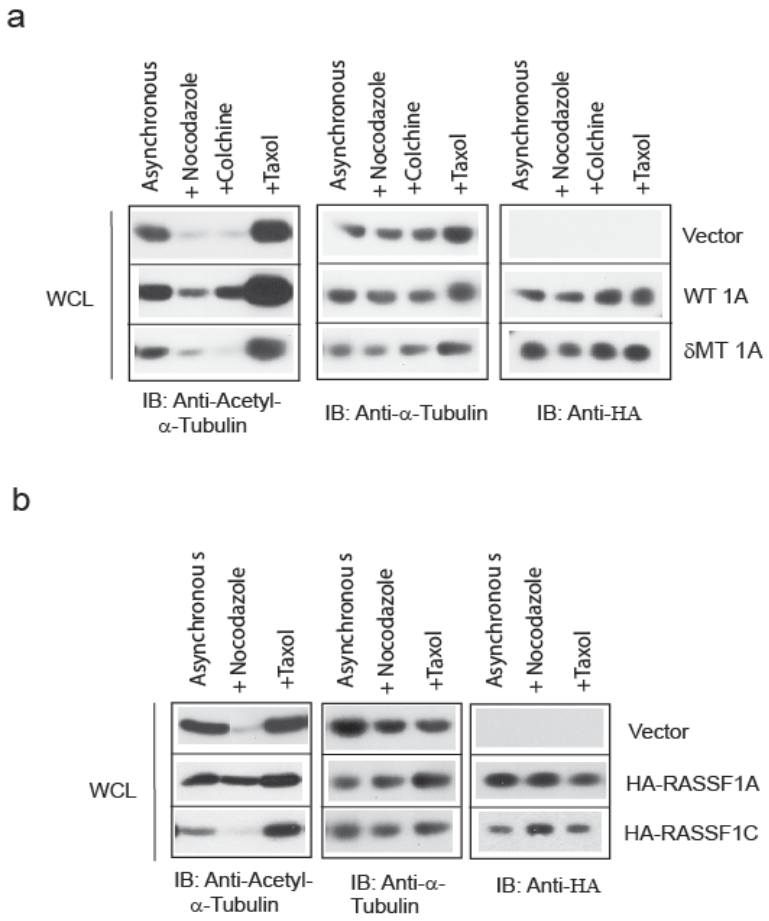

Figure 6.5: RASSF1A plays a role in stabilizing tubulin. U2OS cells were ectopically expressed with either vector, HA tagged RASSF1A (1A) WT or δMT proteins (**a**) or with RASSF1C (**b**). Cells were treated with nocodazole and colchine (microtubule destabilization agents) or with taxol (a microtubule stabilizing agent). Following treatment, cell lysates were generated by RIPA lysis, proteins separated by SDS-PAGE and immunoblotted (IB) as indicated.

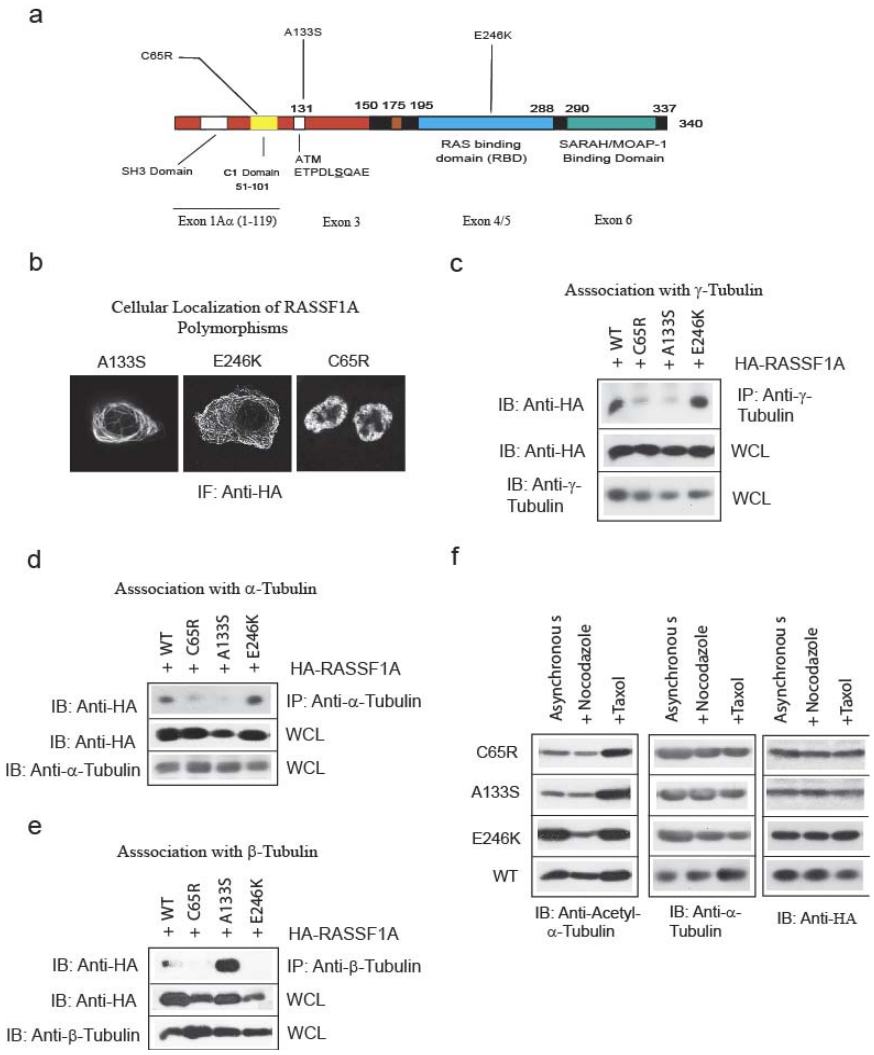

Figure 6.6: Biochemical characterization of RASSF1A polymorphisms. (**a**) Schematic of RASSF1A domains and location of polymorphisms identified in some cancer patients. Polymorphisms are described as such: the C65R denotes a cysteine to arginine change at position 65 of the amino acid sequence. Approximate positions of exons are also indicated. (**b**) U2OS cells were transfected onto square 12 cm X 12 cm coverslips with the indicated HA expression construct. Fourty-eight hours after transfection cells were immunostained with mouse anti-HA antibody and rabbit anti-mouse Alexa 546 secondary antibody. Cellular localization of RASSF1A was visualized by confocal microscopy using a Zeiss microscope. Similar results were obtained in HCT116 cells (data not shown) and a quantification of this is shown in Figure 6.9a. IF, immunoflourescence. (**c, d and e**) HA tagged RASSF1A wild type (WT) or RASSF1A polymorphisms were ectopically expressed in HCT116 cells, treated with 2 μM nocodazole overnight and association with γ-tubulin (**c**), α-tubulin (**d**), or β-tubulin (**e**) was carried out. Associated RASSF1A was recovered by immunoprecipitation (IP) with the indicated antibodies and recovered proteins were separated by SDS-PAGE and immunoblotted (IB) as indicated. (**e**) Stability of α-tubulin was characterized as described in Figure 5b. HCT116 cells were ectopically expressed with the indicated expression mutants of RASSF1A. Following treatment with these agents, cell lysates were generated, proteins separated by SDS-PAGE and immunoblotted (IB) as indicated.

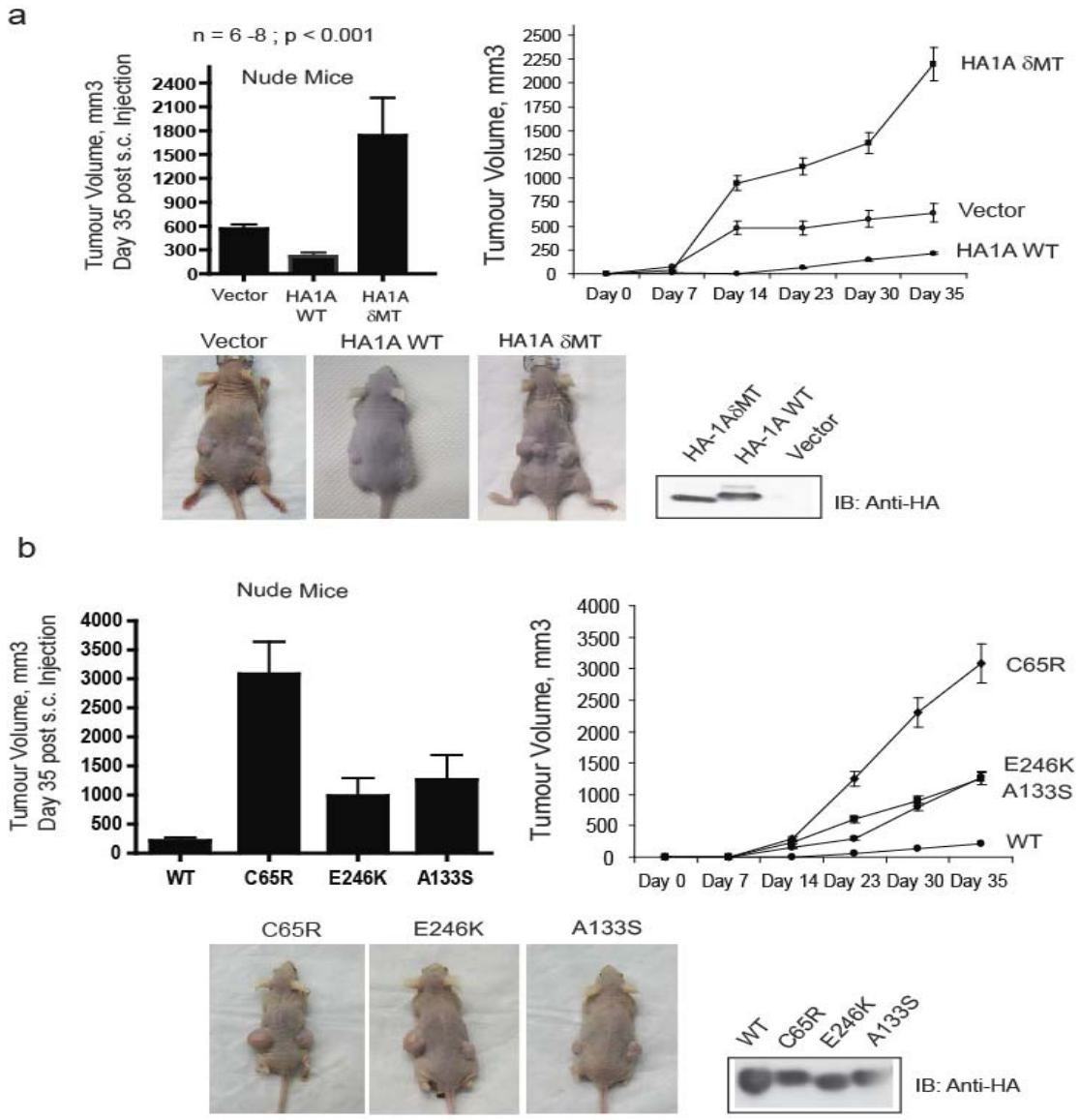

Figure 6.7: Tumor promoting potential of RASSF1A δMT mutant and RASSF1A polymorphisms. Male athymic nude mice were purchased at 6 – 8 weeks of age from Taconic Laboratories and used in tumorigenicity experiments. Once tumors were formed (usually about day 10 to 15), growth was followed until tumors were about 20 mm in size. Tumor volume was calculated based on a spherical appearance using the formula $4/3\pi r^3$. In both **a** and **b**, (i) *top left panel* represents tumor growth at day 35; (ii) *top right panel* is tumor growth increases with time; (iii) *bottom left panel* is a representative mouse showing subcutaneous tumor in the flanks for the nude mice; (iv) *bottom right panel* is an immunoblot of the expression of proteins used in these assays. For each expression construct 6-8 animals were injected on both flanks to give 12-16 measures of tumor growth and significance was evaluated by either Student's T-test (two-tailed) for both (**a**) and (**b**). p values for (**b**): between C65R and WT (< 0.003); between C93A and WT (< 0.004); between E246K and WT (<0.008); and between A133S and WT (<0.01). Experiments in **(a)** and **(b)** were conducted at the same time and thus have the same vector control results. All experiments were carried out using cells from transiently transfected HCT116 cells that give > 60% transfection efficiencies.

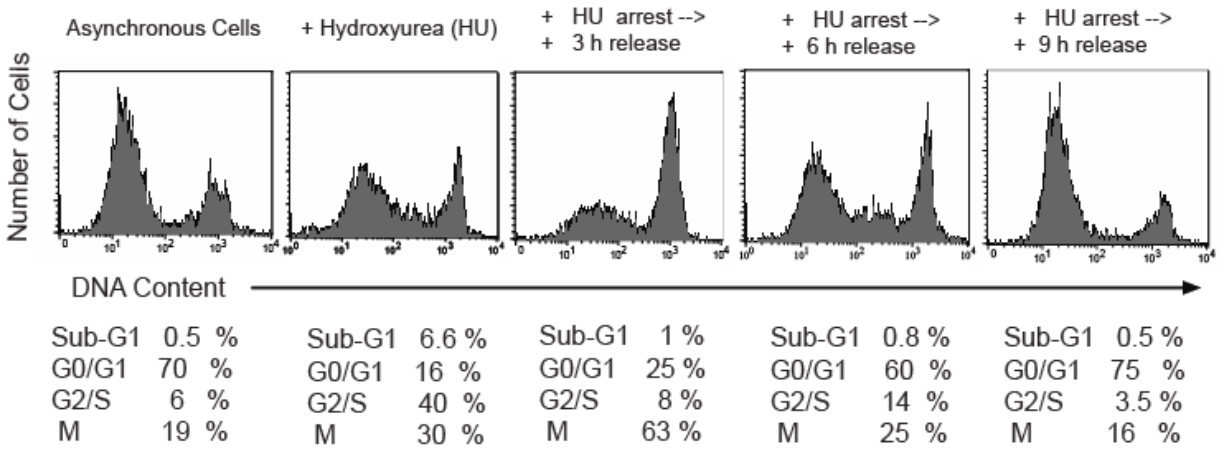

Figure 6.8: Cell cycle profile using hydroxurea arrest and release. U2OS cells were left untreated (asynchronous cells) or treated with hydroxyurea for 16 h followed by release from arrest by adding fresh media to the cell. Release was allowed for the indicated times and FACS analysis carried out to confirm cell cycle profile following arrest and release. Numbers indicated percentage of cells within each given population.

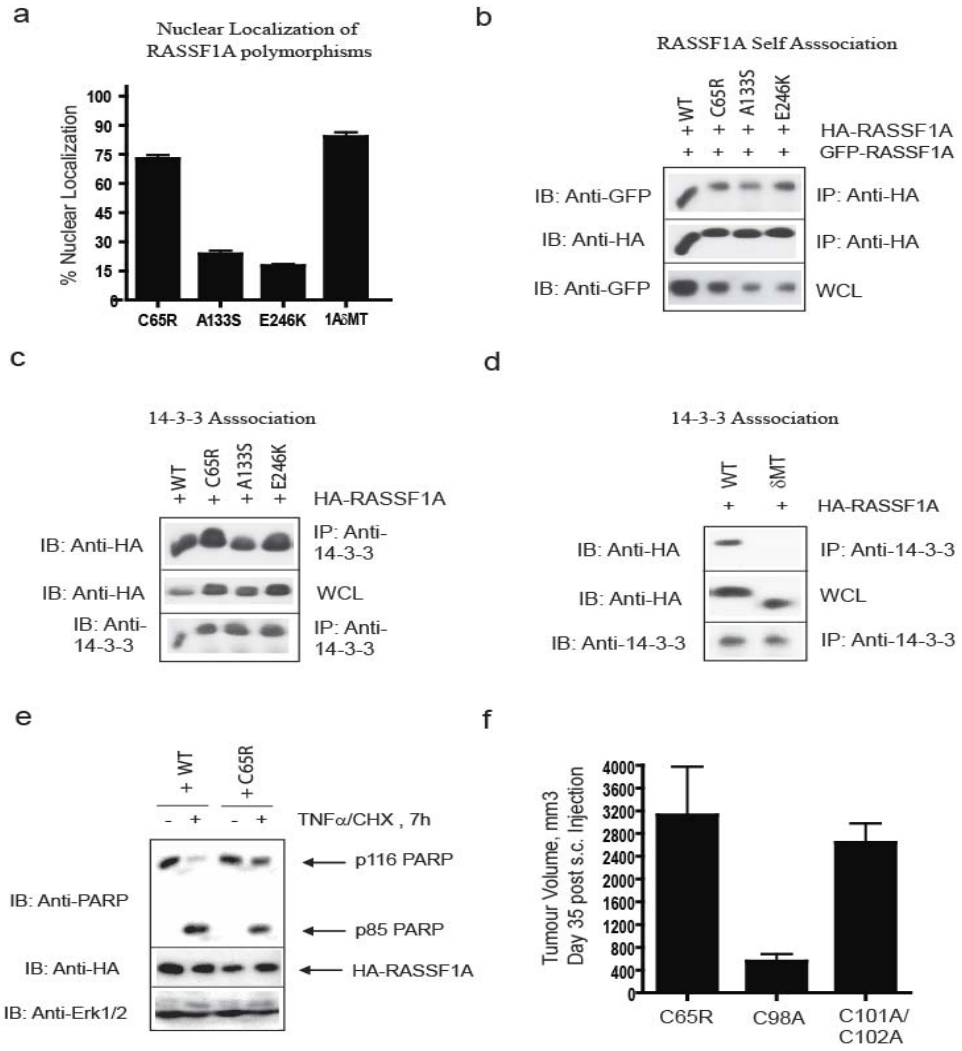

Figure 6.9: Characterization of RASSF1A polymorphisms. (**a**) HCT116 cells were transfected with the indicated expression constructs and imaged on a confocal microscope to determine cellular localization. About 75 – 100 cells were counted and percentage of nuclear staining is graphed. The experiment was repeated three times. IF, immunoflourescence. **(b and c**) HA tagged RASSF1A wild type (WT) or RASSF1A polymorphisms were ectopically expressed in HCT116 cells followed by self association with GFP-RASSF1A (**b**) or association with 14-3-3 (**c**). Associated RASSF1A was recovered by immunoprecipitation (IP) with the indicated antibodies and recovered proteins were separated by SDS-PAGE and immunoblotted (IB) as indicated. (**d**) HA tagged RASSF1A WT or δMT proteins were ectopically expressed in U2OS cells followed by immunoprecipitation (IP) with a pan specific 14-3-3 antibody and recovered proteins were separated by SDS-PAGE and immunoblotted (IB) as indicated. (**e**) HA-RASSF1A WT (WT) or C65R mutant of RASSF1A were ectopically expressed in U2OS cells and associated TNFα/CHX-evoked PARP cleavage (see IB: Anti-PARP) was detected using an anti-PARP antibody in order to detect full length PARP (p116PARP) and cleaved PARP (p85 PARP). Also indicated are expression levels for HA-RASSF1A and anti-Erk1/2 immunoblotting as loading controls. (**f**) Male athymic nude mice were purchased at 6 – 8 weeks of age from Taconic Laboratories and used in tumorigenicity experiments as outlined in Fig. 6.7. For each expression construct 3 animals were injected on both flanks to give 6 measures of tumor growth and significance was evaluated by either Student's T-test (two-tailed). p values between C65R and C98A (< 0.03); between C65R and C101A/C102A (< 0.6).

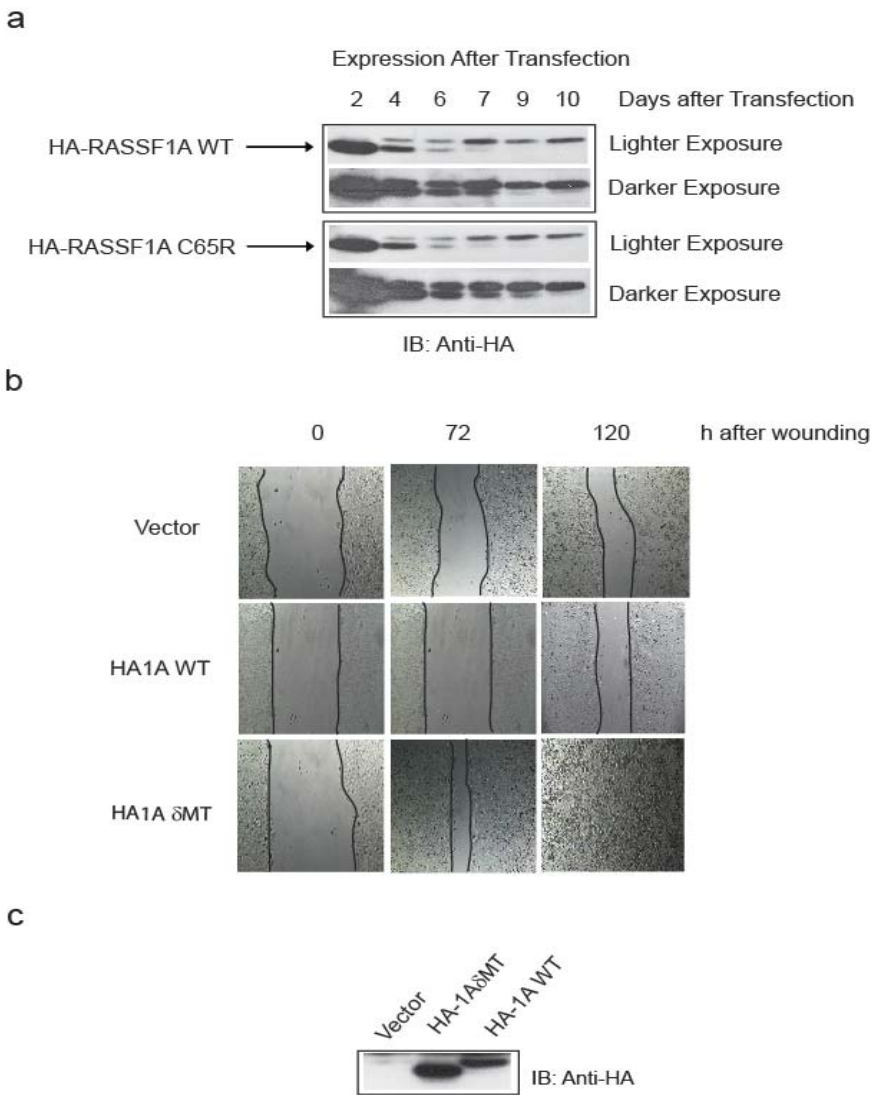

Figure 6.10: Expression of RASSF1A in transfected HCT116 cells and the loss of RASSF1A microtubule association results in increased migration rate of cells. **(a)** HCT116 cells were transfected with the indicated expression constructs and cells maintained in culture for the indicated times. At the indicated times, cells were harvested, lysed in SB lysis buffer and then prepared for immunoblotting as indicated. (**b**) Stable U2OS cells containing either vector control, RASSF1A WT or δMT expression constructs were grown to confluency in a 6 well dish followed by scratching of the center of the well using a pipet tip to "wound" the cells. After the indicated time points, the image was captured to reveal the speed of migration of these cells following wounding. (**c)** Expression of proteins in the stable U2OS cells used in b.

Chapter 7

Discussion

Inflammatory bowel disease (IBD) (such as Crohn's disease [CD] and ulcerative colitis [UC]) are chronic intestinal diseases characterized by inflammation of the gastrointestinal area (the large and small intestine) resulting in abdominal pain, chronic diarrhoea, and weight loss. IBD affects 1 in 1000 individuals and molecularly, it is characterized by hyperactivation of the transcription factor, NFκB, and elevated production of regulated cytokines.[37, 38] The NFκB pathway originates from several receptor dependent mechanisms and shares common elements with some apoptotic components (such as the TNFα receptor, TNF-R1).[208-211] IBD has genetic linkages on several chromosomes including chromosome 1q32 (encoding for IL-10), 1p31 (encoding the IL-23 receptor), chromosome 16q12 (encoding for NOD2), and uncharacterized linkages on 3p21(the chromosomal location for RASSF1A).[22-26] Some IBD genetic linkages have been characterized using mouse knockout models but they generally do not reflect the human disease.[22, 171]

The tumor suppressor gene RASSF1A modulates a broad range of cellular functions that are essential for normal growth control. It has been demonstrated that RASSF1A modulates the cell death pathway by associating with TNF-R1 upon TNFα stimulation.[7, 110] We are now defined a negative of RASSF1A in modulating innate immunity through affecting the transcription factor, NFκB, a key modulator of inflammation. We speculate the RASSF1A is a new susceptibility gene for IBD and an important component to restrict uncontrolled inflammation. Therefore RASSF1A could be considered a link between inflammation and cancer.

The functional association between inflammation and cancer dates back to Virchow[212], who in 1863 hypothesized that cancer arises in sites of inflammation because prolonged irritation, tissue injury, and activated local host response ultimately favored cell proliferation.

Although it is currently understood that simple cell proliferation does not result in cancer, it is also clear that sustained cell proliferation in an environment rich in inflammatory cells, growth factors, activated stroma, enhanced angiogenesis, and DNA-damaging agents may provide the conditions needed for tumor formation and progression. Indeed, it has been estimated that cancer is preceded by chronic inflammation in up to a third of all cases.[213] Examples include chronic bronchitis and lung cancer, papillomavirus infection and cervical cancer hepatitis B and C and liver cancer, asbestosis and mesothelioma, and inflammatory bowel disease and colorectal cancer. Therefore understanding the biological functions of RASSF1A which has been characterized to affect inflammation and cancer formation is very important.

As mentioned earlier, numerous mouse models have been established that have either deletions or mutations in key regulatory elements involved in NFκB activation and TLR function. To varying degrees, these models are useful in understanding the pathogenesis of IBD since Crohn's disease and ulcerative colitis have multifactorial etiologies. An underlying hallmark of IBD is enhanced NFκB activation and elevated production of regulated cytokines. In our current study, we have explored the use of *Rassf1a*$^{-/-}$ mice to model IBD in mice. Following challenge with either components of the bacterial cell wall or with a chemical irritant of the colonic mucosa, we have observed enhanced NFκB activation, elevated production of regulated cytokines, and destruction of the colonic mucosa indicative of the situation that exist with human IBD. Furthermore, we can use our *Rassf1a*$^{-/-}$ mice to test new therapies in the treatment of IBD. We speculate that RASSF1A is a new and novel susceptible gene for IBD on chromosome 3p21 and understanding the molecular mechanisms involved in RASSF1A-dependent modulation of NFκB is greatly needed in understanding the pathogenesis of IBD and how the duration of the inflammatory response is regulated.

Future experiments

Future experiments that will build on our current knowledge of RASSF1A and inflammation include: (1) The generation of two tissue specific knockouts whereby RASSF1A is missing in the intestinal epithelial cells and in macrophages. LPS IP injection experiment (to target TLR4) and the DSS treatment (to induce an acute colitis like phenotype) will be carried on the tissue specific mice (together with untreated wild type mice). We propose that the intestinal epithelial (IE) and macrophage specific RASSF1A knockout may better model IBD in mice. We propose that in patients with IBD, multiple changes may occur within the epithelial layer of the GI system or in cells poised to defend against invading pathogens, such as macrophages, that may result in uncontrolled inflammation. The use of the IE and macrophage specific mouse may answer these questions. It is possible that other gut cells types or non-macrophage cells (such as B and T cells) influence innate immunity in our system and contribute to uncontrolled inflammation in our *Rassf1a*$^{-/-}$ mice.

(2) Once we have determined the specific NFκB/TLR pathway modulated by RASSF1A, we can carry out a detailed analysis of NFκB activity in our tissue specific knockouts following TLR stimulation by looking to ChIP analysis (Chromatin immunoprecipitation), detection of mouse NFκB (mainly the p65 subunit) and monitoring IκBα phosphorylation and degradation levels in mice tissues. Limitations of our techniques include NFκB antibody for ChIP analysis (Chromatin immunoprecipitation), detection of mouse NFκB (mainly the p65 subunit) and monitoring IκBα phosphorylation and degradation levels in mice tissues. In addition, the use of the *Moap-1*$^{-/-}$ single and *Rassf1a*$^{-/-}$*/Moap-1*$^{-/-}$ double knockout mouse will be useful in determining how important MOAP-1 is for the role of RASSF1A as a negative modulator of inflammation. (3) We have determined that TLR2, TLR4, and TLR9 strongly associate with

RASSF1A. Therefore, survival of these mice will further investigated following IP injections of 10 to 15 μg/g body weight with CpG DNA (to target TLR9), and PAM_3CSK_4 (to target TLR2 and TLR6). Once experiments are done, tissue histology (mainly liver and colon) from the treated mice (mainly from overnight stimulations) will be carried on and scored for infiltration of cells, generally using H&E staining and specifically using markers for macrophages (Mac-1) and for natural killer (NK) cells. (4) An analysis of NFκB activity in cells directly involved in inflammation following treatment with either LPS or DSS. These include bone marrow derived macrophages (BMDM), lamina propria lymphocytes (LPL) and intestinal crypt cells (ICC). BMDM are one of the first cells the home into the site of infection and respond to pathogenic insults. LPLs function to regulate the duration and intensity of mucosal immune responses. Lack of LPL can lead to the pathogenesis of spontaneous bowel inflammation in many animal models. ICC cells are directly activated by pathogens and by the actions of macrophages. For all these cells, nuclear extracts will be obtained and NFκB DNA binding levels using an Electophoretic mobility shift assays (to test DNA binding ability of NFkB) and immunostaining for IκBα and p65 NFκB to detect NFkB release and nuclear presence, respectively).

Summary

The specific role for RASSF1A in modulating the NFκB-dependent inflammation will offer a unique chance to investigate the importance of how chronic inflammation (originating from NFκB) may constitute a risk factor for cancers. We hope to better model human IBD in mice and *Rassf1a*$^{-/-}$ mice may be a unique model to test new therapies. A complete understanding of the RASSF1A molecular pathway (linked to NFκB) may offer an alternative target for therapy for

IBD patients and other inflammatory disorders and how inflammation may constitute a risk factor for cancers.

Chapter 8

References

1. Sherr, C.J. Principles of tumor suppression. *Cell* **116**, 235-46 (2004).

2. Sawyers, C. Targeted cancer therapy. *Nature* **432**, 294-7 (2004).

3. Vousden, K.H. Activation of the p53 tumor suppressor protein. *Biochim Biophys Acta* **1602**, 47-59 (2002).

4. Ivanov, V.N., Bhoumik, A. & Ronai, Z. Death receptors and melanoma resistance to apoptosis. *Oncogene* **22**, 3152-61 (2003).

5. Kroemer, G. Mitochondrial control of apoptosis: an introduction. *Biochem Biophys Res Commun* **304**, 433-5 (2003).

6. Dammann, R. et al. Epigenetic inactivation of a RAS association domain family protein from the lung tumour suppressor locus 3p21.3. *Nat Genet* **25**, 315-9 (2000).

7. Baksh, S. et al. The tumor suppressor RASSF1A and MAP-1 link death receptor signaling to Bax conformational change and cell death. *Mol Cell* **18**, 637-50 (2005).

8. Loftus, E.V., Jr. Clinical epidemiology of inflammatory bowel disease: Incidence, prevalence, and environmental influences. *Gastroenterology* **126**, 1504-17 (2004).

9. Bernstein, C.N. et al. The epidemiology of inflammatory bowel disease in Canada: a population-based study. *Am J Gastroenterol* **101**, 1559-68 (2006).

10. Koutroubakis, I., Manousos, O.N., Meuwissen, S.G. & Pena, A.S. Environmental risk factors in inflammatory bowel disease. *Hepatogastroenterology* **43**, 381-93 (1996).

11. Ainley, C., Cason, J., Slavin, B.M., Wolstencroft, R.A. & Thompson, R.P. The influence of zinc status and malnutrition on immunological function in Crohn's disease. *Gastroenterology* **100**, 1616-25 (1991).

12. O'Morain, C., Segal, A.W. & Levi, A.J. Elemental diet as primary treatment of acute Crohn's disease: a controlled trial. *Br Med J (Clin Res Ed)* **288**, 1859-62 (1984).

13. Lochs, H. et al. Comparison of enteral nutrition and drug treatment in active Crohn's disease. Results of the European Cooperative Crohn's Disease Study. IV. *Gastroenterology* **101**, 881-8 (1991).

14. Teahon, K., Bjarnason, I., Pearson, M. & Levi, A.J. Ten years' experience with an elemental diet in the management of Crohn's disease. *Gut* **31**, 1133-7 (1990).

15. Riordan, A.M. et al. Treatment of active Crohn's disease by exclusion diet: East Anglian multicentre controlled trial. *Lancet* **342**, 1131-4 (1993).

16. Teahon, K., Smethurst, P., Pearson, M., Levi, A.J. & Bjarnason, I. The effect of elemental diet on intestinal permeability and inflammation in Crohn's disease. *Gastroenterology* **101**, 84-9 (1991).

17. Orholm, M. et al. Familial occurrence of inflammatory bowel disease. *N Engl J Med* **324**, 84-8 (1991).

18. Asquith, P., Mackintosh, P., Stokes, P.L., Holmes, G.K. & Cooke, W.T. Histocompatibility antigens in patients with inflammatory-bowel disease. *Lancet* **1**, 113-5 (1974).

19. Hugot, J.P. et al. Linkage analyses of chromosome 6 loci, including HLA, in familial aggregations of Crohn disease. G.E.T.A.I.D. *Am J Med Genet* **52**, 207-13 (1994).

20. Hugot, J.P. et al. Mapping of a susceptibility locus for Crohn's disease on chromosome 16. *Nature* **379**, 821-3 (1996).

21. Satsangi, J. et al. Two stage genome-wide search in inflammatory bowel disease provides evidence for susceptibility loci on chromosomes 3, 7 and 12. *Nat Genet* **14**, 199-202 (1996).

22. Wirtz, S. & Neurath, M.F. Mouse models of inflammatory bowel disease. *Adv Drug Deliv Rev* **59**, 1073-83 (2007).

23. Raelson, J.V. et al. Genome-wide association study for Crohn's disease in the Quebec Founder Population identifies multiple validated disease loci. *Proc Natl Acad Sci U S A* **104**, 14747-52 (2007).

24. Paavola, P. et al. Genetic analysis in Finnish families with inflammatory bowel disease supports linkage to chromosome 3p21. *Eur J Hum Genet* **9**, 328-34 (2001).

25. Hampe, J. et al. Evidence for a NOD2-independent susceptibility locus for inflammatory bowel disease on chromosome 16p. *Proc Natl Acad Sci U S A* **99**, 321-6 (2002).

26. Quaglietta, L., te Velde, A., Staiano, A., Troncone, R. & Hommes, D.W. Functional consequences of NOD2/CARD15 mutations in Crohn disease. *J Pediatr Gastroenterol Nutr* **44**, 529-39 (2007).

27. Buning, C. et al. NOD2/CARD15 gene polymorphism in patients with inflammatory bowel disease: is Hungary different? *World J Gastroenterol* **11**, 407-11 (2005).

28. Inohara, N., Ogura, Y., Chen, F.F., Muto, A. & Nunez, G. Human Nod1 confers responsiveness to bacterial lipopolysaccharides. *J Biol Chem* **276**, 2551-4 (2001).

29. Ogura, Y. et al. A frameshift mutation in NOD2 associated with susceptibility to Crohn's disease. *Nature* **411**, 603-6 (2001).

30. Mashimo, H., Wu, D.C., Podolsky, D.K. & Fishman, M.C. Impaired defense of intestinal mucosa in mice lacking intestinal trefoil factor. *Science* **274**, 262-5 (1996).

31. Schmitz, H. et al. Altered tight junction structure contributes to the impaired epithelial barrier function in ulcerative colitis. *Gastroenterology* **116**, 301-9 (1999).

32. Fiocchi, C. Inflammatory bowel disease: etiology and pathogenesis. *Gastroenterology* **115**, 182-205 (1998).

33. Fuss, I.J. et al. Disparate CD4+ lamina propria (LP) lymphokine secretion profiles in inflammatory bowel disease. Crohn's disease LP cells manifest increased secretion of IFN-gamma, whereas ulcerative colitis LP cells manifest increased secretion of IL-5. *J Immunol* **157**, 1261-70 (1996).

34. Toms, C. & Powrie, F. Control of intestinal inflammation by regulatory T cells. *Microbes Infect* **3**, 929-35 (2001).

35. Sans, M. et al. Differential role of selectins in experimental colitis. *Gastroenterology* **120**, 1162-72 (2001).

36. Koizumi, M., King, N., Lobb, R., Benjamin, C. & Podolsky, D.K. Expression of vascular adhesion molecules in inflammatory bowel disease. *Gastroenterology* **103**, 840-7 (1992).

37. de Ridder, L., Benninga, M.A., Taminiau, J.A., Hommes, D.W. & van Deventer, S.J. Infliximab use in children and adolescents with inflammatory bowel disease. *J Pediatr Gastroenterol Nutr* **45**, 3-14 (2007).

38. Baumgart, D.C. & Carding, S.R. Inflammatory bowel disease: cause and immunobiology. *Lancet* **369**, 1627-40 (2007).

39. Madrid, L.V. & Baldwin, A.S., Jr. Regulation of NF-kappaB by oncoproteins and tumor suppressor proteins. *Methods Mol Biol* **223**, 523-32 (2003).

40. Hayden, M.S. & Ghosh, S. Signaling to NF-kappaB. *Genes Dev* **18**, 2195-224 (2004).

41. Delhalle, S., Blasius, R., Dicato, M. & Diederich, M. A beginner's guide to NF-kappaB signaling pathways. *Ann N Y Acad Sci* **1030**, 1-13 (2004).

42. Orlowski, R.Z. & Baldwin, A.S., Jr. NF-kappaB as a therapeutic target in cancer. *Trends Mol Med* **8**, 385-9 (2002).

43. Xiao, C. & Ghosh, S. NF-kappaB, an evolutionarily conserved mediator of immune and inflammatory responses. *Adv Exp Med Biol* **560**, 41-5 (2005).

44. Viatour, P., Merville, M.P., Bours, V. & Chariot, A. Phosphorylation of NF-kappaB and IkappaB proteins: implications in cancer and inflammation. *Trends Biochem Sci* **30**, 43-52 (2005).

45. Wajant, H., Pfizenmaier, K. & Scheurich, P. Tumor necrosis factor signaling. *Cell Death Differ* **10**, 45-65 (2003).

46. Algeciras-Schimnich, A. et al. Molecular ordering of the initial signaling events of CD95. *Mol Cell Biol* **22**, 207-20 (2002).

47. Liu, Z.G. Molecular mechanism of TNF signaling and beyond. *Cell Res* **15**, 24-7 (2005).

48. Chung, J.Y., Park, Y.C., Ye, H. & Wu, H. All TRAFs are not created equal: common and distinct molecular mechanisms of TRAF-mediated signal transduction. *J Cell Sci* **115**, 679-88 (2002).

49. Wu, H. & Arron, J.R. TRAF6, a molecular bridge spanning adaptive immunity, innate immunity and osteoimmunology. *Bioessays* **25**, 1096-105 (2003).

50. Lawrence, T. & Bebien, M. IKKalpha in the regulation of inflammation and adaptive immunity. *Biochem Soc Trans* **35**, 270-2 (2007).

51. Miagkov, A.V. et al. NF-kappaB activation provides the potential link between inflammation and hyperplasia in the arthritic joint. *Proc Natl Acad Sci U S A* **95**, 13859-64 (1998).

52. Ohshima, H., Tazawa, H., Sylla, B.S. & Sawa, T. Prevention of human cancer by modulation of chronic inflammatory processes. *Mutat Res* **591**, 110-22 (2005).

53. Nickoloff, B.J., Ben-Neriah, Y. & Pikarsky, E. Inflammation and cancer: is the link as simple as we think? *J Invest Dermatol* **124**, x-xiv (2005).

54. Kawai, T. & Akira, S. TLR signaling. *Semin Immunol* **19**, 24-32 (2007).

55. Michelsen, K.S. & Arditi, M. Toll-like receptors and innate immunity in gut homeostasis and pathology. *Curr Opin Hematol* **14**, 48-54 (2007).

56. Gerold, G., Zychlinsky, A. & de Diego, J.L. What is the role of Toll-like receptors in bacterial infections? *Semin Immunol* **19**, 41-7 (2007).

57. Miyake, K. Innate immune sensing of pathogens and danger signals by cell surface Toll-like receptors. *Semin Immunol* **19**, 3-10 (2007).

58. O'Neill, L.A. & Bowie, A.G. The family of five: TIR-domain-containing adaptors in Toll-like receptor signalling. *Nat Rev Immunol* **7**, 353-64 (2007).

59. Roy, C.R. & Mocarski, E.S. Pathogen subversion of cell-intrinsic innate immunity. *Nat Immunol* **8**, 1179-87 (2007).

60. Doyle, S.L. & O'Neill, L.A. Toll-like receptors: from the discovery of NFkappaB to new insights into transcriptional regulations in innate immunity. *Biochem Pharmacol* **72**, 1102-13 (2006).

61. Latz, E. et al. TLR9 signals after translocating from the ER to CpG DNA in the lysosome. *Nat Immunol* **5**, 190-8 (2004).

62. Schmausser, B. et al. Expression and subcellular distribution of toll-like receptors TLR4, TLR5 and TLR9 on the gastric epithelium in Helicobacter pylori infection. *Clin Exp Immunol* **136**, 521-6 (2004).

63. Lee, J., Rachmilewitz, D. & Raz, E. Homeostatic effects of TLR9 signaling in experimental colitis. *Ann N Y Acad Sci* **1072**, 351-5 (2006).

64. Kawai, T., Adachi, O., Ogawa, T., Takeda, K. & Akira, S. Unresponsiveness of MyD88-deficient mice to endotoxin. *Immunity* **11**, 115-22 (1999).

65. West, A.P., Koblansky, A.A. & Ghosh, S. Recognition and signaling by toll-like receptors. *Annu Rev Cell Dev Biol* **22**, 409-37 (2006).

66. Takeda, K. & Akira, S. TLR signaling pathways. *Semin Immunol* **16**, 3-9 (2004).

67. Yamamoto, M. et al. Role of adaptor TRIF in the MyD88-independent toll-like receptor signaling pathway. *Science* **301**, 640-3 (2003).

68. Kim, Y. et al. MyD88-5 links mitochondria, microtubules, and JNK3 in neurons and regulates neuronal survival. *J Exp Med* **204**, 2063-74 (2007).

69. Strober, W., Fuss, I.J. & Blumberg, R.S. The immunology of mucosal models of inflammation. *Annu Rev Immunol* **20**, 495-549 (2002).

70. Morris, G.P. et al. Hapten-induced model of chronic inflammation and ulceration in the rat colon. *Gastroenterology* **96**, 795-803 (1989).

71. Okayasu, I. et al. A novel method in the induction of reliable experimental acute and chronic ulcerative colitis in mice. *Gastroenterology* **98**, 694-702 (1990).

72. Boirivant, M., Fuss, I.J., Chu, A. & Strober, W. Oxazolone colitis: A murine model of T helper cell type 2 colitis treatable with antibodies to interleukin 4. *J Exp Med* **188**, 1929-39 (1998).

73. Morrissey, P.J., Charrier, K., Braddy, S., Liggitt, D. & Watson, J.D. CD4+ T cells that express high levels of CD45RB induce wasting disease when transferred into congenic

severe combined immunodeficient mice. Disease development is prevented by cotransfer of purified CD4+ T cells. *J Exp Med* **178**, 237-44 (1993).

74. Hollander, G.A. et al. Severe colitis in mice with aberrant thymic selection. *Immunity* **3**, 27-38 (1995).

75. Powrie, F. T cells in inflammatory bowel disease: protective and pathogenic roles. *Immunity* **3**, 171-4 (1995).

76. Mombaerts, P. et al. Spontaneous development of inflammatory bowel disease in T cell receptor mutant mice. *Cell* **75**, 274-82 (1993).

77. Kuhn, R., Lohler, J., Rennick, D., Rajewsky, K. & Muller, W. Interleukin-10-deficient mice develop chronic enterocolitis. *Cell* **75**, 263-74 (1993).

78. Rudolph, U. et al. Gi2 alpha protein deficiency: a model of inflammatory bowel disease. *J Clin Immunol* **15**, 101S-105S (1995).

79. Wirtz, S. & Neurath, M.F. Gene transfer approaches for the treatment of inflammatory bowel disease. *Gene Ther* **10**, 854-60 (2003).

80. Lindsay, J.O., Ciesielski, C.J., Scheinin, T., Brennan, F.M. & Hodgson, H.J. Local delivery of adenoviral vectors encoding murine interleukin 10 induces colonic interleukin 10 production and is therapeutic for murine colitis. *Gut* **52**, 981-7 (2003).

81. Elson, C.O. et al. Monoclonal anti-interleukin 23 reverses active colitis in a T cell-mediated model in mice. *Gastroenterology* **132**, 2359-70 (2007).

82. Kullberg, M.C. et al. IL-23 plays a key role in Helicobacter hepaticus-induced T cell-dependent colitis. *J Exp Med* **203**, 2485-94 (2006).

83. Duerr, R.H. et al. A genome-wide association study identifies IL23R as an inflammatory bowel disease gene. *Science* **314**, 1461-3 (2006).

84. Hugot, J.P. et al. Association of NOD2 leucine-rich repeat variants with susceptibility to Crohn's disease. *Nature* **411**, 599-603 (2001).

85. Pauleau, A.L. & Murray, P.J. Role of nod2 in the response of macrophages to toll-like receptor agonists. *Mol Cell Biol* **23**, 7531-9 (2003).

86. Kobayashi, K.S. et al. Nod2-dependent regulation of innate and adaptive immunity in the intestinal tract. *Science* **307**, 731-4 (2005).

87. Goyette, P. et al. Gene-centric association mapping of chromosome 3p implicates MST1 in IBD pathogenesis. *Mucosal Immunol* **1**, 131-8 (2008).

88. Leonard, E.J. & Skeel, A.H. Isolation of macrophage stimulating protein (MSP) from human serum. *Exp Cell Res* **114**, 117-26 (1978).

89. Leonard, E.J. & Skeel, A. A serum protein that stimulates macrophage movement, chemotaxis and spreading. *Exp Cell Res* **102**, 434-8 (1976).

90. Agathanggelou, A. et al. Methylation associated inactivation of RASSF1A from region 3p21.3 in lung, breast and ovarian tumours. *Oncogene* **20**, 1509-18 (2001).

91. Burbee, D.G. et al. Epigenetic inactivation of RASSF1A in lung and breast cancers and malignant phenotype suppression. *J Natl Cancer Inst* **93**, 691-9 (2001).

92. Dreijerink, K. et al. The candidate tumor suppressor gene, RASSF1A, from human chromosome 3p21.3 is involved in kidney tumorigenesis. *Proc Natl Acad Sci U S A* **98**, 7504-9 (2001).

93. Kuzmin, I. et al. The RASSF1A tumor suppressor gene is inactivated in prostate tumors and suppresses growth of prostate carcinoma cells. *Cancer Res* **62**, 3498-502 (2002).

94. Tommasi, S. et al. Tumor susceptibility of Rassf1a knockout mice. *Cancer Res* **65**, 92-8 (2005).

95. van der Weyden, L. et al. The RASSF1A isoform of RASSF1 promotes microtubule stability and suppresses tumorigenesis. *Mol Cell Biol* **25**, 8356-67 (2005).

96. Dammann, R., Takahashi, T. & Pfeifer, G.P. The CpG island of the novel tumor suppressor gene RASSF1A is intensely methylated in primary small cell lung carcinomas. *Oncogene* **20**, 3563-7 (2001).

97. Wong, N. et al. Frequent loss of chromosome 3p and hypermethylation of RASSF1A in cholangiocarcinoma. *J Hepatol* **37**, 633-9 (2002).

98. Dammann, R., Yang, G. & Pfeifer, G.P. Hypermethylation of the cpG island of Ras association domain family 1A (RASSF1A), a putative tumor suppressor gene from the 3p21.3 locus, occurs in a large percentage of human breast cancers. *Cancer Res* **61**, 3105-9 (2001).

99. Kuroki, T. et al. Promoter hypermethylation of RASSF1A in esophageal squamous cell carcinoma. *Clin Cancer Res* **9**, 1441-5 (2003).

100. van der Weyden, L. & Adams, D.J. The Ras-association domain family (RASSF) members and their role in human tumourigenesis. *Biochim Biophys Acta* **1776**, 58-85 (2007).

101. Dammann, R. et al. The tumor suppressor RASSF1A in human carcinogenesis: an update. *Histol Histopathol* **20**, 645-63 (2005).

102. Agathanggelou, A., Cooper, W.N. & Latif, F. Role of the Ras-association domain family 1 tumor suppressor gene in human cancers. *Cancer Res* **65**, 3497-508 (2005).

103. Allen, N.P. et al. RASSF6 is a novel member of the RASSF family of tumor suppressors. *Oncogene* **26**, 6203-11 (2007).

104. Vos, M.D. et al. RASSF2 is a novel K-Ras-specific effector and potential tumor suppressor. *J Biol Chem* **278**, 28045-51 (2003).

105. Fujita, H. et al. Local activation of Rap1 contributes to directional vascular endothelial cell migration accompanied by extension of microtubules on which RAPL, a Rap1-associating molecule, localizes. *J Biol Chem* **280**, 5022-31 (2005).

106. Katagiri, K., Maeda, A., Shimonaka, M. & Kinashi, T. RAPL, a Rap1-binding molecule that mediates Rap1-induced adhesion through spatial regulation of LFA-1. *Nat Immunol* **4**, 741-8 (2003).

107. Vos, M.D., Martinez, A., Ellis, C.A., Vallecorsa, T. & Clark, G.J. The pro-apoptotic Ras effector Nore1 may serve as a Ras-regulated tumor suppressor in the lung. *J Biol Chem* **278**, 21938-43 (2003).

108. Ponting, C.P. & Benjamin, D.R. A novel family of Ras-binding domains. *Trends Biochem Sci* **21**, 422-5 (1996).

109. Newton, A.C. Protein kinase C. Seeing two domains. *Curr Biol* **5**, 973-6 (1995).

110. Foley, C.J. et al. Dynamics of RASSF1A/MOAP-1 association with death receptors. *Mol Cell Biol* **28**, 4520-35 (2008).

111. Kim, S.T., Lim, D.S., Canman, C.E. & Kastan, M.B. Substrate specificities and identification of putative substrates of ATM kinase family members. *J Biol Chem* **274**, 37538-43 (1999).

112. Bott, L. et al. [Ataxia-telangiectasia: a review]. *Arch Pediatr* **13**, 293-8 (2006).

113. Scheel, H. & Hofmann, K. A novel interaction motif, SARAH, connects three classes of tumor suppressor. *Curr Biol* **13**, R899-900 (2003).

114. Ortiz-Vega, S. et al. The putative tumor suppressor RASSF1A homodimerizes and heterodimerizes with the Ras-GTP binding protein Nore1. *Oncogene* **21**, 1381-90 (2002).

115. Chan, E.H. et al. The Ste20-like kinase Mst2 activates the human large tumor suppressor kinase Lats1. *Oncogene* **24**, 2076-86 (2005).

116. Hwang, E. et al. Structural insight into dimeric interaction of the SARAH domains from Mst1 and RASSF family proteins in the apoptosis pathway. *Proc Natl Acad Sci U S A* **104**, 9236-41 (2007).

117. Hesson, L.B. et al. CpG island promoter hypermethylation of a novel Ras-effector gene RASSF2A is an early event in colon carcinogenesis and correlates inversely with K-ras mutations. *Oncogene* **24**, 3987-94 (2005).

118. Cuschieri, L., Nguyen, T. & Vogel, J. Control at the cell center: the role of spindle poles in cytoskeletal organization and cell cycle regulation. *Cell Cycle* **6**, 2788-94 (2007).

119. Luders, J. & Stearns, T. Microtubule-organizing centres: a re-evaluation. *Nat Rev Mol Cell Biol* **8**, 161-7 (2007).

120. Soldati, T. & Schliwa, M. Powering membrane traffic in endocytosis and recycling. *Nat Rev Mol Cell Biol* **7**, 897-908 (2006).

121. Liu, L., Tommasi, S., Lee, D.H., Dammann, R. & Pfeifer, G.P. Control of microtubule stability by the RASSF1A tumor suppressor. *Oncogene* **22**, 8125-36 (2003).

122. Song, M.S. et al. The tumour suppressor RASSF1A regulates mitosis by inhibiting the APC-Cdc20 complex. *Nat Cell Biol* **6**, 129-37 (2004).

123. Rong, R., Jin, W., Zhang, J., Sheikh, M.S. & Huang, Y. Tumor suppressor RASSF1A is a microtubule-binding protein that stabilizes microtubules and induces G2/M arrest. *Oncogene* **23**, 8216-30 (2004).

124. Vos, M.D. et al. A role for the RASSF1A tumor suppressor in the regulation of tubulin polymerization and genomic stability. *Cancer Res* **64**, 4244-50 (2004).

125. Dallol, A. et al. RASSF1A interacts with microtubule-associated proteins and modulates microtubule dynamics. *Cancer Res* **64**, 4112-6 (2004).

126. Agathanggelou, A. et al. Identification of novel gene expression targets for the Ras association domain family 1 (RASSF1A) tumor suppressor gene in non-small cell lung cancer and neuroblastoma. *Cancer Res* **63**, 5344-51 (2003).

127. Moshnikova, A., Frye, J., Shay, J.W., Minna, J.D. & Khokhlatchev, A.V. The growth and tumor suppressor NORE1A is a cytoskeletal protein that suppresses growth by inhibition of the ERK pathway. *J Biol Chem* **281**, 8143-52 (2006).

128. Liu, L., Amy, V., Liu, G. & McKeehan, W.L. Novel complex integrating mitochondria and the microtubular cytoskeleton with chromosome remodeling and tumor suppressor RASSF1 deduced by in silico homology analysis, interaction cloning in yeast, and colocalization in cultured cells. *In Vitro Cell Dev Biol Anim* **38**, 582-94 (2002).

129. Song, M.S. et al. The centrosomal protein RAS association domain family protein 1A (RASSF1A)-binding protein 1 regulates mitotic progression by recruiting RASSF1A to spindle poles. *J Biol Chem* **280**, 3920-7 (2005).

130. Riederer, B.M. Microtubule-associated protein 1B, a growth-associated and phosphorylated scaffold protein. *Brain Res Bull* **71**, 541-58 (2007).

131. Liu, L., Vo, A. & McKeehan, W.L. Specificity of the methylation-suppressed A isoform of candidate tumor suppressor RASSF1 for microtubule hyperstabilization is determined by cell death inducer C19ORF5. *Cancer Res* **65**, 1830-8 (2005).

132. Dallol, A. et al. Depletion of the Ras association domain family 1, isoform A-associated novel microtubule-associated protein, C19ORF5/MAP1S, causes mitotic abnormalities. *Cancer Res* **67**, 492-500 (2007).

133. Danial, N.N. & Korsmeyer, S.J. Cell death: critical control points. *Cell* **116**, 205-19 (2004).

134. Thorburn, A. Death receptor-induced cell killing. *Cell Signal* **16**, 139-44 (2004).

135. Cain, K., Bratton, S.B. & Cohen, G.M. The Apaf-1 apoptosome: a large caspase-activating complex. *Biochimie* **84**, 203-14 (2002).

136. Ho, A.T. & Zacksenhaus, E. Splitting the apoptosome. *Cell Cycle* **3**, 446-8 (2004).

137. Denecker, G. et al. Death receptor-induced apoptotic and necrotic cell death: differential role of caspases and mitochondria. *Cell Death Differ* **8**, 829-40 (2001).

138. Watson, A.J. Necrosis and apoptosis in the gastrointestinal tract. *Gut* **37**, 165-7 (1995).

139. Merritt, A.J. et al. The role of p53 in spontaneous and radiation-induced apoptosis in the gastrointestinal tract of normal and p53-deficient mice. *Cancer Res* **54**, 614-7 (1994).

140. Thompson, C.B. Apoptosis in the pathogenesis and treatment of disease. *Science* **267**, 1456-62 (1995).

141. Festoff, B.W. Amyotrophic lateral sclerosis: current and future treatment strategies. *Drugs* **51**, 28-44 (1996).

142. Fesik, S.W. Promoting apoptosis as a strategy for cancer drug discovery. *Nat Rev Cancer* **5**, 876-85 (2005).

143. Fadeel, B. & Orrenius, S. Apoptosis: a basic biological phenomenon with wide-ranging implications in human disease. *J Intern Med* **258**, 479-517 (2005).

144. Guo, C. et al. RASSF1A is part of a complex similar to the Drosophila Hippo/Salvador/Lats tumor-suppressor network. *Curr Biol* **17**, 700-5 (2007).

145. Matallanas, D. et al. RASSF1A elicits apoptosis through an MST2 pathway directing proapoptotic transcription by the p73 tumor suppressor protein. *Mol Cell* **27**, 962-75 (2007).

146. Oh, H.J. et al. Role of the tumor suppressor RASSF1A in Mst1-mediated apoptosis. *Cancer Res* **66**, 2562-9 (2006).

147. Praskova, M., Khoklatchev, A., Ortiz-Vega, S. & Avruch, J. Regulation of the MST1 kinase by autophosphorylation, by the growth inhibitory proteins, RASSF1 and NORE1, and by Ras. *Biochem J* **381**, 453-62 (2004).

148. Rabizadeh, S. et al. The scaffold protein CNK1 interacts with the tumor suppressor RASSF1A and augments RASSF1A-induced cell death. *J Biol Chem* **279**, 29247-54 (2004).

149. Shivakumar, L., Minna, J., Sakamaki, T., Pestell, R. & White, M.A. The RASSF1A tumor suppressor blocks cell cycle progression and inhibits cyclin D1 accumulation. *Mol Cell Biol* **22**, 4309-18 (2002).

150. Ashida, R. et al. AP-1 and colorectal cancer. *Inflammopharmacology* **13**, 113-25 (2005).

151. Deng, Z.H., Wen, J.F., Li, J.H., Xiao, D.S. & Zhou, J.H. Activator protein-1 involved in growth inhibition by RASSF1A gene in the human gastric carcinoma cell line SGC7901. *World J Gastroenterol* **14**, 1437-43 (2008).

152. Song, M.S. & Lim, D.S. Control of APC-Cdc20 by the tumor suppressor RASSF1A. *Cell Cycle* **3**, 574-6 (2004).

153. Liu, L., Baier, K., Dammann, R. & Pfeifer, G.P. The tumor suppressor RASSF1A does not interact with Cdc20, an activator of the anaphase-promoting complex. *Cell Cycle* **6**, 1663-5 (2007).

154. Zhang, Z. et al. Inactivation of RASSF2A by promoter methylation correlates with lymph node metastasis in nasopharyngeal carcinoma. *Int J Cancer* **120**, 32-8 (2007).

155. Tommasi, S. et al. RASSF3 and NORE1: identification and cloning of two human homologues of the putative tumor suppressor gene RASSF1. *Oncogene* **21**, 2713-20 (2002).

156. Hesson, L. et al. Frequent epigenetic inactivation of RASSF1A and BLU genes located within the critical 3p21.3 region in gliomas. *Oncogene* **23**, 2408-19 (2004).

157. Eckfeld, K. et al. RASSF4/AD037 is a potential ras effector/tumor suppressor of the RASSF family. *Cancer Res* **64**, 8688-93 (2004).

158. Vavvas, D., Li, X., Avruch, J. & Zhang, X.F. Identification of Nore1 as a potential Ras effector. *J Biol Chem* **273**, 5439-42 (1998).

159. Steiner, G. et al. High-density mapping of chromosomal arm 1q in renal collecting duct carcinoma: region of minimal deletion at 1q32.1-32.2. *Cancer Res* **56**, 5044-6 (1996).

160. Almeida, A. et al. GAC1, a new member of the leucine-rich repeat superfamily on chromosome band 1q32.1, is amplified and overexpressed in malignant gliomas. *Oncogene* **16**, 2997-3002 (1998).

161. Kros, J.M. et al. Genetic aberrations in oligodendroglial tumours: an analysis using comparative genomic hybridization (CGH). *J Pathol* **188**, 282-8 (1999).

162. Ried, T. et al. Comparative genomic hybridization of formalin-fixed, paraffin-embedded breast tumors reveals different patterns of chromosomal gains and losses in fibroadenomas and diploid and aneuploid carcinomas. *Cancer Res* **55**, 5415-23 (1995).

163. Riemenschneider, M.J. et al. Amplification and overexpression of the MDM4 (MDMX) gene from 1q32 in a subset of malignant gliomas without TP53 mutation or MDM2 amplification. *Cancer Res* **59**, 6091-6 (1999).

164. Zanke, B. et al. A hematopoietic protein tyrosine phosphatase (HePTP) gene that is amplified and overexpressed in myeloid malignancies maps to chromosome 1q32.1. *Leukemia* **8**, 236-44 (1994).

165. Chen, J. et al. The t(1;3) breakpoint-spanning genes LSAMP and NORE1 are involved in clear cell renal cell carcinomas. *Cancer Cell* **4**, 405-13 (2003).

166. Aoyama, Y., Avruch, J. & Zhang, X.F. Nore1 inhibits tumor cell growth independent of Ras or the MST1/2 kinases. *Oncogene* **23**, 3426-33 (2004).

167. Katagiri, K. et al. Crucial functions of the Rap1 effector molecule RAPL in lymphocyte and dendritic cell trafficking. *Nat Immunol* **5**, 1045-51 (2004).

168. Hull, J. et al. Haplotype mapping of the bronchiolitis susceptibility locus near IL8. *Hum Genet* **114**, 272-9 (2004).

169. Ikeda, M. et al. Ras-association domain family protein 6 induces apoptosis via both caspase-dependent and caspase-independent pathways. *Exp Cell Res* **313**, 1484-95 (2007).

170. Sherwood, V., Manbodh, R., Sheppard, C. & Chalmers, A.D. RASSF7 is a member of a new family of RAS association domain-containing proteins and is required for completing mitosis. *Mol Biol Cell* **19**, 1772-82 (2008).

171. Sollid, L.M. & Johansen, F.E. Animal models of inflammatory bowel disease at the dawn of the new genetics era. *PLoS Med* **5**, e198 (2008).

172. Kenny, E.F. & O'Neill, L.A. Signalling adaptors used by Toll-like receptors: an update. *Cytokine* **43**, 342-9 (2008).

173. Inohara, N. & Nunez, G. The NOD: a signaling module that regulates apoptosis and host defense against pathogens. *Oncogene* **20**, 6473-81 (2001).

174. Inohara, N., Ogura, Y. & Nunez, G. Nods: a family of cytosolic proteins that regulate the host response to pathogens. *Curr Opin Microbiol* **5**, 76-80 (2002).

175. Gutierrez, O. et al. Induction of Nod2 in myelomonocytic and intestinal epithelial cells via nuclear factor-kappa B activation. *J Biol Chem* **277**, 41701-5 (2002).

176. Inohara, N. et al. Host recognition of bacterial muramyl dipeptide mediated through NOD2. Implications for Crohn's disease. *J Biol Chem* **278**, 5509-12 (2003).

177. Ogura, Y. et al. Nod2, a Nod1/Apaf-1 family member that is restricted to monocytes and activates NF-kappaB. *J Biol Chem* **276**, 4812-8 (2001).

178. Ogura, Y. et al. Genetic variation and activity of mouse Nod2, a susceptibility gene for Crohn's disease. *Genomics* **81**, 369-77 (2003).

179. Hanahan, D. & Weinberg, R.A. The hallmarks of cancer. *Cell* **100**, 57-70 (2000).

180. Lowe, S.W., Cepero, E. & Evan, G. Intrinsic tumour suppression. *Nature* **432**, 307-15 (2004).

181. 20Agathanggelou, A. et al. Methylation associated inactivation of RASSF1A from region 3p21.3 in lung, breast and ovarian tumours. *Oncogene* **20**, 1509-18. (2001).

182. Pihan, G. & Doxsey, S.J. Mutations and aneuploidy: co-conspirators in cancer? *Cancer Cell* **4**, 89-94 (2003).

183. Richter, A.M., Pfeifer, G.P. & Dammann, R.H. The RASSF proteins in cancer; from epigenetic silencing to functional characterization. *Biochim Biophys Acta* (2009).

184. Donninger, H., Vos, M.D. & Clark, G.J. The RASSF1A tumor suppressor. *J Cell Sci* **120**, 3163-72 (2007).

185. Sherwood, V., Manbodh, R., Sheppard, C. & Chalmers, A.D. RASSF7 is a Member of a New Family of RAS Association Domain-Containing Proteins and is Required for Completing Mitosis. *Mol Biol Cell* (2008).

186. Moshnikova, A., Kuznetsov, S. & Khokhlatchev, A.V. Interaction of the growth and tumour suppressor NORE1A with microtubules is not required for its growth-suppressive function. *BMC Res Notes* **1**, 13 (2008).

187. Raynaud-Messina, B. & Merdes, A. Gamma-tubulin complexes and microtubule organization. *Curr Opin Cell Biol* **19**, 24-30 (2007).

188. Liu, L., Vo, A., Liu, G. & McKeehan, W.L. Putative tumor suppressor RASSF1 interactive protein and cell death inducer C19ORF5 is a DNA binding protein. *Biochem Biophys Res Commun* **332**, 670-6 (2005).

189. Adachi, M., Zhang, Y.B. & Imai, K. Mutation of BAD within the BH3 domain impairs its phosphorylation-mediated regulation. *FEBS Lett* **551**, 147-52 (2003).

190. Parvin, J.D. The BRCA1-dependent ubiquitin ligase, gamma-tubulin, and centrosomes. *Environ Mol Mutagen* (2009).

191. Frew, I.J. & Krek, W. Multitasking by pVHL in tumour suppression. *Curr Opin Cell Biol* **19**, 685-90 (2007).

192. Senda, T., Shimomura, A. & Iizuka-Kogo, A. Adenomatous polyposis coli (Apc) tumor suppressor gene as a multifunctional gene. *Anat Sci Int* **80**, 121-31 (2005).

193. Bhat, K.M. & Setaluri, V. Microtubule-associated proteins as targets in cancer chemotherapy. *Clin Cancer Res* **13**, 2849-54 (2007).

194. Fisk, H.A., Mattison, C.P. & Winey, M. Centrosomes and tumour suppressors. *Curr Opin Cell Biol* **14**, 700-5 (2002).

195. van der Weyden, L. et al. Loss of Rassf1a cooperates with Apc(Min) to accelerate intestinal tumourigenesis. *Oncogene* **27**, 4503-8 (2008).

196. Liu, L. & McKeehan, W.L. Sequence analysis of LRPPRC and its SEC1 domain interaction partners suggests roles in cytoskeletal organization, vesicular trafficking, nucleocytosolic shuttling, and chromosome activity. *Genomics* **79**, 124-36 (2002).

197. Mili, S. & Pinol-Roma, S. LRP130, a pentatricopeptide motif protein with a noncanonical RNA-binding domain, is bound in vivo to mitochondrial and nuclear RNAs. *Mol Cell Biol* **23**, 4972-82 (2003).

198. Finsterer, J. Leigh and Leigh-like syndrome in children and adults. *Pediatr Neurol* **39**, 223-35 (2008).

199. Filosto, M. et al. Neuropathology of mitochondrial diseases. *Biosci Rep* **27**, 23-30 (2007).

200. Darin, N. et al. Genotypes and clinical phenotypes in children with cytochrome-c oxidase deficiency. *Neuropediatrics* **34**, 311-7 (2003).

201. Fenton, S.L. et al. Identification of the E1A-regulated transcription factor p120 E4F as an interacting partner of the RASSF1A candidate tumor suppressor gene. *Cancer Res* **64**, 102-7 (2004).

202. Fernandes, E.R. & Rooney, R.J. The adenovirus E1A-regulated transcription factor E4F is generated from the human homolog of nuclear factor phiAP3. *Mol Cell Biol* **17**, 1890-903 (1997).

203. Fajas, L. et al. Cyclin A is a mediator of p120E4F-dependent cell cycle arrest in G1. *Mol Cell Biol* **21**, 2956-66 (2001).

204. Fajas, L. et al. pRB binds to and modulates the transrepressing activity of the E1A-regulated transcription factor p120E4F. *Proc Natl Acad Sci U S A* **97**, 7738-43 (2000).

205. Rizos, H. et al. Association of p14ARF with the p120E4F transcriptional repressor enhances cell cycle inhibition. *J Biol Chem* **278**, 4981-9 (2003).

206. la Cour, T. et al. Analysis and prediction of leucine-rich nuclear export signals. *Protein Eng Des Sel* **17**, 527-36 (2004).

207. Brameier, M., Krings, A. & MacCallum, R.M. NucPred--predicting nuclear localization of proteins. *Bioinformatics* **23**, 1159-60 (2007).

208. Carmody, R.J. & Chen, Y.H. Nuclear factor-kappaB: activation and regulation during toll-like receptor signaling. *Cell Mol Immunol* **4**, 31-41 (2007).

209. Courtois, G. & Gilmore, T.D. Mutations in the NF-kappaB signaling pathway: implications for human disease. *Oncogene* **25**, 6831-43 (2006).

210. Basseres, D.S. & Baldwin, A.S. Nuclear factor-kappaB and inhibitor of kappaB kinase pathways in oncogenic initiation and progression. *Oncogene* **25**, 6817-30 (2006).

211. Karin, M. Nuclear factor-kappaB in cancer development and progression. *Nature* **441**, 431-6 (2006).

212. Balkwill, F. & Mantovani, A. Inflammation and cancer: back to Virchow? *Lancet* **357**, 539-45 (2001).

213. Ames, B.N., Gold, L.S. & Willett, W.C. The causes and prevention of cancer. *Proc Natl Acad Sci U S A* **92**, 5258-65 (1995).